Examination of "Primary", "Secondary", and "Tertiary" Structural Elements of Bis-Amino Acids: Progress toward "Fauxteins"

By

Matthew F. L. Parker

B. S. Binghamton University, 2003

M. S. Binghamton University, 2005

Submitted to the Graduate Faculty of the

Kenneth P. Dietrich School of Arts and

Sciences in partial fulfillment

of the requirements for the degree of

Doctor of Philosophy

University of Pittsburgh

2015

UNIVERSITY OF PITTSBURGH

KENNETH P. DIETRICH SCHOOL OF ARTS AND SCIENCES

This dissertation was presented

By

Matthew F. L. Parker

It was defended on

July 20th, 2015

and approved by

Dr. Seth Horne, Associate Professor, Department of Chemistry

Dr. Peng Liu, Assistant Professor, Department of Chemistry

Dr. Christian E. Schafmeister, Professor, Department of Chemistry, Temple University

Dissertation Advisor: Dr. David H. Waldeck, Professor, Department of Chemistry

Examination of "Primary", "Secondary", and "Tertiary" Structural Elements of Bis-Amino Acids: Progress toward "Fauxteins"

Matthew F. L. Parker, PhD

University of Pittsburgh, 2015

Proteins are in a category all their own as supramolecular entities enriched with both chirality and functionality. Inspired by them, we have created a new class of building blocks, called Bis-Amino Acids, for making molecules several kilodaltons in size that possess high degrees of both functionality and chirality. Bis-amino acids can assemble into shape-programmable macromolecules, called Spiroligomers that connect through pairs of amide bonds. They serve as water-soluble, rigid scaffolds capable of presenting collections of functional groups in different spatial orientations by virtue of their sequence, shape and stereochemistry of each chiral building block.

This dissertation utilizes these unique building block as scaffolding for the presentation of functional groups in localized domains. A short spiroligomer sequence is used to presents a donor and acceptor pair facially for measuring electron-transfer in water. The same cleft motif is used to present a pair of hydrogen bonding donors to catalyze an aromatic Claisen rearrangement. Methods are developed to improve and expand the chemistry to make the bis-amino acids as well as their assembly into spiroligomers. Lastly, spiroligomers are utilized as intermediate building materials forming sequences of two and three connected by short, flexible linkers and cross-linked them into assemblies. We envision the use of these macromolecules, called "Fauxteins" to position multiple functional groups over large surface areas for mimicry of protein-protein interactions, recreation of complex active sites of enzymes, and form unique, chiral pockets for host-guest molecular recognition.

TABLE OF CONTENTS

LIST OF TABLES

LIST OF FIGURES

LIST OF SCHEMES

PREFACE

I can imagine that such a long PhD, spanning effectively two academic advisors at two different research institutions would mean that I have twice as many people who have contributed and deserve to be recognized and thanked…and that would in fact be the case. Chiefly among them are Prof Christian E. Schafmeister and Professor David H. Waldeck for their unconditional support, patience, and guidance. If my PhD was a boat, Professor Waldeck is my Anchor that without I would have surely been long lost as sea by now. Professor Schafmeister is my Captain, pushing us through the blue expanse that is the ocean of science. Through their combined efforts, this boat might actually reach shore.

I am thankful to my labmates, including Dr. Sharad Gupta, Dr. Zack Brown, Dr. Mahboubeh Kheirabadi, Jae Eun Cheong, Conrad Pfeiffer, Justin Northrup, Stephanie Kumor, and the rest of the Schafmeister group past and present. I would also like to thank Dr. Subhasis Chakrabarti, Dr. Prasun Mukherjee, Brittney Graff, and Daniel Lamont from the Waldeck group and Dr. Silvia Osuna from the Houk group.

I am also thankful to my committee members, Prof. Seth Horne and Prof. Peng Lui for their hard work, thoughtful criticism, and time to aid in the completing of my PhD.

List of Abbreviations

ACN	Acetonitrile
AcMe	Acetone
AcOH	Acetic acid
Boc	tert-Butoxycarbonyl
Boc2O	Di-tert-butyl dicarbonate
Cbz	Carboxybenzyl
DIC	Diisopropylcarbodiimide
DCM	Dichloromethane
DIPEA	N,N-Diisoproylethylamine
DKP	Diketopiperazine
DMAP	4-Methyldiaminopyridine
DMF	N,N-Dimethylformamide
EtOAc	Ethyl acetate
Fmoc	9-Fluorenylmethoxycarbonyl
HATU	O-(7-azabenzotriazol-1-yl)-tetramethyluronium hexafluorophosphate
HFIP	Hexafluoroisopropanol
HMBC	Heteronuclear multiple bond correlation spectroscopy
HMQC	Heteronuclear multiple quantum coherence
HOAt	Hydroxyazabenzotriazole
HPLC	High performance liquid chromatography
LC-MS	Liquid chromatography with mass spectrometry
MeIm	Methylimidazole
MeOH	Methyl alcohol
MS	Mass spectrometry
pNZ	Carboxy-para-Nitrobenzyl
TFA	Trifluoroacetic acid
THF	Tetrahydrofuran
TIPS	Triisopropylsilane

1.0 Introduction

1.1 Proteins and the Mimicry of Protein Structure

Proteins are nature's nanomachines, catalyzing chemical reactions with high specificity and carrying out molecular recognition selectively. Proteins accomplish such marvels by forming well-defined three-dimensional structures and precisely positioning collections of functional groups. [1] Furthermore, proteins accomplish this large diversity of tasks with only a small collection of 20 amino acids. Proteins' formula for success seems inherently simple, yet the rules that govern the crucial transformations of a linear peptide sequence into the well-ordered globular structures proteins adopt to provide function, are very complex and not fully understood. [2,3]

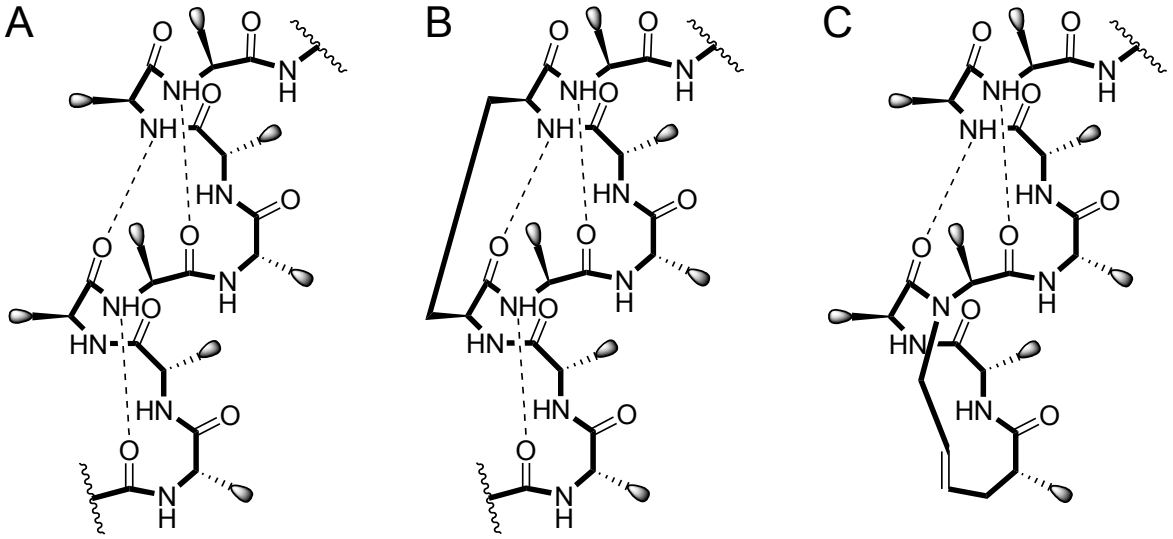

Figure 1-1. 2D structures of α-helix (A) and two methods of α-helix stabilization: stapled peptides (B) and hydrogen bonding surrogates (C).

Several research efforts are concerned with emulating the functional group organizing capabilities and functions of proteins. Such efforts include stabilization of peptides via stapled peptides and hydrogen bonding surrogates, shown in Figure 1-1. [4,5] Both of these examples utilize alkene-derived peptide sequences and olefin methasis to

form additional bonds that promote and stabilize an α-helix conformation as in the case of stapled peptides (Figure 1-1B) or emulate an intermolecular hydrogen bond as in the case of hydrogen bond surrogates (Figure 1-1C).

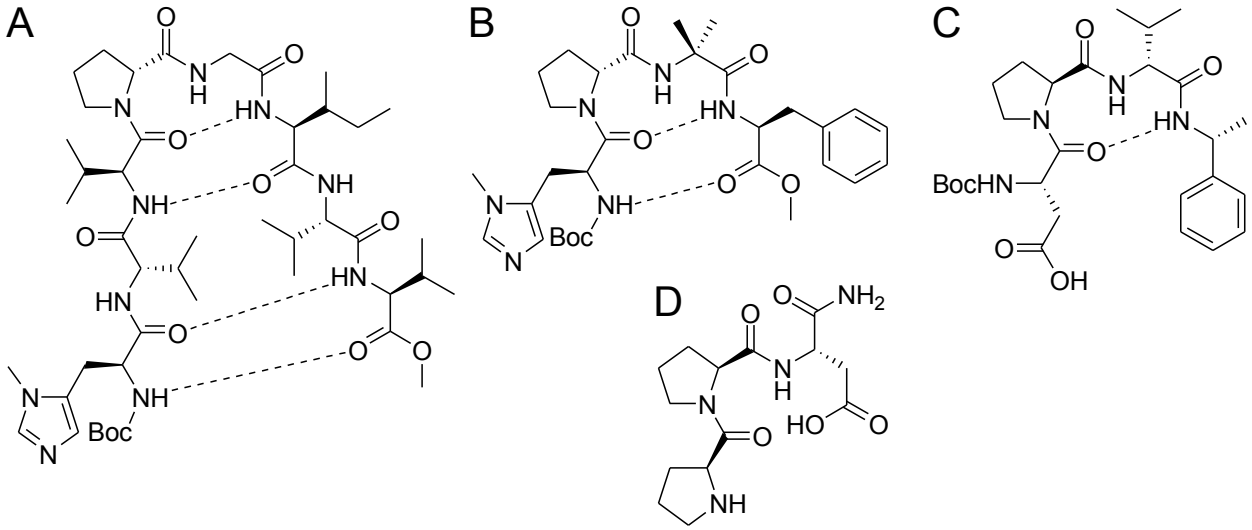

Figure 1-2. 2D structures of small peptides used as asymmetric catalysts. (A) and (B) are acylation catalysts. (C) is an epoxidation catalyst. (D) is an aldol catalyst.

Alternatively, the use of smaller peptide scaffolds have been invoked to direct the presentation of chemical reactive functional groups, hydrogen bonding groups, and steric bias to effect asymmetric catalysis. [6-8] Figure 1-2 illustrates some examples of peptide ranging in size from three to eight residues that have demonstrated to successfully perform asymmetric acylation reactions (Figure 1-2A and B), asymmetric epoxidation reactions (Figure 1-2C) and asymmetric aldol reactions (Figure 1-2D) as just a few examples. Based on these catalysts ability to demonstrate asymmetric induction, it is reasonable to suggest that a strong conformational preference exists. However, non-polar solvents and, in some cases, subzero temperatures are required in order to achieve and stabilize the conformation necessary to provide asymmetric induction.

Beyond the use of proteogenic amino acids to form small oligomers, classes of compounds called "foldamers" have been utilized as scaffolds to present functional groups. Foldamers are defined as "any oligomers that fold into a conformationally ordered state in solution, the structures of which are stabilized by a collection of noncovalent interactions between nonadjacent monomer units". [9] Figure 1-3 highlights some examples of various foldamer designs. Most of them are variation of amino acids and form amide bonds, while others depart significantly. To date, most foldamers adopt a helical structure. [10-18] Despite the triumphs of these various research directions, they still heavily rely on folding in order to obtain structure.

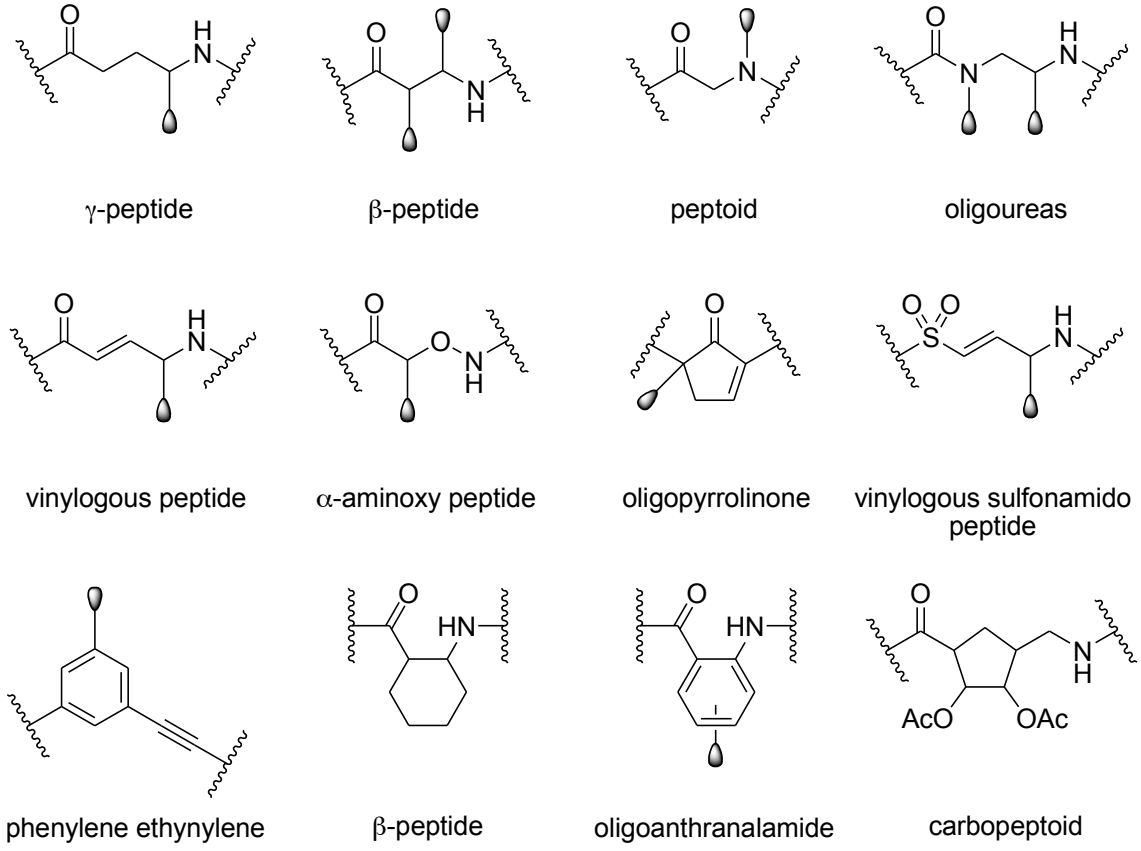

Figure 1-3. 2-D structures of general representations of various foldamers.

1.2 Spiroligomers

Spiroligomers offer a dramatic departure from these protein-inspired research directions. [19] The key element that separates spiroligomers from everything else is that spiroligomers are connected through pairs of amide bonds, as their name entails, providing a more conformationally restricting, polycyclic backbone. The shape and presentation of functional groups are not formed via folding and stabilized by noncovalent interactions, but instead are a result of the monomer structure, connectivity and the rich stereochemistry installed in each building block. Figure 1-4 shows the general concept of spiroligomers. There are 4 monomer classes synthesized to date: Pro4 class, Pip4 class, Pip5 class and the Hin class (shown in Figure 1-4). The Pro4 class is most developed so only its synthesis will be discussed in detail.

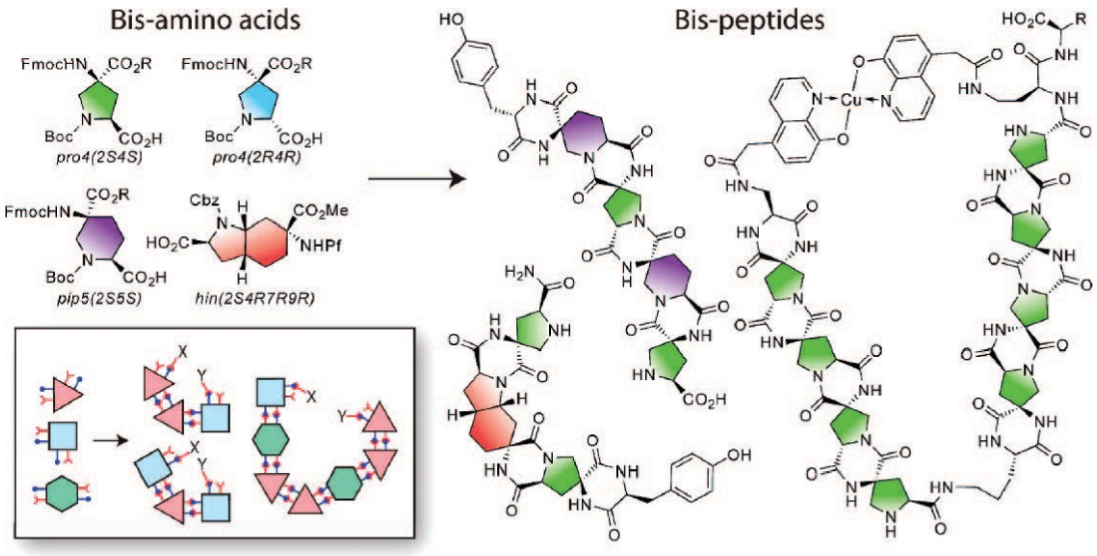

Figure 1-4. General concepts of spiroligomers including example of monomer and previously synthesized oligomers.

Each member of the Pro4 monomer class has two stereocenters and thus the Pro4 class contains four stereoisomers. All four stereoisomers have been synthesized from 4-trans-hydroxyproline (compound **5**) as shown in Scheme 1-1. Compound **5** is protected with a benzyl carbamate using Cbz-Cl and $NaHCO_3$ in 1:10 dioxane/water mixture. The C-4 hydroxyl group is then oxidized to the corresponding ketone with Jones reagent in AcMe. The C-2 carboxylic acid is then converted to the tert-butyl ester with isobutylene and catalytic H_2SO_4 in DCM to yield compound **6**. Compound **6** is subjected to the Bucherer Berg's reaction using KCN, $(NH_4)_2CO_3$ in 1:1 EtOH/water mixture to convert the ketone to a 5:1 diastereomeric mixture of hydantoins (compounds **7a** and **7b**). The hydantoins are separated with column chromatography.

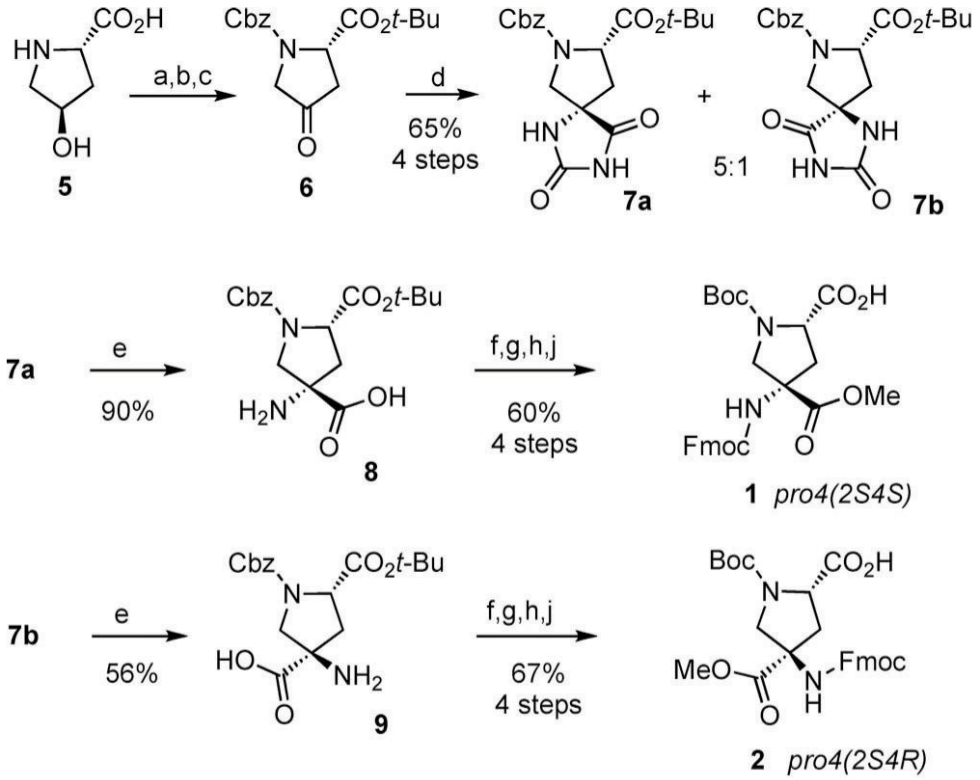

Scheme 1-1. Synthesis of Pro4 class of monomers. (a) $NaHCO_3$, Cbz-Cl, 1:10 Diox/ H_2O; (b) Jones reagent, AcMe; (c) isobutylene, H_2SO_4 (cat.), DCM; (d) $(NH_4)_2CO_3$, KCN, 1:1 EtOH/H_2O; (e) i. $(Boc)_2O$, DMAP, THF ; ii. 2 M KOH; (f) Fmoc-OSu, DIPEA, DCM; (g) MeOH, DIC, DMAP, DCM, 0 °C to rt; (h) 1:2 TFA/DCM; (j) H_2, 10% Pd/C, $(Boc)_2O$, THF

Each pure stereoisomer is converted to its amino acid form via base hydrolysis in two steps. First the hydantoin imide and amide are converted to tert-butyl carbamates using Boc_2O and catalytic DMAP in THF followed by base hydrolysis of the bis-Boc hydantoin via addition of 2M KOH (aq). The amino acid is recovered after neutralization and precipitation of the basic aqueous solution to provide compounds **8** and **9** from **7a** and **7b**, respectively. Compound **8** is protected with a fluorenylmethyl carbamate using Fmoc-OSu and DIPEA in DCM and esterified with MeOH, DIC, and catalytic DMAP in DCM. The tert-butyl ester is cleaved using 1:2 TFA/DCM mixture and the benzyl carbamate (Cbz) is converted to a tert-butyl carbamate (Boc) using Boc_2O and Pd/C in THF under a H_2 atmosphere to yield compound **1**. Similar, Compound **9** is converted to compound **2**.

The other two stereoisomers of Pro4 are synthesized from 4-*cis*-hydroxyproline (compound **10**), which is obtained from epimerization of compound **5** in three steps as shown in Scheme 1-2. Compound **5** is refluxed in a 2:1 Ac_2O/AcOH mixture followed by reflux in 2M HCl (aq). Compound **10** is isolated via freebasing with TEA and recrystallized from EtOH/water. Compound **10** is then converted to compounds **3** and **4** using the same protocols described for compounds **1** and **2**.

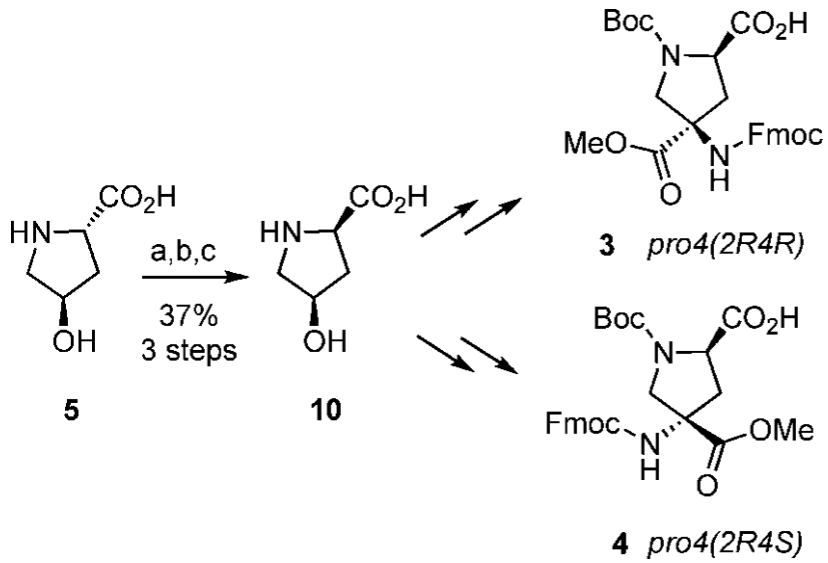

Scheme 1-2. Synthesis of Pro4 class of monomers. (a) Ac_2O, AcOH, reflux; (b) 2 M HCl (aq), reflux; (c) (i) free base with TEA; (ii) recryst. from $EtOH/H_2O$.

Compounds **1**-**4** are now able to be assembled into oligomers using solid support and are designed to be amenable touse in Fmoc solid phase synthesis. Scheme 1-3 shows the overall strategy for oligomer assembly and rigidification. Each building block is attached through a single amide bond with the C-2 carboxylic acid and the C-4 amino group after the Fmoc is cleaved. Once the oligomer is assembled, the remaining protecting groups are cleaved and the oligomer is liberated from the solid support. The oligomer is then rigidified via a methanolysis reaction in which each available amine forms an amide bond with the C-4 carboxy methyl ester of the proceeding building block to yield a diketopiperazine (DKP) ring.

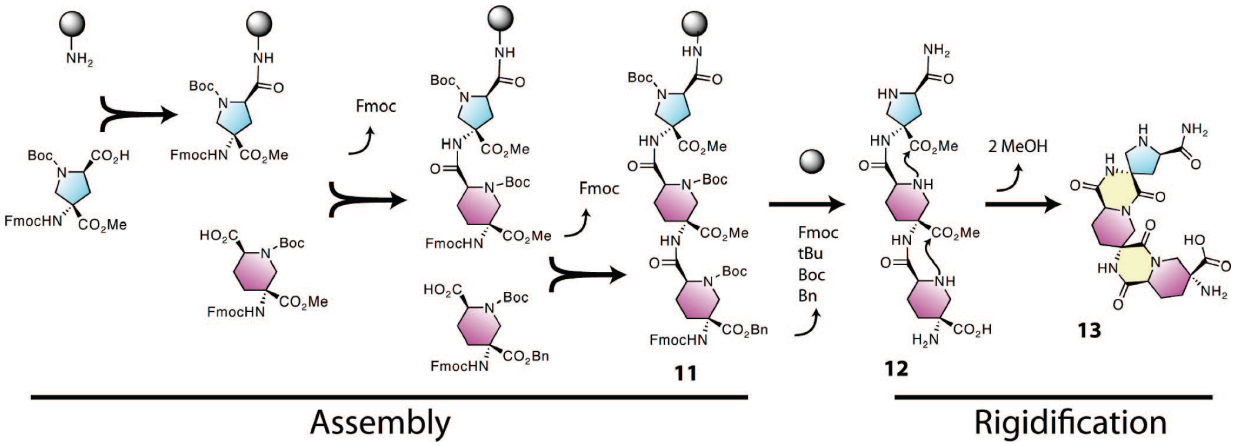

Scheme 1-3. Solid phase oligomers assembly and rigidification.

Many examples of these oligomers have been synthesized and characterized using multiple building blocks to create unique shapes and different techniques to characterize these structures. Among these techniques are multi-dimensional NMR, Fluorescence Resonance Energy Transfer (FRET), and double electron-electron resonance (DEER). All have contributed to our growing knowledge of the global structure and conformational preferences of the spiroligomers. [19]

1.3 References

[1] Creighton, T. *Proteins Structures and Molecular Properties*; W.H. Freeman, **1993**

[2] Dill, K.; Ozkan, S.; Weikl, T.; Chodera, J.; Voelz, V. *Curr. Op. in Struct. Bio*. **2007**, 17, 342

[3] Cheng, R.; Gellman, S.; DeGrado, W.; *Chem. Rev*. **2001**, 101, 3219

[4] Patgiri, A.; Jochim, A.; Arora, P. *Acc. Chem. Res* **2008**, 41, 1289

[5] Walensky, L. D.; Kung, A. L.; Escher, I.; Malia, T. J.; Barbuto, S.; Wright, R. D. *Science* **2004**, 305, 1466

[6] Miller, S. J.; Acc. Chem. Res. **2004,** 37, 601-610

[7] Peris, G.; Jakobsche, C. E.; Miller, S. J.; *Am. Chem. Soc.*, **2007**, 129 (28), 8710-8711

[8] Krattiger, P; Kovasy, R.; Revell, J. D.; Ivan, S.; Wennemers, H; *Org. Lett.*, **2005**, 7 (6), 1101-11-3.

[9] Hill, D.; Mio, M.; Prince, R.; Hughes, T.; Moore, J. *Chem. Rev*. **2001**, 101, 3893

[10] Cho, C.Y.; Moran, E.J.; Cherry, S.R.; Stephans, J.C.; Fodor, S.P.A.; Adams, C.L.; Sundaram, A.; Jacobs, J.W.; Schultz, P.G.; *Science*, **1993**, *261*, 1303-1305.

[11] Hagihara, M.; Anthony, N.J.; Stout, T.J.; Clardy, J.; Schreiber, S.L.; *J. Am. Chem. Soc.*, **1992**, *114*, 6568-6570.

[12] Barron, A.E.; Zuckermann, R.N.; *Curr. Opin. Chem. Biol.*, **1999**, *3*, 681-687.

[13] Nowick, J.S.; Powell, N.A.; Martinez, E.J.; Smith, E.M.; Noronha, G.; *J. Org. Chem.*, **1992**, *57*, 3763-3765.

[14] Seebach, D.; Matthews, J.L.; *Chem. Commun.*, **1997**, *21*, 2015-2022.

[15] Appella, D.J.; Christianson, L.A.; Klein, D.A.; Powell, D.R.; Huang, X.; Barchi, J.J., Jr.; Gellman, S.H. *Nature*, **1997**, *387*, 381-384.

[16] Nelson, J.C.; Saven, J.G.; Moore, J.S.; Wolynes, P.G.; *Science*, **1997**, *277*, 1793-1796.

[17] Gellman, S.H.; *Acc. Chem. Res.*, **1998**, *31*, 173-180.

[18] Goodman, C.;Choi, S.; Shandler, S.; DeGrado W. *Nature Chem. Bio*. **2007**, 5, 252

[19] Schafmeister, C.E.; Brown, Z.Z.; Gupta, S. *Acc. Chem. Res*. **2008**, 41, 1387

2.0 Spiroligomer Donor-Bridge-Acceptor (DBA) Molecular Scaffolds for Probing Electron Transfer Processes

Chapter 2 details our use of bis-amino acids for presenting a dimethylaniline donor and pyrene acceptor moiety that is water-soluble for probing electron-transfer in water. Highlights of this work are the first electron transfer measurements performed in water at ambient conditions. A 3-fold rate enhancement was observed for the cleft forming molecule in water. This interesting finding has resulted in the synthesis of additional molecules with the intent to further probe this electron-transfer process.

A portion of this work was published in:

J. Am. Chem. Soc., **2009**, *131* (6), pp 2044–2045

Acknowledgments: Dr. Subhasis Chakrabarti executed all physical chemistry experiments

2.1 Introduction

Organic Scaffolds, peptides, and oligomers continue to play an important role for understanding how positioning of chemical functionalities in space control chemical reactivity and how functional groups communicate through energy and electron transfer processes. [1-5] Figure 2-1 illustrates a few examples of Donor-Bridge-Acceptor (DBA) molecular scaffolds used to probe energy and electron transfer processes. Figure 2-1A shows a bis-steroid DBA scaffold that was used to test the distance dependence of coulombic energy transfer. [1] The fused poly-ring system provided a rigid backbone to position an anthracyl (energy donor) and a naphthyl (energy acceptor) groups approximately 20 Å apart. Figure 2-1B shows an example of probing distance dependence of singlet-singlet energy transfer by the Förster mechanism using a series of poly-proline peptides of varying length. [2] Poly-prolines adopt a PPII helix, which is relatively more rigid than other polypeptides. Furthermore, the PPII helices containing different numbers of prolines act as a series of molecular rulers, which separate the naphthyl (energy donor) and a dansyl (energy acceptor) groups and enabled the observation of the relationship between intergroup distance and the efficiency of energy transfer between groups. Figure 2-1C shows an example of a poly-norborane DBA scaffold that was used to investigate solvent-mediated electronic coupling and electron transfer processes. [3-5] The *cis*-conformations of the norborane ring systems provide an inherent curvature in the scaffold, ultimately forming a cleft between and providing facial presentation of the anthracyl (electron donor) and the maleate (electron acceptor).

These three examples of organic scaffolds represent two extremes of organic scaffolding and both offer benefits as well as restrictions. The bis-steroid and poly-

norborane are completely rigid systems but are very lipophilic, limiting their application to the study of energy and electron transfer processes in nonpolar solvents. The poly-peptide on the other hand is significantly less constrained and relies on folding to present functionality, so solvent and temperature conditions strongly govern the resulting helical presentation. A scaffold that is both rigid and water-soluble would allow the exploration of energy and electron transfer processes in water, which could help us to understand these physical processes in biological systems.

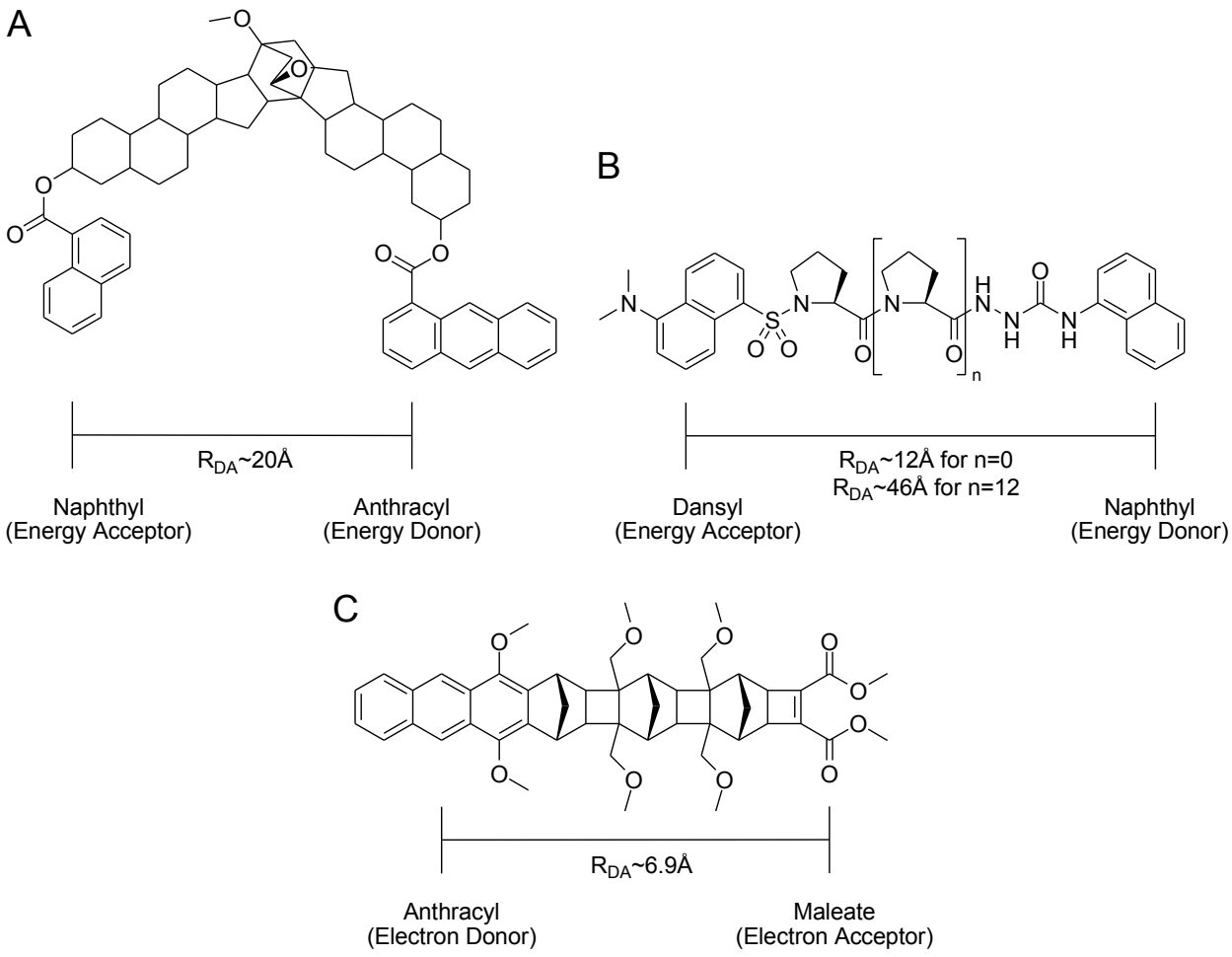

Figure 2-1. Examples of organic scaffold possessing donor and acceptor moieties to measure energy transfer. (A) shows a bis-steroid bridge for energy transfer. (B) shows a poly-proline bridge used for energy transfer. (C) shows a poly-norborane bridge used for electron transfer.

The importance of water in determining the activation energy for election transfer (ET) reactions is well appreciated. Water molecules influence electron transport in biomolecules and play a key role in biologically vital processes in living cells. [6-8] Recent theoretical work shows that placement of a few water molecules between electron donor and acceptor moieties can change the electronic tunneling probabilities between them. [9-11] Prior to our work, there have only been studies that probed electron tunneling in frozen water. [12,13] We demonstrate the first example of water mediated ET in ambient aqueous conditions.

Spiroligomers offer a unique scaffold that combines the benefits of preorganization, like the bis-steroid and poly-norborane, and the water solubility of poly-proline. As shown in Chapter 1, the structure and presentation of groups on sprioligomers are controlled by the stereochemistry and number of component monomers. This chapter describes the design and synthesis of spiroligomers containing a pyrene (electron acceptor) and dimethylaniline (electron donor) for studying the photoinduced ET rates through water. [14,15]

2.2 Results & Discussion

We set out to develop a water-soluble DBA molecule that we could use to study electron transfer in water. We developed a small spiroligomer that bears a cleft that holds a pyrene donor ~4.5 Å away from a dimethylaniline acceptor. Previous studies with spiroligomers as molecular rulers have provided evidence that the separation between two functional groups on a bis-amino acid monomer is ~ 5 Å, therefore only a single Pro4 monomer was used to present the donor and acceptor moieties. [16]

The general design is shown in Figure 2-2. The dimethylaniline (DMA) chromophore is displayed on a diketopiperazine (DKP) ring with the C-4 quaternary amino acid of the Pro4 monomer. The DMA chromophore can be synthetically accessed from a commercially available substituted phenylalanine derivative. Figure 2-2B and C shows 3D and 2D structures, respectively, of the DBA scaffold using the 2S4S stereoisomer of Pro4 (compound **11**). Although, the Spiroligomer DBA design possesses several degrees of freedom and can adopt several conformations, the Amber94 minimumized structure of this DBA scaffold shows that D-SSS-A (**11**) can display a cleft (Figure 2-2B). As shown, the closed DKP and the stereochemistry of the C-4 of the Pro4 monomer and the DMA amino acid orient the chromophore on the same face as the pyrrolidine nitrogen where the pyrene chromophore was installed via a carboxamide linkage using commercially available pyrene-1-carboxylic acid. Lastly, the C-2 carboxylic acid was modified with a lysine tri-peptide to enhance the water-solubility of the system. When the 2R4R stereoisomer of Pro4 was used (Figure 2-2D and E), the DMA chromophore orients to the C-2 carboxylic acid and no distinct cleft is observed in the Amber94 minimized structure (Figure 2-2D).

The DBA scaffold using the 2R4R stereoisomer of Pro4 was synthesized and used as a control molecule (compound **12**).

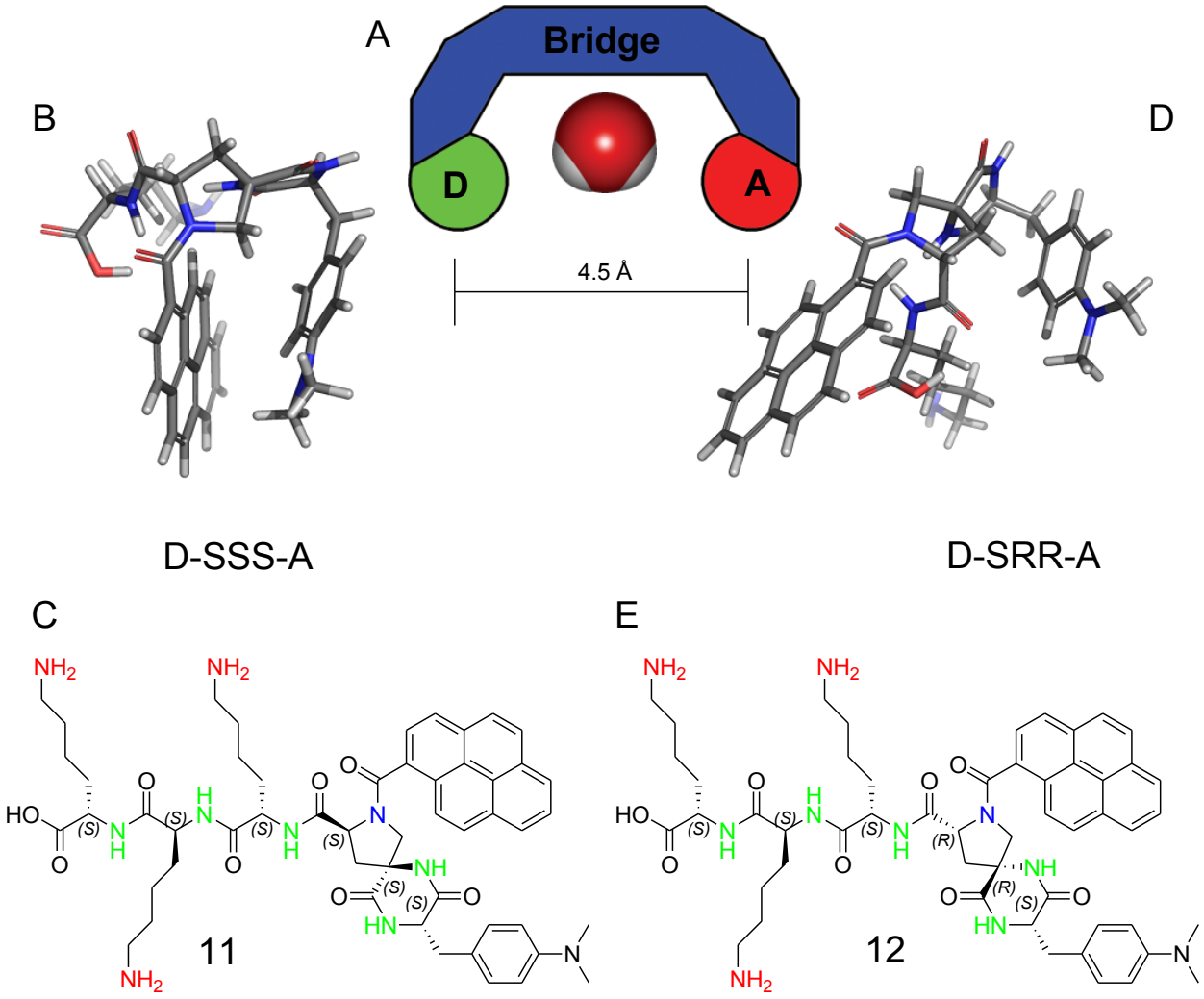

Figure 2-2. Bis-peptide Donor-Bridge-Acceptor (DAB) for studying electron transfer processes in water. (A) shows the general design schematic. (B) and (D) are the 3D models using 2S4S and 2R4R stereochemistry, respectively. (C) and (E) are the 2D structures of D-SSS-A (compound **11**) and D-SRR-A (compound **12**).

The molecules were synthesized using standard Fmoc solid phase synthesis. The ideal point of resin attachment is the C terminus of the tri-lysine unit followed by the Pro4 monomer, DMA amino acid, and attachment of the pyrene last. However, the design does

require that three different sets of amines be orthogonally protected. All of the amino acids were Fmoc protected as well as the C-4 amino group on Pro4 (highlighted green in Figure 2-2C and E). The epsilon amino groups on the lysines were Boc protected so that side chain deprotection would accompany liberation from the solid support (highlighted red in Figure 2-2C and E). The pyrrolidine amine on Pro4 was protected with an allyl carbamate (highlighted blue in Figure 2-2C and E). The Alloc group was chosen because it is orthogonal to both Fmoc and Boc protecting groups and can be easy cleaved on solid support.

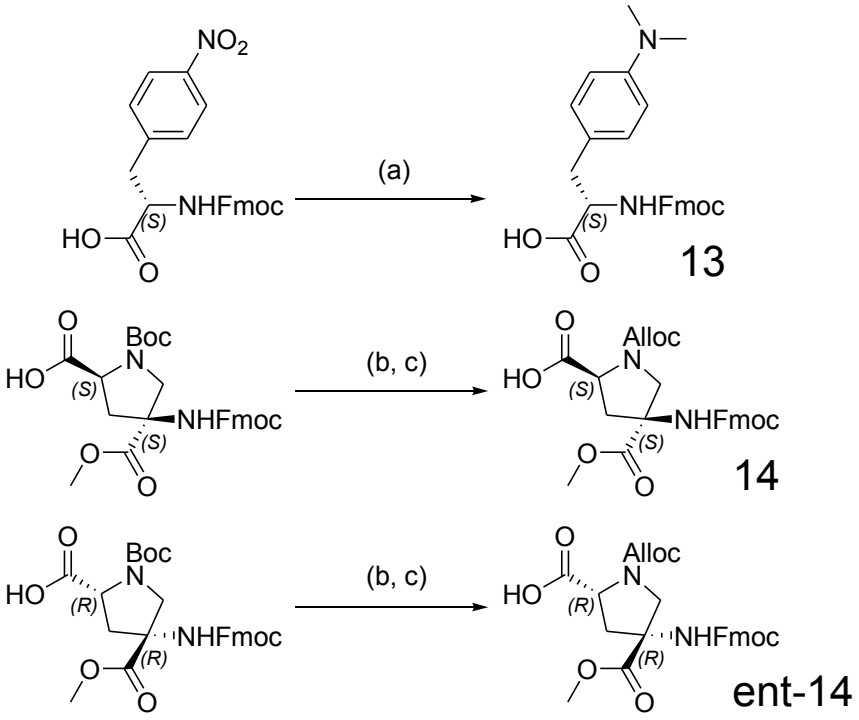

Scheme 2-1. Synthesis of DMA Amino acid (**13**) and Alloc protected Pro4 (**14**, **ent-14**). a) CH_2O (aq), Pd/C, H_2, THF, MeOH; b) 1:2 TFA, DCM; c) Alloc-Cl, DIPEA, DCM

The synthesis of the DMA amino acid (**13**) and the Alloc protected Pro4 (**14, ent-14**) are shown in Scheme 2-1. The DMA amino acid (**13**) was synthesized from a commercially available Fmoc-protected nitro derivative of phenylalanine via a reductive alkylation with

formaldehyde and Pd/C in THF/MeOH with H_2. The Pro4 monomer was modified via removal of the Boc group with TFA/DCM 1:2 followed by Alloc protection with the Alloc-Cl and TEA in DCM. Both the 2S4S and 2R4R stereoisomers of Pro4 were converted to the Alloc protected derivative (**14** and **ent-14**).

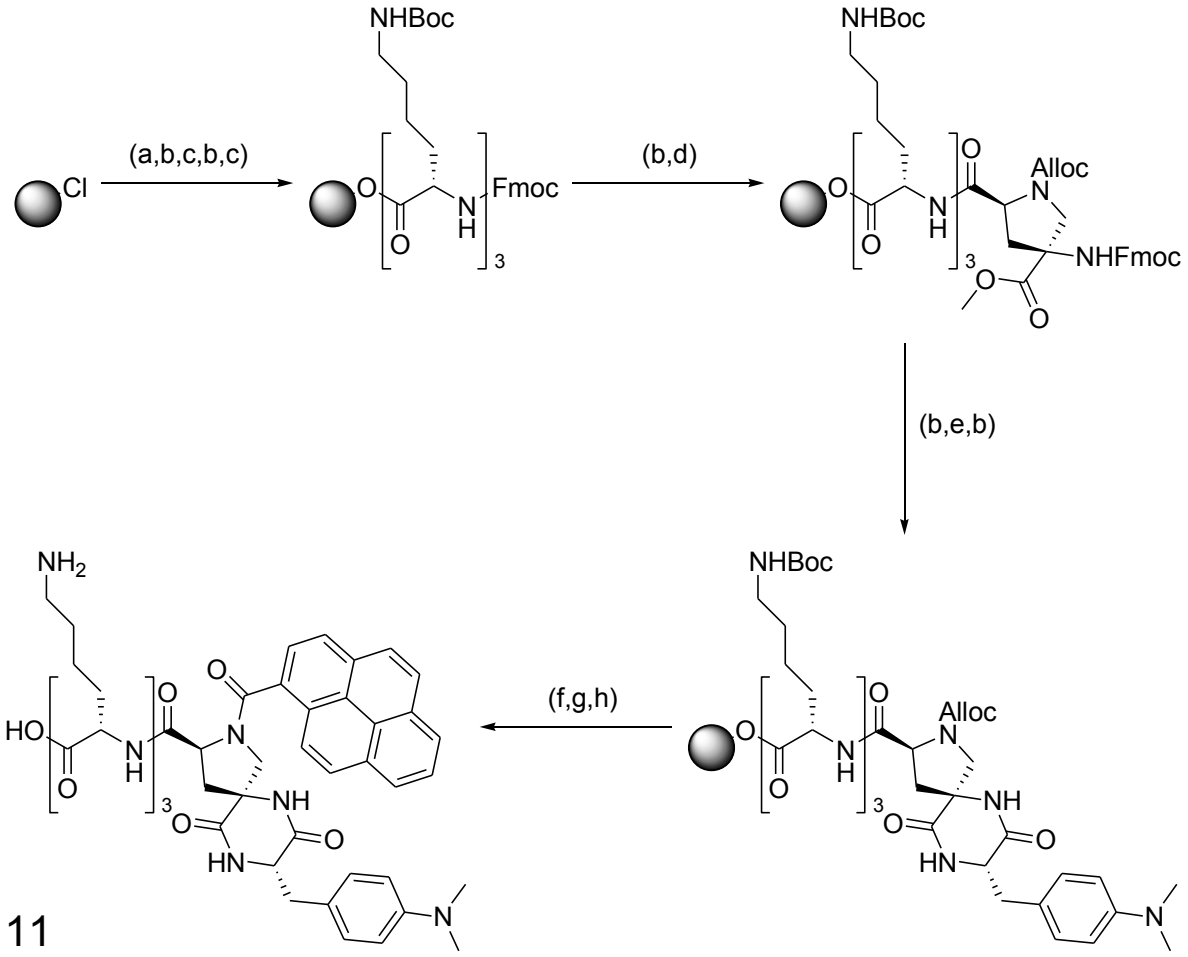

Scheme 2-2. Synthesis of DBA scaffolds. a) Fmoc-Lys(Boc)-OH, DIPEA, DCM; b) 1:4 piperidine/DMF; c) Fmoc-Lys(Boc)-OH, HATU, DIPEA, NMP; d) Pro4ssAHFM (**14**), HATU, DIPEA, NMP; e) Fmoc-DMA-OH (**13**), HATU, DIPEA, NMP; f) $(PPh_3)_4Pd$, BH_3:DMA, DCM; g) Py-COOH, HATU, DIPEA, NMP; h) 38:1:1 TFA/TIPS/H_2O.

The DBA spiroligomers were synthesized using Trityl resin as the solid support (Scheme 2-2). The first lysine residue was attached via S_N1 nucleophilic displacement using Fmoc-Lysine(Boc)-OH and DIPEA in DCM. The Fmoc group was cleaved with a 1:4

piperdine in DMF. The second lysine was attached via HATU coupling using Fmoc-Lysine(Boc)-OH, HATU and DIPEA in NMP. The Fmoc group was cleaved and the third lysine was introduced in identical fashion followed by Fmoc cleavage. The Alloc protected Pro4 monomer (**14** or **ent-14**) was then attached via HATU coupling followed by Fmoc cleavage. The DMA amino acid (**13**) was then attached and an extended Fmoc deprotection resulted in the spontaneous closure to the DKP ring.

The Alloc group was removed using $(PPh_3)_4Pd$ and BH_3:DMA in DCM and the pyrene-1-carboxylic acid was attached using HATU coupling. The Boc protecting groups were removed and the resin cleavage was affected using 48:1:1 TFA/H_2O/TIPS to yield the DBA scaffolds D-SSS-A (**11**) from compound (**14**) and D-SRR-A (**12**) from (**ent-14**), which were purified using reverse phase HPLC.

NMR analyses of the DBA spiroligomers (**11**) and (**12**) were performed in D_2O and deuterated DMSO, which was used as a control solvent for the ET experiments. At low temperature, significant broadening was observed due to aggregated states and slow exchanging among conformations. However, as the temperature was increased, coalescence was observed to two distinct conformations which were attributed to the *cis* and *trans* amide rotamers of pyrenyl amide. This along with overlap in the aliphatic regions due to the lysine side chains, made full assignment impractical. The aromatic region of the NMR was easy to interpret and provided detailed information about the presence and absence of the molecular cleft (Figure 2-3). Two different sets of doublets can be observed for each of the two sets of protons on the DMA ring. Integration of these two distinct sets of doublets suggested that these two conformations exist in a 2:1 ratio. This was consistent for each solvent for D-SSS-A and D-SRR-A. Even more intriguing was

that for the cleft-bearing D-SSS-A, one set of doublets were shifted further up field than the other and further up field than expected for this particular type of aromatic proton.

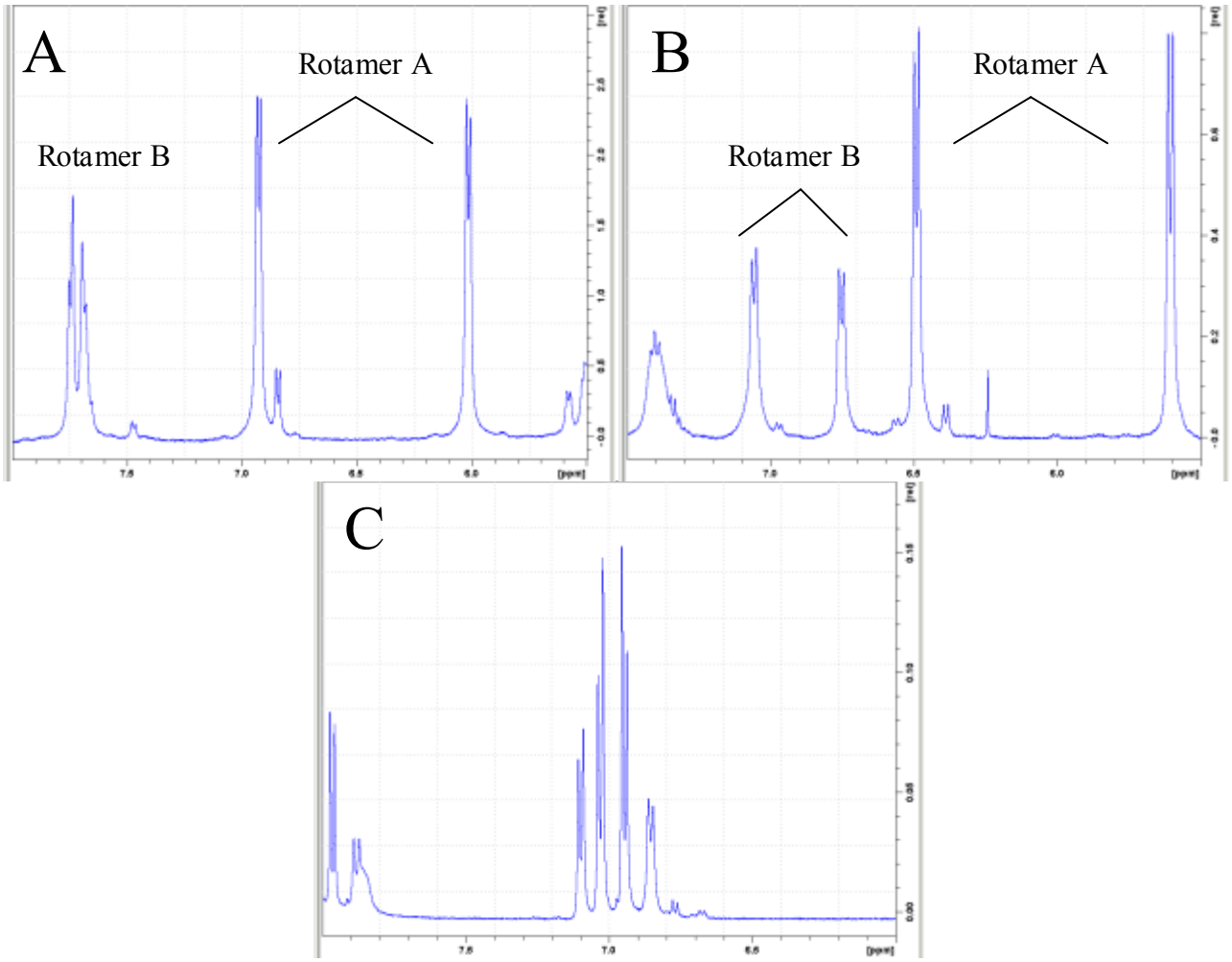

Figure 2-3. 1H NMR spectra for D-SSS-A (**11**) in D_2O and DMSO, (A) and (B) respectively, and D-SRR-A (**12**) in D_2O (C) at 333K. Only aromatic region is shown for visual clarity.

The two conformations observed by NMR were attributed to the cis and trans amide rotamers about the pyrrolidine-pyrene carboxamide bond, which would be expected to exchange slowly on the NMR time scale even at elevated temperatures. Closer inspection of the cleft-bearing D-SSS-A showed that a cleft is only present in the trans-amide conformation and no clear-defined cleft is present in the cis-amide conformation. The

conformations of the cis and trans amide rotamers and their presentation of donor and acceptor moieties are illustrated in Figure 2-4. Also illustrated is the shielding cone and deshielding torus, highlighted in green and red respectively. In the trans rotamer, the DMA moiety is presented to the shielding cone, which would cause an upfield shift in the NMR spectra for the proton lying in the shielding cone. This is consistent with what was observed for the higher populated conformer in both D_2O and deuterated DMSO for D-SSS-A. The cis rotamer, the DMA moiety is presented to the deshielding torus and is attributed to the lower populated conformer observed in the NMR spectra. NMR Analyses of the DBA spiroligomers confirm that a cleft is formed and that similar conformational preference was exhibited in both D_2O and deuterated DMSO.

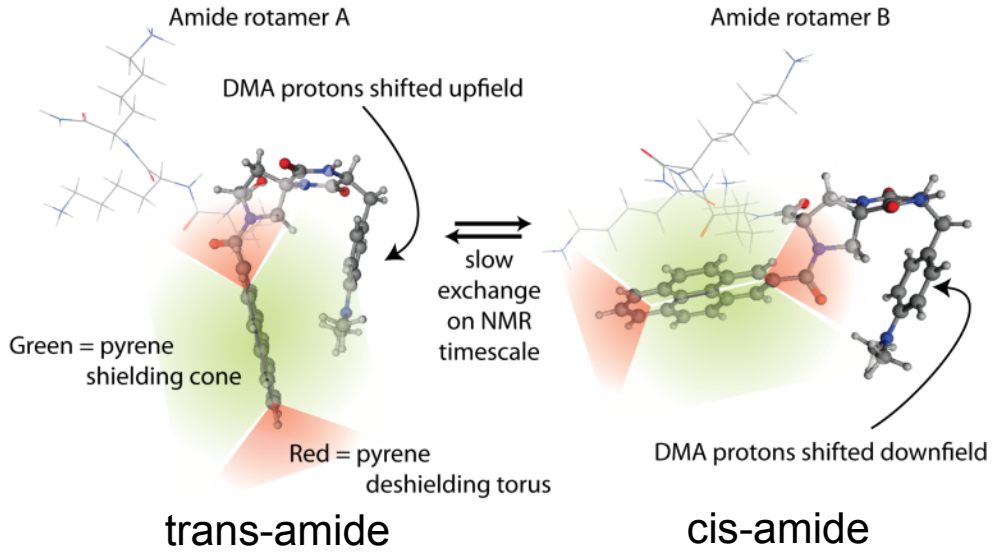

Figure 2-4. 3D model of two rotameric conformers of compound D-SSS-A (**11**). The pyrene shielding cone is highlighted in green and the pyrene deshielding torus is highlighted in red.

Time-resolved fluorescence was used to investigate electron transfer properties of the DBA spiroligomers D-SSS-A (**11**) and D-SRR-A (**12**). The fluorescence decay for both molecules in DMSO and H_2O possess two time components, which we attributed to the two

rotamer species observed from NMR: the shorter decay for the cleft-forming, higher populated conformer and the longer decay for the less populated conformer. The ET rate constants, k_{ET}, were derived for each DBA spiroligomer in both DMSO and H_2O over a range of temperatures. A proportional temperature dependence was observed for each trial and a ~3 fold increase of k_{ET} was observed for the cleft-forming DBA D-SSS-A (**11**) in water. This is attributed to an enhancement from tunneling mediated by water molecules.

Solvent	Temperature (K)	Lifetime τ_1 (ps)	A_1 (%)	Lifetime τ_2 (ps)	A_2 (%)	k_{ET} (s^{-1})
Water	283	807	65	15600	35	1.24 E+09
Water	296	599	64	12766	36	1.67 E+09
Water	306	592	62	11103	38	1.69 E+09
Water	319	484	62	11236	38	2.07 E+09
Water	326	498	64	11767	36	2.01 E+09
Water	334.5	404	61	8034	39	2.48 E+09
Water	344.5	418	64	7497	36	2.39 E+09
DMSO	283	2000.00	69	17915.64	31	5.00 E+08
DMSO	296	1687.59	67	15538.10	33	5.93 E+08
DMSO	306	1587.91	65	14045.17	35	6.30 E+08
DMSO	319	1488.44	67	12860.16	33	6.72 E+08
DMSO	326	1293.93	67	11591.00	33	7.73 E+08
DMSO	334.5	1386.79	64	10523.04	36	7.21 E+08
DMSO	344.5	1277.60	66	9867.35	34	7.83 E+08

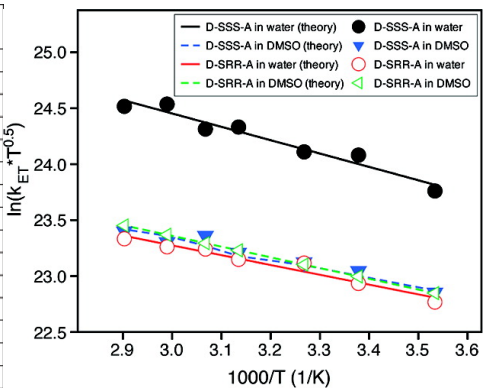

Figure 2-5. Photophysical Data for D-SSS-A (**11**) and D-SRR-A (**12**). Decay law fitting parameters for D-SSS-A and the ET rate plotted versus temperature.

The presence of two time components in the lifetime data as well as two states found in the NMR prompted further interest in DBA scaffold using sing photon counting. However, these experiments required the use of laser equipment with an excitation wavelength of 375 nm. The current DBA scaffold does not absorb at 375 nm and therefore is unsuitable for this analysis. In order to shift the excitation wavelength, a chemical modification was made to the pyrene moiety to affect a bathochromic shift of its absorbance spectra. Previously, a series of pyrene-bridged peptides and pyrene-peptide macrocycles have been shown to possess a sufficient absorbance at 375 nm. [17] Figure 2-6 shows the absorbance spectra and structure of these compounds. According to this

precedent, an additional carboxamide functionality appended to the pyrene moiety on the DBA scaffold will cause the desired bathochromic shift.

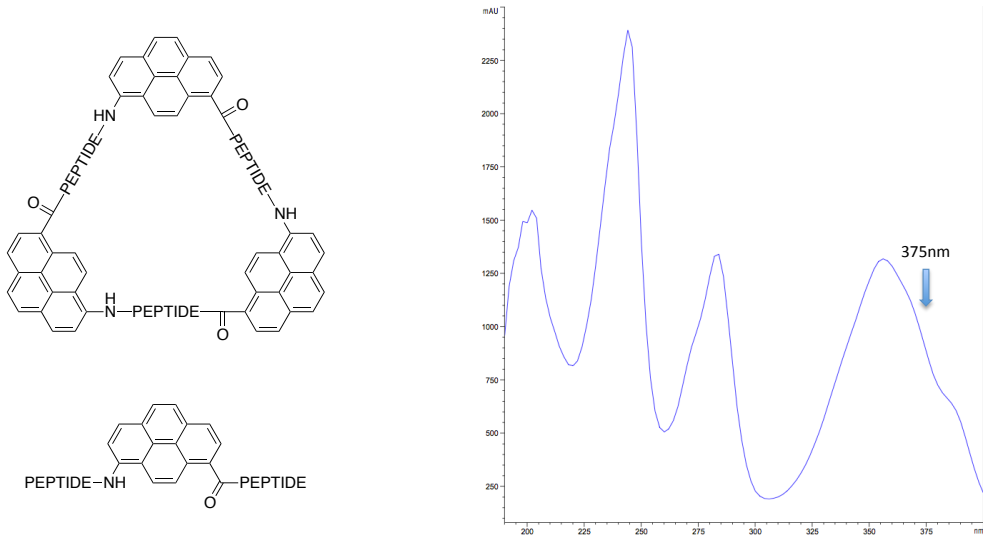

Figure 2-6. 2D structures and absorbance spectra of pyrene containing peptides.

This chemical modification was easily incorporated into the DBA design and was implemented by converting the pyrene-1-carboxylic acid to compound **16**. This was accomplished by first converting the carboxylic acid to the corresponding methyl ester using MeI, Na_2CO_3 in DMF followed by nitration with HNO_3 in Ac_2O at 70°C. The nitration resulted in a mixture of three regioisomers. Separation at this stage was unsuccessful. The mixture was reduced to the free amine using Pd/C with H_2 in THF. Separation at this stage was successful. Three fractions were collected. Fraction 1 contains a single unknown compound we will call X. Fraction 3 contains a single unknown compound Z. Fraction 2 contains a mixture of three unknown compounds X, Y, and Z. Compounds X, Y, and Z correspond to compounds **15a**, **15b**, and **15c**. NMR analysis was conducted to assign each unknown with its regioisomer product.

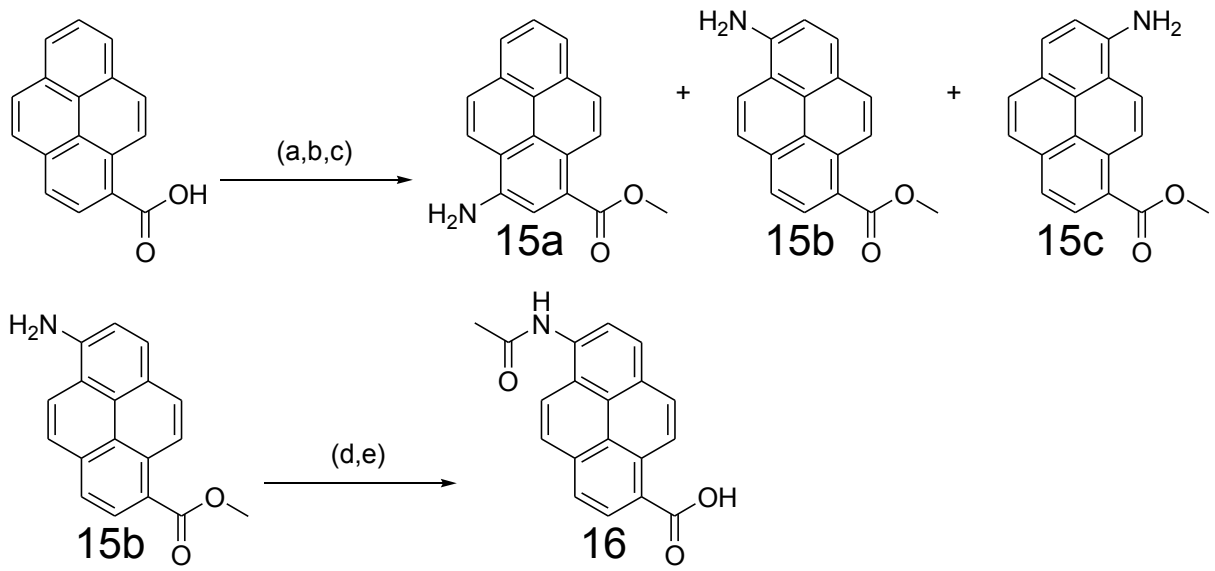

Scheme 2-3. Synthesis of modified pyrene. a) Na_2CO_3, MeI, DMF; b) HNO_3, Ac_2O; c) Pd/C, H_2, THF; d) Ac_2O, DIPEA, DCM; e) KOTMS, DCM

Full NMR analysis, shown in Figure 2-7, was conducted on fractions 1 and 3 in order to assign unknown compounds X, Y, and Z. From the 1H spectrum, it was apparent that unknown Y was the 1,3 disubstituted pyrene (**15a**). The C-2 of the 1,3 disubstituted pyrene would provide a characteristic singlet that was not observed in either 1H spectra. The Cosy spectrum provided assignment of each signal to the four spin systems of pyrene; labeled A, B, C, and D (shown in Figure 2-7). The aniline carbon, which has a very characteristic chemical shift range at 140-150 ppm, was an excellent NMR handle to aid in differentiating between the remaining pyrene regioisomers. The HMBC spectrum showed that the aniline carbon coupled into different spins systems of the pyrene in each fraction. For unknown X, the aniline carbon clearly coupled into the C and D spin systems. This was consistent with the 1,6 disubstituted pyrene (**15b**). For unknown Z, the aniline carbon clearly coupled into the C and B spin systems. This was consistent with the 1,8 disubstituted pyrene (**15c**). The summary of the final assignments is compound **15a** is unknown Y, compound **15b** is

unknown X, and compound **15c** is unknown Z. Compound **15b** was isolated in greatest quantity and was used for the remainder of the synthesis.

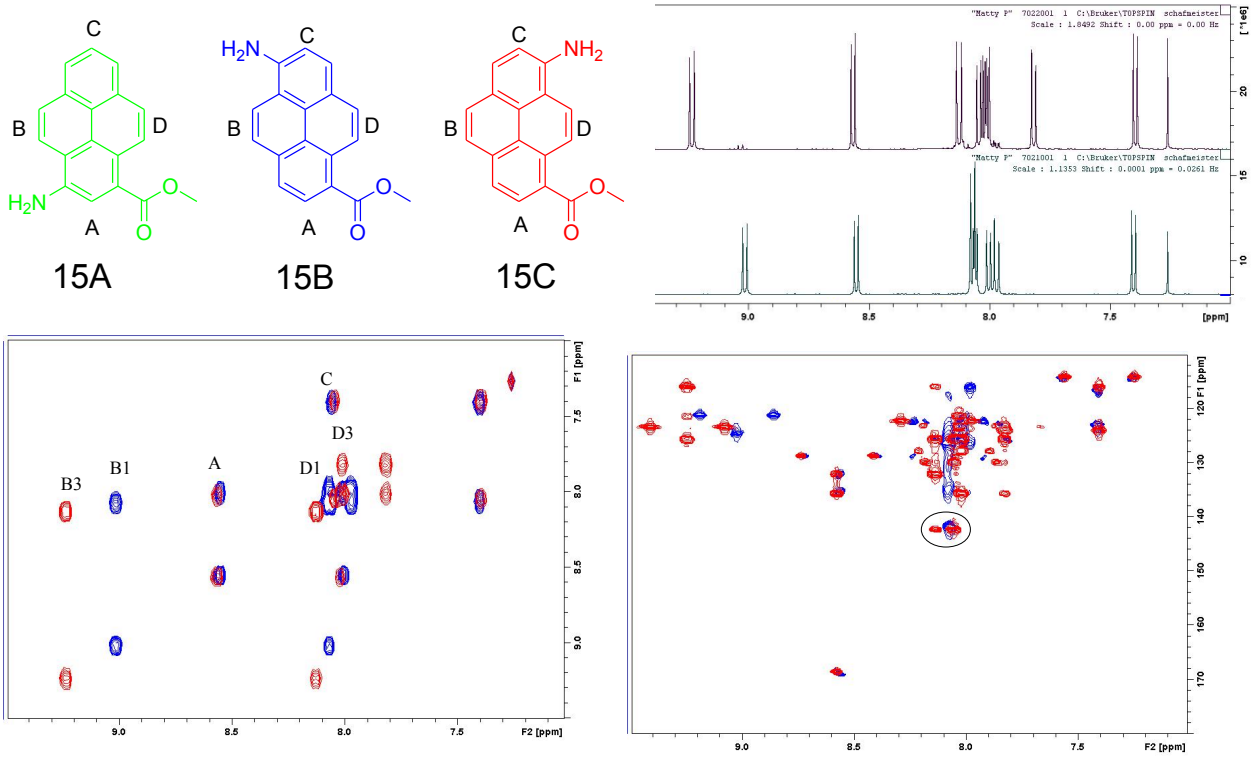

Figure 2-7. NMR analysis of amino pyrene-1-carboxymethyl ester. The 2D structures of the three isomers are shown with labels for the four spin systems. 1H NMR of fractions 1 and 3 are shown as well as overlays of the Cosy and HMBC spectra of fractions 1 and 3. For the overlays, fraction 1 is colored red and fraction 3 is colored blue

To complete the synthesis, compound **15b** was converted to the carboxamide with Ac_2O and DIPEA in DCM followed by hydrolysis of the methyl ester with KOTMS in DCM to yield the compound **16**. Compound **16** was introduced into the DBA scaffold the same as for D-SSS-A and D-SRR-A, as shown in Scheme 2-2. Compound **16** yielded two new DBA molecules: D-SSS-A* (**17**) and D-SRR-A* (**18**), shown in Figure 2-8. Additional experiments using these two DBA scaffolds are ongoing.

D-SSS-A* D-SRR-A*

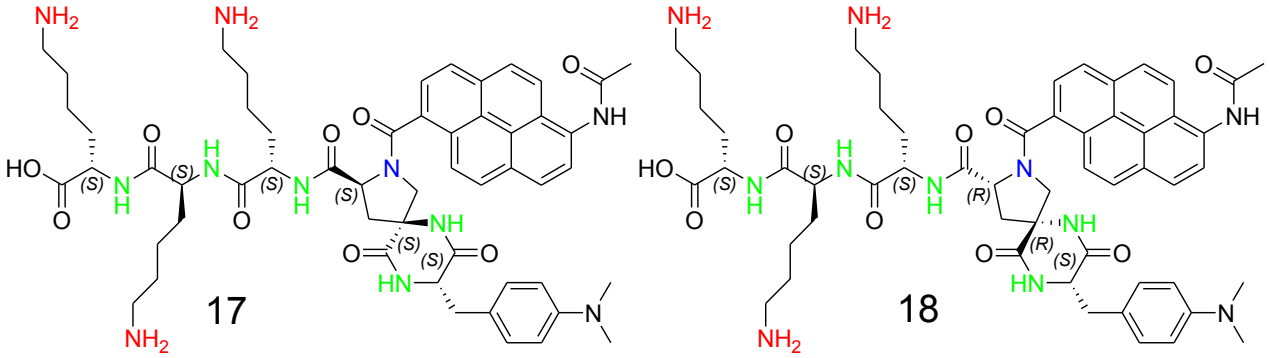

Figure 2-8. 2D Structures of D-SSS-A* (17) and D-SRR-A* (18).

2.3 Conclusion

Two DBA scaffolds were synthesized, one of which possessed a cleft that could accommodate a water molecule for photoinduced electron transfer studies. A 3-fold enhancement of electron transfer rate was observed for the cleft forming DBA in water but not in DMSO and no water-mediated rate enhancement was observed for the non-cleft forming DBA. However, all DBA scaffolds showed two time components in both solvents. In the NMR characterization, two distinct conformations were observed for both DBA scaffolds in both water and DMSO that could be attributed to two amide rotamers. Further studies of this duality can now be conducted with the synthesis of a new modified DBA scaffolds designed to be suitable for single photon counting experiments.

2.4 Eperimental Details

General Methods. Anhydrous N-methylpyrrolidinone, Anhydrous Dimethylformamide, Anhydrous Dichloromethane, Redistilled Diisopropylethylamine, Tetrakis(triphenylphosphine) palladium0, Borane:dimethylamine complex, Diisopropylcarbodiimide, Pyrenecarboxylic acid, Allyl chloroformate, and 37% Formaldehyde solution were purchased from Aldrich. Methanol, Tetrahydrofuran, Triethylamine and Trifluoroacetic acid were purchased from Alfa Aesar. Palladium on Carbon and O-(7-Azabenzotriazole-1-yl)-N, N,N'N'-tetramethyluronium hexafluorophosphate (HATU) were purchased from Genscript, Fmoc-4-nitrophenylanaline was purchased from TCI organics. Fmoc-Lys(Boc)-OH was purchased from Novabiochem. Flash Chromatography was perfored on an ISCO CombiFlash Companion with cartridges filled with Bodman 32-63 D (60.) grade silica gel. Analytical HPLC-MS analysis was performed on a Hewlett-Packard Series 1200 with a Waters Xterra MS C18 column (3.5um packing, 4.6 mm x 100mm) with a solvent system of water/acetonitrile with 0.1% formic acid at a flow rate of 0.8mL/min. Preparatory Scale HPLC purification was performed on a Varian Prostar Prep HPLC with a Waters Xterra column (5um packing, 19mm x 100mm) with a solvent system of water/acetonitrile with 0.1% formic acid at a flow rate of 12mL/min. NMR experiments were performed on a Bruker 500mHz NMR with a chemical shifts (δ) reported relative to DMSO-d6 or CDCl3 residual solvent peaks. HRESIQTOFMS analysis was performed by Ohio State University.

Solution Synthesis

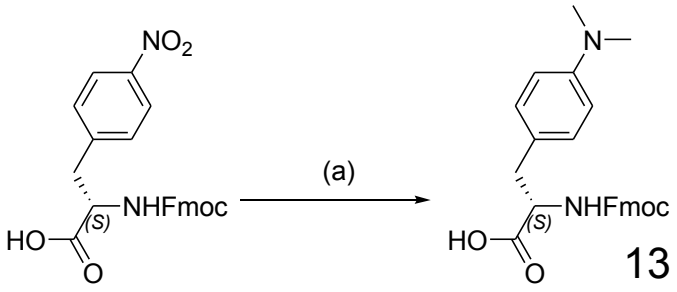

Fmoc-4-nitrophenylalanine a) $CH_2O_{(n)}$, Pd/C, H_2, THF, MeOH

(S)-2-(((9H-fluoren-9-yl)methoxy)carbonylamino)-3-(4-(dimethylamino) phenyl)propanoic acid (13):

To a solution of Fmoc-4-nitrophenylalanine (1g, 2.3mmoles) in THF/MeOH (46mL, 1:1) was added 37% $CH_2O_{(n)}$ (aq) (690uL, 9.2mmoles, 4equiv) followed by Pd/C (69mg). The reaction mixture was then degassed and charged with H_2 (g) and stirred overnight then chromatographed on silica (gradient elution over 16 column volumes from 0-5% MeOH in DCM). The desired fractions were combined and concentrated to yield a yellow solid (860mg, 2.0mmoles, 87%). ^{1}H NMR (500 MHz, rt, $CDCl_3$): δ 9.19 (br s, 1H), 7.77 (d, J = 7.6 Hz, 2H), 7.60 (t, J = 7.0 Hz, 2H), 7.41 (t, J = 7.4 Hz, 7.6 Hz, 2H), 7.32 (t, J = 7.4 Hz, 7.6 Hz, 2H), 7.10 (d, J = 8.2 Hz, 2H), 6.86 (d, J = 8.2 Hz, 2H), 5.53 (d, J = 7.7 Hz, 1H), 4.66 (q, J = 7.3 Hz, 3.0 Hz, 7.3 Hz, 1H), 4.35 (q, J = 7.3 Hz, 3.00 Hz, 7.30 Hz, 1H), 4.22 (t, J = 7.0 Hz, 7.0 Hz, 1H), 3.18 (m, 2H), 2.89 (s, 6H); ^{13}C NMR (125MHz, rt, $CDCl_3$): δ 155,82, 147.80, 143.88, 141.30, 130.53, 127.70, 127.07, 125.25, 125.15, 119.98, 115.57, 66.92, 55.19, 47.18, 42.29, 36.97; LRESIQMS calcd for $C_{26}H_{27}N_2O_4$ ($M + H^+$) 431.1971, measured 431.1967.

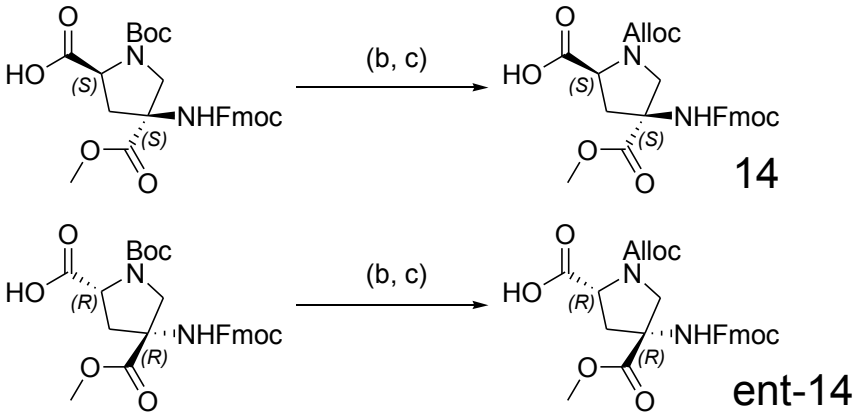

a) TFA, DCM (1:2); b) Alloc-Cl, DIPEA, DCM

(2*S*,4*S*)-4-(((9*H*-fluoren-9-yl)methoxy)carbonylamino)-1-(allyloxycarbonyl)-4-(methoxycarbonyl)pyrrolidine-2-carboxylic acid (14):

To a solution of Pro4ss (**1**) (1g, 1.96mmoles) in DCM (14mL) was added TFA (7mL). The reaction mixture was stirred for 4 hours then concentrated under reduced pressure. The residue was diluted with PhMe and concentrated under reduced pressure and further dried over night under high vacuum. The residue was dissolved in DCM (20mL) and DIPEA (1.03mL, 5.88mmoles, 3equiv) was added followed by Alloc-Cl (230uL, 2.15mmoles, 1.1equiv). The reaction mixture was stirred overnight then diluted with EtOAc. The solution was washed with sat. NH_4Cl (aq) x 3, sat. NaCl (aq) x 2, dried over Na_2SO_4, filtered, and concentrated under reduced pressure. The residue was chromatographed on silica (gradient elution over 16 column volumes from 0-5% MeOH in DCM). The desired fractions were combined and concentrated to yield a yellow solid (914mg, 1.85mmoles, 94%yield). ^{1}H NMR (500 MHz, 365K, DMSO-d6): δ 8.49 (bs, 1H), 8.11 (d, J = 7.5 Hz, 2H), 7.92 (d, J = 7.1 Hz, 2H), 7.64 (t, J = 7.3 Hz, 7.4 Hz, 2H), 7.56 (t, J = 7.3 Hz, 7.2 Hz, 2H), 6.17 (m, 1H), 5.52 (t, J = 16.7 Hz, 16.7 Hz, 1H), 5.43 (dd, J = 10.5 Hz, 17.9 Hz, 10.5 Hz, 1H), 4.77 (m, 2H), 4.54 (m, 4H), 4.29 (dd, J = 11.2 Hz, 24.2 Hz, 11.2 Hz, 1H), 3.82 (s, 3H), 3.80 (m, 1H),

3.11 (m, 1H);); ^{13}C NMR (125MHz, 365K, DMSO-d6): δ 174.8, 171.8, 157.6, 155.6, 155.6, 143.6, 141.0, 133.5, 128.7, 128.4, 128.2, 126.8, 116.4, 67.3, 65.1, 55.0, 54.8, 52.2, 50.9, 37.2; LRESIQMS calcd for $C_{132}H_{138}N_{10}O_{40}$ (M + H^+) 494.1689, measured 494.2.

(2R,4R)-4-(((9*H*-fluoren-9-yl)methoxy)carbonylamino)-1-(allyloxycarbonyl)-4-(methoxycarbonyl)pyrrolidine-2-carboxylic acid (ent-14):

To a solution of Pro4rr (**3**) (1g, 1.96mmoles) in DCM (14mL) was added TFA (7mL). The reaction mixture was stirred for 4 hours then concentrated under reduced pressure. The residue was diluted with PhMe and concentrated under reduced pressure and further dried over night under high vacuum. The residue was dissolved in DCM (20mL) and DIPEA (1.03mL, 5.88mmoles, 3equiv) was added followed by Alloc-Cl (230uL, 2.15mmoles, 1.1equiv). The reaction mixture was stirred overnight then diluted with EtOAc. The solution was washed with sat. NH_4Cl (aq) x 3, sat. NaCl (aq) x 2, dried over Na_2SO_4, filtered, and concentrated under reduced pressure. The residue was chromatographed on silica (gradient elution over 16 column volumes from 0-5% MeOH in DCM). The desired fractions were combined and concentrated to yield a yellow solid (882mg, 1.78mmoles, 91%yield). ^{1}H NMR (500 MHz, 365K, DMSO-d6): δ 8.49 (bs, 1H), 8.11 (d, J = 7.5 Hz, 2H), 7.92 (d, J = 7.1 Hz, 2H), 7.64 (t, J = 7.3 Hz, 7.4 Hz, 2H), 7.56 (t, J = 7.3 Hz, 7.20 Hz, 2H), 6.17 (m, 1H), 5.52 (t, J = 16.7 Hz, 16.7 Hz, 1H), 5.43 (dd, J = 10.5 Hz, 17.9 Hz, 10.5 Hz, 1H), 4.77 (m, 2H), 4.54 (m, 4H), 4.29 (dd, J = 11.2 Hz, 24.2 Hz, 11.2 Hz, 1H), 3.82 (s, 3H), 3.80 (m, 1H), 3.11 (m, 1H);); ^{13}C NMR (125MHz, 365K, DMSO-d6): δ 174.8, 171.8, 157.6, 155.6, 155.6, 143.6, 141.0, 133.5, 128.7, 128.4, 128.2, 126.8, 116.4, 67.3, 65.1, 55.0, 54.8, 52.2, 50.9, 37.2; LRESIQMS calcd for $C_{132}H_{138}N_{10}O_{40}$ (M + H^+) 494.1689, measured 494.2.

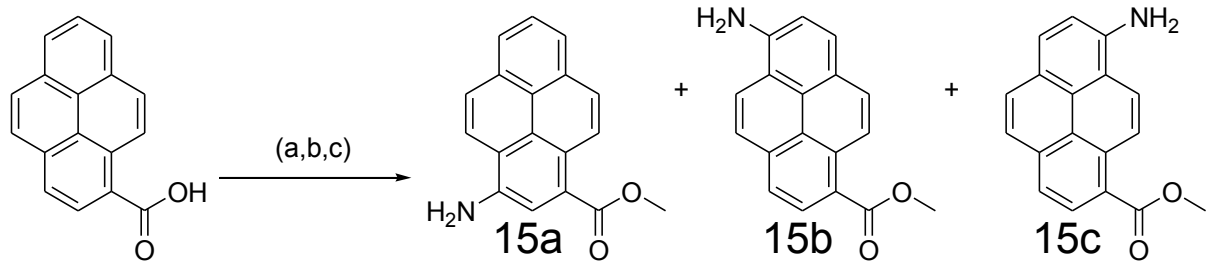

Pyrene-1-carboxylic acid a) Na_2CO_3, MeI, DMF; b) HNO_3, Ac_2O; c) Pd/C, H_2, THF d) Ac_2O, DIPEA, DCM; e) KOTMS, DCM

Methyl 6-aminopyrene-1-carboxylate (15b):

To a solution of Pyrene-1-carboxylic acid (250mg, 1.02mmoles) in DMF (10mL) was added Na_2CO_3 (215mg, 2.04mmoles, 2equiv) followed by MeI (70uL, 1.12mmoles, 1.1equiv). The reaction mixture was stirred overnight then added dropwise to a stirring solution of water (100mL) at 0°C. The precipitate was collected and washed with cold water. The resulting solid was suspended in Ac_2O (10mL) and a 0.4 M HNO3 solution in Ac_2O (5mL, 2.04mmoles, 2equiv) was added. The reaction mixture was heated to 70°C and stirred overnight then concentrated under reduced pressure. The residue was suspended in THF (20mL) and Pd/C (30mg) was added. The reaction mixture was then degassed and charged with H_2 (g) and stirred overnight then chromatographed on silica (isocratic elution of PhMe). The desired fractions were combined and concentrated to yield a red solid (118mg, 429umoles, 42%). ^{1}H NMR (500 MHz, rt, $CDCl_3$): δ 9.03 (d, J=9.1 Hz, 1H), 8.56 (d, J=8.3 Hz, 1H), 8.07 (m, 3H), 8.01 (d, J=8.3 Hz, 1H), 7.98 (d, J=9.1 Hz, 1H), 7.41 (d, J=8.3 Hz, 1H), 4.08 (s, 3H); ^{13}C NMR (125MHz, rt, $CDCl_3$): δ 168.8, 141.8, 135.2, 134.9, 132.3, 128.6, 126.3, 125.7, 125.3, 124.5, 123.0, 122.6, 122.2, 121.1, 117.1, 116.1, 114.3, 52.2; LRESIQMS calcd for $C_{18}H_{13}NO_2$ ($M + H^+$) 276.0946, measured 276.2.

Methyl 3-aminopyrene-1-carboxylate (15a):

Isolated as a mixture of **15a**, **15b**, and **15c** from purification of **15b**.

Methyl 8-aminopyrene-1-carboxylate (15c):

Isolated from purification of **15b**. The desired fractions were combined and concentrated to yield a red solid (53mg, 193umoles, 19%). ^{1}H NMR (500 MHz, rt, $CDCl_3$): δ 9.25 (d, J=10.0 Hz, 1H), 8.57 (d, J=8.6 Hz, 1H), 8.14 (d, J=10.0 Hz, 1H), 8.03 (m, 3H), 7.83 (d, J=8.6 Hz, 1H), 7.40 (d, J=8.6 Hz, 1H), 4.08 (s, 3H); ^{13}C NMR (125MHz, rt, $CDCl_3$): δ 168.5, 142.3, 135.5, 131.9, 129.9, 128.7, 127.9, 125.5, 124.4, 123.8, 123.4, 122.2, 121.4, 115.9, 114.1, 52.1; LRESIQMS calcd for $C_{18}H_{13}NO_2$ (M + H^+) 276.0946, measured 276.2.

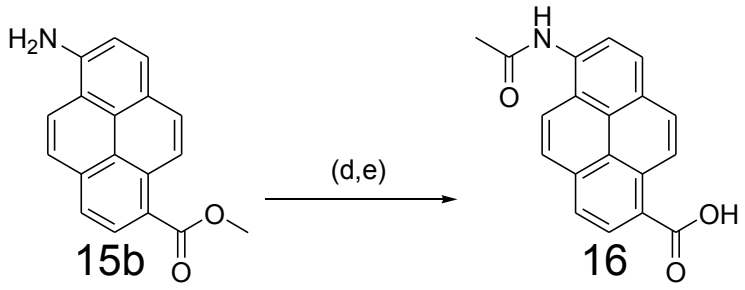

d) Ac_2O, DIPEA, DCM; e) KOTMS, DCM

6-acetamidopyrene-1-carboxylic acid (16):

To a solution of **15b** (110mg, 400umoles) in DCM (8mL) was added Ac_2O (1mL) followed by TEA (1mL). The reaction was stirred overnight then concentrated under reduced pressure. The residue was diluted in THF (20mL) and KOTMS (513mg, 4mmoles, 10equiv) was added. The reaction mixture was stirred overnight then chromatographed by reverse-phase chromatography (gradient elution over 18 column volumes from water (0.1% formic acid) to MeCN in water (0.1% formic acid). Desired fractions were combined and freeze-dried to a white powder (910mg, 300umoles, 75%). ^{1}H NMR (500 MHz, rt, DMSO-D6): δ 10.41 (s, 1H), 9.18 (d, J=9.0 Hz, 1H), 8.59 (d, J=9.0 Hz, 1H), 8.46 (d, J=9.0, 1H), 8.33 (m, 5H),

2.26 (s, 3H); ^{13}C NMR (125MHz, rt, $CDCl_3$): δ 167.7, 133.6, 130.4, 128.9, 128.7, 127.4, 126.8, 126.1, 124.9, 124.4, 123.9, 123.7, 123.0; LRESIQMS calcd for $C_{19}H_{13}NO_3$ ($M + H^+$) 304.0895, measured 305.1.

Solid Phase Synthesis

General procedure (A): Attachment to Trityl resin

To a solution of the amino acid (10 equivalents based on resin loading) in DCM (3mL/mmole of amino acid) was added DIPEA (5 equivalents based on resin loading). The reaction mixture was added to a portion of resin in a solid phase reactor. The reaction mixture was stirred for 4 hours. The resin was filtered and washed with DMF, DCM, IPA, DCM and DMF.

General procedure (B): HATU coupling

To a solution of amino acid (3 equivalents based on resin loading) and HATU (3 equivalents based on resin loading in NMP (5mL/mmole of amino acid) was added DIPEA (6 equivalents based on resin loading). The reaction mixture was agitated for 5 minutes then added to a pre-swelled (with DMF) portion of resin in a solid phase reactor and stirred for 45 minutes. The resin was filtered and washed with DMF, DCM, IPA, DCM and DMF.

General procedure (C): Fmoc deprotection

A solution of 20% of piperidine in DMF (15mL/mmole based on resin loading) was added to a pre-swelled (with DMF) portion of resin in a solid phase reactor and stirred for 15 minutes. The resin was filtered and washed with DMF, DCM, IPA, DCM and DMF.

General procedure (D): Alloc deprotection

A solution of borane:dimethylamine complex (6 equivalents based on resin loading) in DCM (10mL/mmole based on resin loading) was added to a pre-swelled (with DMF)

portion of resin in a solid phase reactor and stirred for 5 minutes. To this solution was added a solution of tetrakis(triphenylphosphine)palladium(0) (0.1 equivalents based on resin loading) in DCM (10mL/mmole based on resin loading). The reaction mixture was stirred for 1 hour. The resin was filtered and washed with DMF, DCM, IPA, DCM and DMF.

General procedure (E): Liberation from Wang resin

A solution of 5% TIPS and 5% water in TFA (25 mL/mmole based on resin loading was added to a portion of resin (successively washed with DCM and MeOH, and thoroughly dried under vacuum) and stirred for 4 hours. The resin was filtered and rinsed with TFA. The filtrate was concentrated, reconstituted in 50% MeCN in water (0.1% formic acid) and freeze-dried.

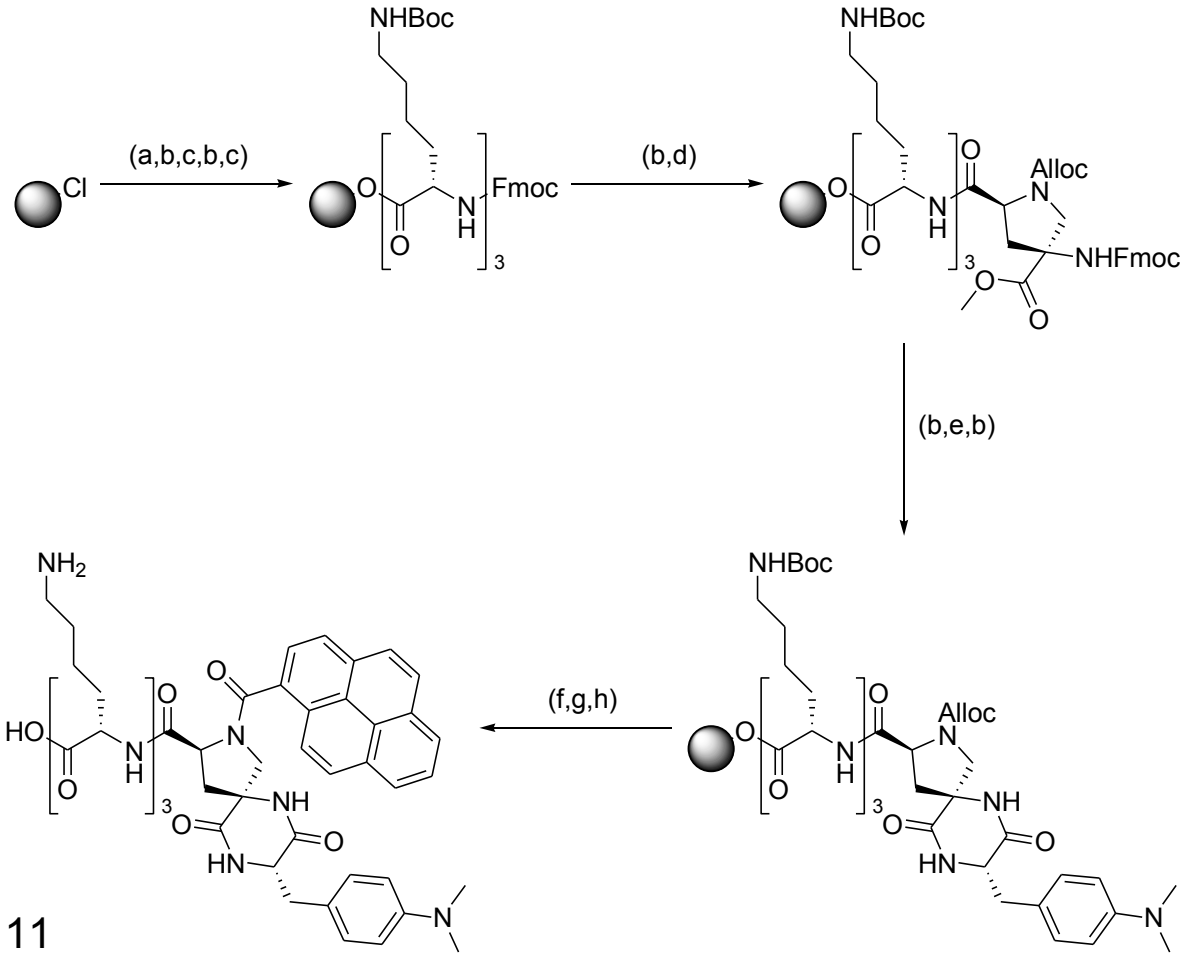

D-SSS-A (11)

Trityl resin (100mg, 100umoles loading) was placed in a 4mL solid phase reactor. Fmoc-Lys(Boc)-OH (703mg, 1.5mmoles) was attached according to general procedure (A) using DCM (4.5mL) and DIPEA (116uL, 750umoles). The terminal Fmoc group was removed according to general procedure (C) using 20% piperidine in DMF (2.25mL).

Fmoc-Lys(Boc)-OH (211mg, 450umoles) was coupled according to general procedure (B) using HATU (171mg, 450umoles), NMP (2.25mL), and DIPEA (156uL, 900umoles). The terminal Fmoc group was removed according to general procedure (C) using 20% piperidine in DMF (2.25mL).

Fmoc-Lys(Boc)-OH (211mg, 450umoles) was coupled according to general procedure (B) using HATU (171mg, 450umoles), NMP (2.25mL), and DIPEA (156uL, 900umoles). The terminal Fmoc group was removed according to general procedure (C) using 20% piperidine in DMF (2.25mL).

14 (223mg, 450umoles) was coupled according to general procedure (B) using HATU (171mg, 450umoles), NMP (2.25mL), and DIPEA (156uL, 900umoles). The terminal Fmoc group was removed according to general procedure (C) using 20% piperidine in DMF (2.25mL).

Fmoc-DMA-OH (194mg, 450umoles) was coupled according to general procedure (B) using HATU (171mg, 450umoles), NMP (2.25mL), and DIPEA (156uL, 900umoles). The terminal Fmoc group was removed according to general procedure (C) using 20% piperidine in DMF (2.25mL) and the reaction time was extended to 2 hour.

The Alloc group was removed according to general procedure (D) using borane:dimethylamine complex (53mg, 900umoles) in DCM (2.5mL) and tetrakis(triphenylphosiphine)palladium(0) (17mg, 15umoles) in DCM (2mL). Pyrene-1-carboxylic acid (111mg, 450umoles) was coupled according to general procedure (B) using HATU (171mg, 450umoles), NMP (2.25mL), and DIPEA (156uL, 900umoles).

11 was liberated from the resin according to general procedure (E) using 3.75 mL of the cleavage cocktail. The residue was reconstituted in 50% MeCN in water (0.1% formic acid) and purified by reverse-phase chromatography (gradient elution over 30 minutes from water (0.1% formic acid) to 50% MeCN in water (0.1% formic acid). Desired fractions were combined and freeze-dried to yield a white powder.

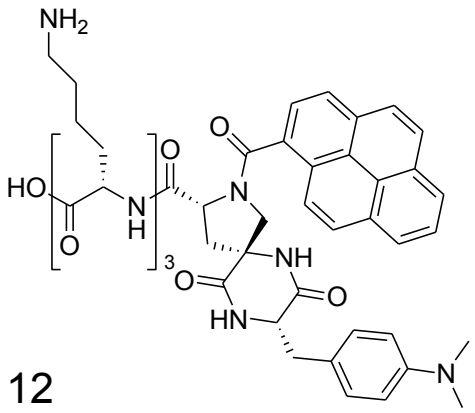

12

D-SRR-A (12):

Trityl resin (100mg, 100umoles loading) was placed in a 4mL solid phase reactor. Fmoc-Lys(Boc)-OH (703mg, 1.5mmoles) was attached according to general procedure (A) using DCM (4.5mL) and DIPEA (116uL, 750umoles). The terminal Fmoc group was removed according to general procedure (C) using 20% piperidine in DMF (2.25mL).

Fmoc-Lys(Boc)-OH (211mg, 450umoles) was coupled according to general procedure (B) using HATU (171mg, 450umoles), NMP (2.25mL), and DIPEA (156uL, 900umoles). The terminal Fmoc group was removed according to general procedure (C) using 20% piperidine in DMF (2.25mL).

Fmoc-Lys(Boc)-OH (211mg, 450umoles) was coupled according to general procedure (B) using HATU (171mg, 450umoles), NMP (2.25mL), and DIPEA (156uL, 900umoles). The terminal Fmoc group was removed according to general procedure (C) using 20% piperidine in DMF (2.25mL).

Ent-14 (223mg, 450umoles) was coupled according to general procedure (B) using HATU (171mg, 450umoles), NMP (2.25mL), and DIPEA (156uL, 900umoles). The terminal Fmoc group was removed according to general procedure (C) using 20% piperidine in DMF (2.25mL).

Fmoc-DMA-OH (194mg, 450umoles) was coupled according to general procedure (B) using HATU (171mg, 450umoles), NMP (2.25mL), and DIPEA (156uL, 900umoles). The terminal Fmoc group was removed according to general procedure (C) using 20% piperidine in DMF (2.25mL) and the reaction time was extended to 2 hour.

The Alloc group was removed according to general procedure (D) using borane: dimethylamine complex (53mg, 900umoles) in DCM (2.5mL) and tetrakis (triphenylphosiphine) palladium(0) (17mg, 15umoles) in DCM (2mL). Pyrene-1-carboxylic acid (111mg, 450umoles) was coupled according to general procedure (B) using HATU (171mg, 450umoles), NMP (2.25mL), and DIPEA (156uL, 900umoles).

12 was liberated from the resin according to general procedure (E) using 3.75 mL of the cleavage cocktail. The residue was reconstituted in 50% MeCN in water (0.1% formic acid)

and purified by reverse-phase chromatography (gradient elution over 30 minutes from water (0.1% formic acid) to 50% MeCN in water (0.1% formic acid). Desired fractions were combined and freeze-dried to yield a white powder.

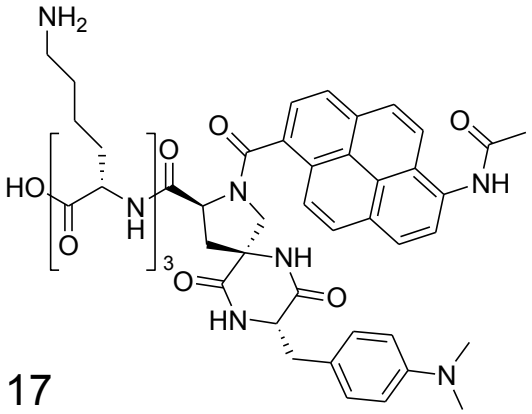

17

D-SSS-A* (17):

Trityl resin (100mg, 100umoles loading) was placed in a 4mL solid phase reactor. Fmoc-Lys(Boc)-OH (703mg, 1.5mmoles) was attached according to general procedure (A) using DCM (4.5mL) and DIPEA (116uL, 750umoles). The terminal Fmoc group was removed according to general procedure (C) using 20% piperidine in DMF (2.25mL).

Fmoc-Lys(Boc)-OH (211mg, 450umoles) was coupled according to general procedure (B) using HATU (171mg, 450umoles), NMP (2.25mL), and DIPEA (156uL, 900umoles). The terminal Fmoc group was removed according to general procedure (C) using 20% piperidine in DMF (2.25mL).

Fmoc-Lys(Boc)-OH (211mg, 450umoles) was coupled according to general procedure (B) using HATU (171mg, 450umoles), NMP (2.25mL), and DIPEA (156uL, 900umoles). The terminal Fmoc group was removed according to general procedure (C) using 20% piperidine in DMF (2.25mL).

14 (223mg, 450umoles) was coupled according to general procedure (B) using HATU (171mg, 450umoles), NMP (2.25mL), and DIPEA (156uL, 900umoles). The terminal Fmoc group was removed according to general procedure (C) using 20% piperidine in DMF (2.25mL).

Fmoc-DMA-OH (194mg, 450umoles) was coupled according to general procedure (B) using HATU (171mg, 450umoles), NMP (2.25mL), and DIPEA (156uL, 900umoles). The terminal Fmoc group was removed according to general procedure (C) using 20% piperidine in DMF (2.25mL) and the reaction time was extended to 2 hour.

The Alloc group was removed according to general procedure (D) using borane:dimethylamine complex (53mg, 900umoles) in DCM (2.5mL) and tetrakis(triphenylphosiphine)palladium(0) (17mg, 15umoles) in DCM (2mL). **16** (111mg, 450umoles) was coupled according to general procedure (B) using HATU (171mg, 450umoles), NMP (2.25mL), and DIPEA (156uL, 900umoles).

17 was liberated from the resin according to general procedure (E) using 3.75 mL of the cleavage cocktail. The residue was reconstituted in 50% MeCN in water (0.1% formic acid) and purified by reverse-phase chromatography (gradient elution over 30 minutes from water (0.1% formic acid) to 50% MeCN in water (0.1% formic acid). Desired fractions were combined and freeze-dried to yield a white powder.

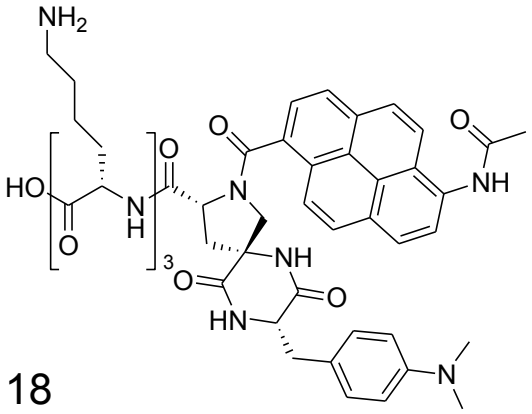

18

D-SRR-A* (18):

Trityl resin (100mg, 100umoles loading) was placed in a 4mL solid phase reactor. Fmoc-Lys(Boc)-OH (703mg, 1.5mmoles) was attached according to general procedure (A) using DCM (4.5mL) and DIPEA (116uL, 750umoles). The terminal Fmoc group was removed according to general procedure (C) using 20% piperidine in DMF (2.25mL).

Fmoc-Lys(Boc)-OH (211mg, 450umoles) was coupled according to general procedure (B) using HATU (171mg, 450umoles), NMP (2.25mL), and DIPEA (156uL, 900umoles). The terminal Fmoc group was removed according to general procedure (C) using 20% piperidine in DMF (2.25mL).

Fmoc-Lys(Boc)-OH (211mg, 450umoles) was coupled according to general procedure (B) using HATU (171mg, 450umoles), NMP (2.25mL), and DIPEA (156uL, 900umoles). The terminal Fmoc group was removed according to general procedure (C) using 20% piperidine in DMF (2.25mL).

Ent-14 (223mg, 450umoles) was coupled according to general procedure (B) using HATU (171mg, 450umoles), NMP (2.25mL), and DIPEA (156uL, 900umoles). The terminal Fmoc group was removed according to general procedure (C) using 20% piperidine in DMF (2.25mL).

Fmoc-DMA-OH (194mg, 450umoles) was coupled according to general procedure (B) using HATU (171mg, 450umoles), NMP (2.25mL), and DIPEA (156uL, 900umoles). The terminal Fmoc group was removed according to general procedure (C) using 20% piperidine in DMF (2.25mL) and the reaction time was extended to 2 hour.

The Alloc group was removed according to general procedure (D) using borane:dimethylamine complex (53mg, 900umoles) in DCM (2.5mL) and tetrakis(triphenylphosiphine)palladium(0) (17mg, 15umoles) in DCM (2mL). **16** (111mg, 450umoles) was coupled according to general procedure (B) using HATU (171mg, 450umoles), NMP (2.25mL), and DIPEA (156uL, 900umoles).

18 was liberated from the resin according to general procedure (E) using 3.75 mL of the cleavage cocktail. The residue was reconstituted in 50% MeCN in water (0.1% formic acid) and purified by reverse-phase chromatography (gradient elution over 30 minutes from water (0.1% formic acid) to 50% MeCN in water (0.1% formic acid). Desired fractions were combined and freeze-dried to yield a white powder

2.5 References

[1] Latt, S.A.; Cheung, H. T.; Blout, E. R.; *J. Am. Chem. Soc*. **1965**, 87, 995.

[2] Stryer, L.; Haugland, R. P., Proc. *Natl. Acad. Sci*. **1967**, 58, 720.

[3] Zimmt, M. B.; Waldeck, D. H. *J. Phys. Chem. A*. **2003**, *107*, 3580.

[4] Read, I.; Napper, A.; Kaplan, R.; Zimmt, M. B.; Waldeck, D. H. *J. Am*. *Chem. Soc.* **1999**, *121*, 10976.

[5] Kumar, K.; Kurnikov, I.; Beratan, D. N.; Waldeck, D. H.; Zimmt, M. B. *J. Phys. Chem. A*. **1998**, **102**, 5529.

[6] Beratan, D. N.; Onuchic, J. N. *Protein Electron Transfer*; Bendall, D. S., Ed.; BIOS Scientific Publishers Ltd.: Oxford, 1996; p 23.

[7] Berg, J. M..; Stryer, L.; Tymoczko J. L. *Biochemistry*, 5th Ed.; Freeman: New York, 2002.

[8] Page, C. C.; Moser, C. C.; Chen, X.; Dutton, P. L. *Nature* **1999**, *402*, 47.

[9] Lin, J.; Balabin, I. A.; Beratan, D. N. *Science* **2005**, 310, 1311.

[10] Migliore, A.; Corni, S.; Felice, R. D.; Molinari, E. *J. Phys. Chem. B* **2006**, *110*, 23796.

[11] Miyashita, O.; Okamura, M. Y.; Onuchic, J. N. *Proc. Natl. Acad. Sci*. *U.S.A*. **2005**, *102*, 3558.

[12] Wenger, O.S.; Leigh, R. M.; Villahermosa, H. B.; Gray, H. B.; Winkler, J. R. *Science*, **2005**, *307*, 99.

[13] Ponce, H. B.; Gray, H. B.; Winkler, J. R. *J. Am. Chem. Soc*. **2000**, *122*, 8187.

[14] Nadeau, J. M.; Liu, M.; Waldeck, D. H.; Zimmt, M. B. *J. Am. Chem. Soc*. **2003**, *125*, 15973.

[15] Galoppini, E.; Fox, M. A. *J. Am. Chem. Soc.* **1996**, *118*, 2299.

[16] Pornsuwan, S.; Bird, G.; Schafmeister, C. E.; Saxena, S.; *J. Am. Chem. Soc.* 2006, *128*, 3876–3877.

[17] Yoshida, K.; Kawamura, S.; Morita, T.; Kimura, S. JACS, **2006**, 128, 8034-8041.

3.0 Acceleration of an aromatic Clasien rearrangement via a designed spiroligozyme catalyst that mimics the ketosteroid isomerase catalytic dyad

Chapter 3 details our use of bis-amino acids for presenting a phenol and a benzoic acid moiety on for catalysis of an aromatic Claisen rearrangement of a prenyl coumarin. Highlights of this work are the first demonstration of a synthetic Claisen catalyst based on oxygen hydrogen bonding. A 58-fold reactivity enhancement was observed for the best computational design. Several catalysts were investigated experimentally and computationally for structure function analysis.

A portion of this work was published in:

J. Am. Chem. Soc., **2014**, *136* (10), pp 3817-3827

Acknowledgements: Dr. Silvia Osuna executed all advanced theoretical experiments.

3.1 Introduction

One century after its discovery,[2] the [3,3]-sigmatropic rearrangement of allyl vinyl ethers (i.e. the Claisen rearrangement) continues to be extensively investigated and applied in the synthesis of natural products and complex organic molecules.[3,4] Many efforts have been devoted to develop small molecule- and bio-catalysts for this synthetically powerful reaction.[5,6] Attractive non-covalent interactions are responsible for much of the rate accelerations and stereoselectivities observed in enzyme catalysis, and active site residues can stabilize the transition state by electrostatic and non-covalent interactions.[7] A variety of dual hydrogen-bond donor organocatalysts such as ureas, thio-ureas, guanidinium groups and bis-imidazoliums have been reported in the literature for Claisen rearrangements.[6,8-13] Some biological catalysts have also been identified,[14-16] and de novo computational design strategies for developing an aromatic Claisen biocatalyst have been carried out.[17] We are developing a new approach to the development of organocatalysts called "spiroligozymes" wherein we use transition state modeling to identify constellations of reactive functional groups and then build those functional groups onto a spiroligomer scaffold to see if they can act as organocatalysts.[18] In this manuscript, we describe the design and synthesis of a series of bis-amino acid monomers fused to amino acids through diketopiperazines, that accelerate the Claisen rearrangement of 1,1-dimethylallyl coumarin. This paper reports the successful mimicry of the catalytic dyad of bacterial ketosteroid isomerase (KSI) in a small spiroligozyme and the catalysis of an aromatic Claisen rearrangement of a 1,1-dimethylallyl coumarin.

Aromatic Claisen rearrangements are typically performed in the temperature range of 180-225ºC,[19] and proceed through a concerted pericyclic pathway followed by a

keto/enol tautomerization that restores aromaticity. The cyclic transition state of the Claisen rearrangement is key for understanding a number of phenomena. These include the effect of solvent on the rate of the reaction,[20-27] substituent effects, and stereoselectivity.[4] There is one well-established enzyme-catalyzed Claisen rearrangement, the chorismate to prephenate transformation catalyzed by chorismate mutase.[28-33] The Claisen rearrangement of O-prenylated tyrosines in a prenyltransferase from the TruF enzyme family has also been proposed,[16] and catalytic antibodies have been developed for the chorismate to prephenate conversion.[34-36]

Considerable acceleration of the Claisen rearrangement can be achieved employing hydrogen-bonding solvents, especially water.[25,26,28,37-40] In 1987, Carpenter and coworkers first reported the acceleration of the Claisen rearrangement of chorismic acid and related compounds in aqueous media.[28] The rate of the aromatic Claisen rearrangement of allyl naphthyl ether was also increased in aqueous suspensions relative to other organic solvents such as toluene, dimethylformamide, acetonitrile and methanol.[41] Sharpless reported “on-water” catalysis of a Diels-Alder reaction and aromatic Claisen rearrangement. Several examples from his lab illustrated the substantial rate acceleration of the reactions when insoluble reactants were stirred in aqueous suspension. This “on water” catalysis has prompted several computational studies to unravel the origin of the rate acceleration in water and hydrogen-bonding solvents.[20,21,26,28,38,42] It was found that the aqueous acceleration of the Claisen rearrangement is due to a greater stabilization of the transition state by specific interactions with first shell solvent molecules.[17,38,43-45] Jorgensen and coworkers computationally studied the acceleration of the Claisen rearrangement in water. The model

consisted of two explicit water molecules around the core heteroatom of the allyl vinyl ether.[21]

Curran et al. discovered that dual hydrogen-bonding catalysts such as ureas and thioureas accelerate the Claisen rearrangement and measured modest rate accelerations using NMR experiments.[9] In addition, protonated catalysts including those based on guanidinium,[11] quinolinium thioamide,[46] and ammonium[26,47] structures were also studied. The latter positively charged catalysts tend to activate electrophiles more strongly than the neutral compounds.[10] Jacobsen and co-workers have developed diphenylguanadinium salts as stereoselective Claisen rearrangement catalysts for a variety of substituted allyl vinyl ethers and β-ketoester derivatives.[11,13] The mechanism by which the guanidinium catalysts promote the Claisen rearrangement was also studied both experimentally and theoretically.[6,12] The catalysis is mainly achieved by stabilization of the developing negative charge on the oxallyl fragment, and by a secondary attractive interaction between the π-system of the catalyst and the partially positive allyl cation fragment.[12] Kozlowski and co-workers designed a bisamidinium catalyst salt able to catalyze the Claisen rearrangement through a two-point hydrogen bonding stabilization of the negatively charged ether oxygen in the transition state.[8]

The most prominent biological example of a Claisen rearrangement is the enzyme Chorismate mutase, which catalyzes the Claisen rearrangement of chorismate to prephenate more than a million fold relative to the uncatalyzed process.[15] Hilvert and co-workers have also studied the enzyme-catalyzed Cope rearrangement of carbachorismate to carbaprephenate in the enzyme Bacillus subtilis chorismate mutase (BsCM).[14] They showed that a positively charged residue at position 88 or 90 is essential for stabilization of

the transition state of the enzymatic chorismate rearrangement. [14] Borden and Houk studied models for this rearrangement and tested differents theozymes to determine the effect of different side chains in chorismate mutase.[48] Bertran et al. performed a QM/MM study where two different transition states were located for the chorismate conversion to prephenate. It was found that the enzyme stabilizes one of the transition states (TS) by means of hydrogen bonding interactions, while the other TS located, corresponded to the preferred one in vacuum and in water. [49] They found that aqueous solution and BsCM active site environments reduce the free energy barriers more than in the gas phase for both reactions. The catalytic effect was mainly attributed to the enhanced electrostatic stabilization of the transition state relative to the starting substrate in the Claisen rearrangement.[50]

Very recently, LynF, a prenyltransferase from the TruF enzyme family was characterized. [16] This enzyme performs O-prenylation of tyrosine, serine and threonine in cyclic peptides. It was found that at physiological temperature and in aqueous buffer, O-prenylated tyrosine derivatives undergo spontaneous Claisen rearrangements.

In recent years, novel enzyme catalysts for the Kemp elimination,[51,52] retro-aldol[53] and Diels-Alder[54] reactions have been designed, making use of the so-called "Inside-Out" approach. The first step of this protocol involves quantum mechanical calculations of the ideal arrangement of catalytic groups around the transition state of a reaction; these computed complexes are called theozymes (short for theoretical enzymes).[55-57] Theozymes serve as models for active site structures and for the prediction of activation barriers relative to the uncatalyzed reaction in aqueous solution. The arrangement of functional groups in the theozyme geometry is then incorporated into

protein scaffolds from the Protein Data Bank[58] using the computational package RosettaMatch. [59] The active sites of the generated proteins are then minimized and repacked, and amino acids in the vicinity of the active site are mutated to stabilize the ideal transition state geometry. This process is performed using the RosettaDesign package. [60,61] The Inside-Out approach has been satisfactorily applied in the above-mentioned cases (Kemp elimination, retro-Aldol and Diels-Alder reaction), but it has some important limitations. Up until now, most active designed enzymes still perform quite poorly in comparison with the natural existing enzymes (i.e. natural enzymes have average kcat/kuncat of ~1011 whereas artificial enzymes developed through computational modeling and directed evolution have k_{cat}/k_{uncat} values that range from 102 to 105). [52-54,62] In part, this is due to the difficulty of designing a protein with the same ideal geometry of functional groups as present in the theozyme.

The design and testing of small-molecule "enzyme mimics" has been a tempting but frustrating target for organic chemists,[63-67] and occasional success has been reported.[10,68,69] We conceived the melding of the Inside-Out approach with our recent successes in spiroligozyme syntheses to mount catalytic groups from theozymes on a spiroligomer scaffold.[70] Spiroligomers are shape-programmable macromolecules constructed by assembling stereochemically pure, cyclic, functionalized bis-amino acids through pairs of amide bonds to create rigidified scaffolds that present functional groups in controlled three-dimensional constellations by virtue of the sequence, shape and stereochemistry inherent in each chiral building block.[71-73] Previously, spiroligomers have been utilized as catalysts for the aldol reaction and transesterification

reaction.[18,70] We now report a combined computational and experimental approach to use spiroligozymes as catalysts for the aromatic Claisen rearrangement.

3.2 Results and Discussion

Bacterial Ketosteroid Isomerase (KSI) is heavily utilized as a model system for investigating fundamental aspects of enzyme catalysis.[1,74,75] Its natural function is the isomerization of the position of a double bond in steroids. The mechanism involves a general base that deprotonates the steroid forming a dienolate, which is stabilized via hydrogen bonding with a tyrosine-16 residue and a protonated aspartic acid-104 residue (see Figure 1a). The stabilized intermediate is reprotonated and the double bond isomerized. The hydrogen bonding catalytic dyad was considered a promising modality for the stabilization of the growing negative charge in the transition state of the Claisen rearrangement (Figure 1). It was proposed by Gerlt and Gassman that the formation of short, strong hydrogen bonds (SSHB, also called low-barrier hydrogen bonds LBHB) between the KSI oxyanion hole and the reaction intermediate stabilizes the transition state of the reaction.[76,77] There has been an intense debate about the role of SSHBs in enzyme catalysis.[78,79]

We designed a series of bio-inspired spiroligozyme catalysts that display a carboxylic acid and a phenol on a spiroligomer backbone that resembles the hydrogen bonding catalytic dyad of KSI (see Figure 1b). The use of a phenol and carboxylic acid is a stark departure from the currently utilized organocatalysts for the Claisen rearrangement, which generally rely on N-H hydrogen-bond donors. The optimized theozyme for the aromatic Claisen rearrangement using the KSI catalytic dyad (i.e. Asp/Tyr, see Figure 1b) suggests that a 105 fold acceleration with respect to the background reaction could be

achieved (at M06-2X/6-311+G(d,p)//M06-2X/6-31G(d) and in CPCM implicit solvation for CH2Cl2 with e = 4).

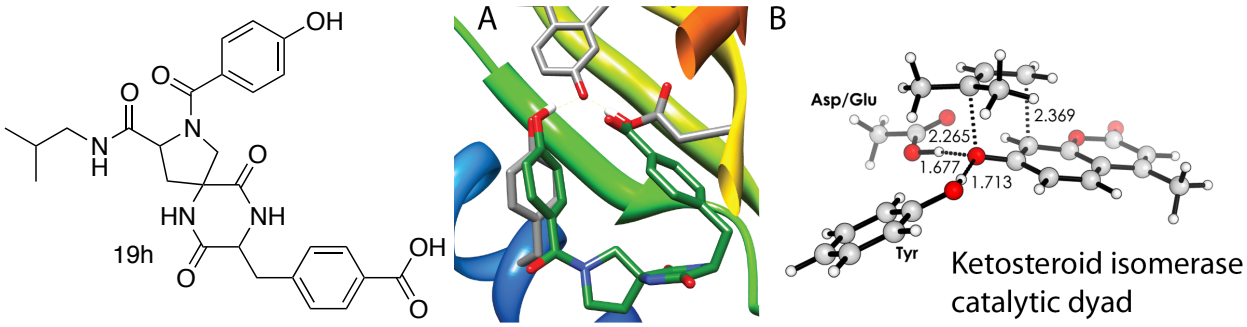

Figure 3-1. (a) Molecular model overlay of the active site of KSI (pdb code 3OWU[1]) with the spiroligomer mimetic 19h. KSI is displayed as a rainbow ribbon with Y16 and D103 shown in grey. Equilenin is bound and also shown in grey. The spirocyclic catalyst 19H is displayed as dark green and is overlayed matching the oxygens of the catalytic residues. (b) The theoretical enzyme model for the KSI catalytic dyad.

Selection of the scaffold to tether the catalytic residues was accomplished by matching carboxylic acid/phenol functionalized Amber 94[80] minimized spiroligomer structural motifs that we have synthetic access to against the crystal structure data for KIS as shown in Figure 1a (pdb code 3OWU).1 A scaffold previously used for studying electron transfer in water was selected as a starting point for further optimization.[81] The scaffold features a single bis-amino acid building block with one functional group introduced via a 2,5-dioxopiperazine (DKP) ring and the other introduced via amide linkage at the pyrrolidine nitrogen forming a well defined cleft between the two catalytic residues.

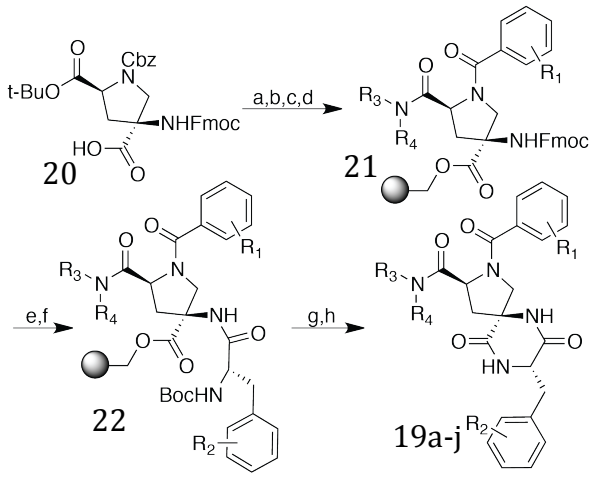

Scheme 3-1. Solid phase assembly of Claisen catalysts 19a-j. a) HMBA Resin (1.1eq), MSNT (2eq), NMI (2eq), DCM (0.1M); b) 33% HBr in AcOH/DCM (1:1, 0.1M); c) Benzoic Acid derivative (3eq), HATU (3eq), DIPEA (6eq), NMP (0.2M); d) Substituted Amine (6eq), PyAOP (3eq), NMP (0.2M); (e) 20% Piperidine in DMF (0.1M); f) N-Boc-Amino Acid (3eq), HATU (3eq), DIPEA (6eq), NMP (0.2M); g) TFA/DCM (1:1, 0.1M); h) 10% DIPEA in MeCN (0.05M).

A series of molecules of this scaffold type were synthesized using solid phase synthesis on HMBA resin (Scheme 1).[82] The bis-amino acid[83] **20** was attached to HMBA resin with MSNT and NMI in DCM. The benzyl carbamate and *tert*-butyl ester were then removed by treatment with 33% HBr in AcOH as a 1:1 volumetric mixture with DCM. This treatment causes acetylation of all remaining hydroxyl groups on the resin. The benzoic acid derivative was introduced using HATU and DIPEA in NMP. The C-2 carboxylic acid was converted to an amide using PyAOP and the amine R_3R_4NH in NMP to form the resin bound intermediate **21**. The Fmoc group was removed using a 20% solution of piperidine in DMF. The phenylalanine derivative was then introduced using HATU and DIPEA in NMP to produce intermediate **22**. The tert butyl carbamate, ester and ether were removed with treatment with a 1:1 volumetric mixture of TFA and DCM. The DKP was closed and subsequent cleavage from the resin was affected with a 10% solution of DIPEA

in MeCN. Purification with C18 reverse phase HPLC yielded the pure catalysts **19a-j** in 60-70% isolated yields (Table 1).

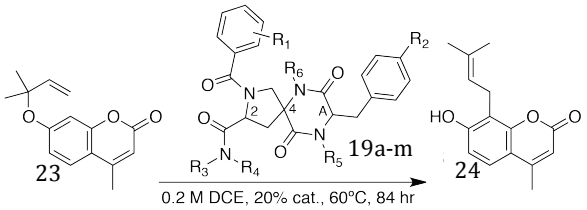

Entry	Catalyst	C-2	C-4	A	R_1	R_2	R_3/R_4	R_5	R_6	k_{rel}
1	none	-	-	-	-	-	-	-	-	1
2	19a	*S*	*S*	*S*	4-COOH	OH	iBu/H	H	H	11
3	19b	*S*	*S*	*S*	4-COOH	OH	H/H	H	H	10
4	19c	*S*	*S*	*S*	4-COOH	OH	iBu/iBu	H	H	10
5	19d	*S*	*S*	*R*	4-COOH	OH	iBu/H	H	H	2
6	19e	*S*	*S*	*S*	4-COOH	H	iBu/H	H	H	2
7	PhCOOH	-	-	-	-	-	-	-	-	2
8	19f	*S*	*S*	*S*	3-COOH	OH	iBu/H	H	H	8
9	19g	*S*	*S*	*S*	2-COOH	OH	iBu/H	H	H	4
10	19h	*S*	*S*	*S*	4-OH	COOH	iBu/H	H	H	30
11	19i	*S*	*S*	*S*	3-OH	COOH	iBu/H	H	H	6
12	19j	*S*	*S*	*S*	2-OH	COOH	iBu/H	H	H	4
13	DPCB*	-	-	-	-	-	-	-	-	14
14	19k	*S*	*S*	*S*	4-OH	COOH	iBu/H	H	Bn	42
15	19l	*S*	*S*	*S*	3-OH	COOH	iBu/H	Bn	H	40
16	19m	*S*	*S*	*S*	2-OH	COOH	iBu/H	Bn	Bn	58

Table 3-1. Kinetic data for the aromatic Claisen rearrangement of **23** to **24**

The series of catalysts **19a-j** and controls were tested for acceleration of the aromatic Claisen rearrangement of the 1,1-dimethylallyl coumarin substrate **23**. Catalyst was added at 20 mol% relative to the substrate **23** at 0.2 M in dichloroethane. The reaction vessels were sealed and stirred magnetically at 60°C for 84 hours. High-density polypropylene vessels had to be used because untreated glass vessels lead to decomposition of the reagent, presumably catalyzed by trace acid. The reactions were analyzed by HPLC-MS. Percent conversions were obtained by comparison of the area contributions from the product **24** and starting material peaks. Rate constants were determined by fitting the concentration of product with respect to time using a first order

kinetics model. Table 1 lists relative rate constants for the catalysts as well as benzoic acid and diphenylguanidinium BARF catalyst.[11]

The compound **19a** displayed a 11-fold rate enhancement relative to the background reaction (entries 1-2). **19a** was designed to display a terephthalic acid and a tyrosine in order to project a carboxylic acid and a phenol alcohol towards each other. Molecular modeling suggested that this would direct the terephthalic acid and phenol towards each other so that they could both simultaneously act as hydrogen bond donors to a single ether oxygen atom. This close approach of these two hydrogen-bonding groups is promoted by the stereochemistry of the spirofused pyrrolidine and diketopiperazine ring onto which the groups are mounted (Figure 1a). This close-approach is analogous to the close-approach that is achieved when a pyrene and a para-dimethylaniline group are displayed in place of the terephthalic acid and phenol.[81] The C-2 amide was modified to primary and tertiary amides (entries 3 and 4) to create the catalysts **19b** and **19c** which are more soluble in dichloroethane and this does not effect the catalytic rate, suggesting that the C2 amide is not involved in hydrogen bond stabilization of the transition state. The cooperativity of the two hydrogen bond donor groups was probed by altering the stereochemistry of the bicyclic backbone to create **19d**, which modeling suggests would pull the two donors away from each other (entry 5) – and the activity of **19d** drops to two-fold above background, which is similar to the activity of benzoic acid alone (entry 7). The cooperativity was further probed by removing the phenol alcohol using phenylalanine in place of tyrosine to form **19e** (entry 6) and its activity is equivalent to **19d** and benzoic acid. Altering the substitution of the carboxylic acid on the benzoic acid derivative to *meta* (**19f**) and *ortho* (**19g**) leads to less well-aligned hydrogen bond donor groups by modeling

and leads to lower activity catalysts (entries 8 and 9). Swapping the positions of the alcohol and the carboxylic acid (**19h**) brings the carboxylic acid and phenol alcohol in better alignment to simultaneously donate two hydrogen bonds to a single oxygen and increased the relative rate to 30-fold over background (entry 10). Altering the position of the alcohol on the benzoic acid derivative to meta (**19i**) and ortho (**19j**) also leads to less-well-aligned hydrogen bond donor groups by modeling and led to less active catalysts (entries 11 and 12). Diphenyl guanidinium BARF (DPGB; entry 13) is a prototype of a series of asymmetric catalysts of the Claisen rearrangement developed by the Jacobsen group.[11] Under these reaction conditions DPGB generated the product **24** with a krel of 14, however concomitant with product formation, significant amounts of side-products were formed, as observed by analytical reverse phase C18 HPLC analysis during the course of the reaction. Among these side-products, the free coumarin was observed indicating that the guanidinium catalyst is effective, under these reaction conditions, at breaking the ether linkage between the coumarin oxygen and allylic carbon, possibly by acting as a Bronsted acid.

Modeling suggests that the diketopiperazine ring of the BPC scaffold exists in a boat-like conformation. The boat conformation and the rotamer preferences of the functional groups could be altered through *N*-alkylation of the amide nitrogens within the diketopiperazine ring and this could alter the presentation of the phenol and carboxylic acid groups and change their catalytic activity. Dichloroethane solutions of **19a-j** were cloudy at room temperature although clear at 60ºC which we attributed to diketopiperazine-tape formation at room temperature.[84] N-alkylation could also improve the solubility of the catalysts in the dichloroethane solvent because it would disrupt

hydrogen-bonded tape-formation. We created three N-alkylated versions of **19h**, the mono N-benzylated catalysts **19k** and **19l**, and the di-N-benzylated catalyst **19m**.

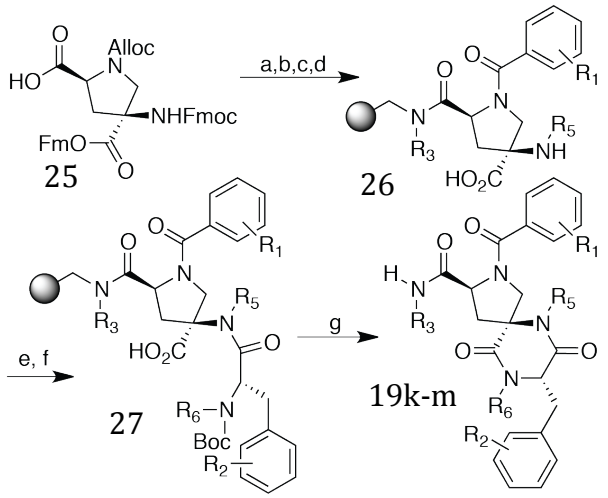

Scheme 3-2. Solid phase assembly of spiroligomer Claisen catalysts 19k-m. a) Substituted Amino Resin (1 eq), HATU (1eq) DIPEA (2eq), NMP (0.2M); b) $(P(Ph_3)_4)Pd(0)$ (0.3eq), BH_3:DMA (6eq), DCM (0.1M); c) Benzoic Acid Derivative (3eq), HATU (3eq), DIPEA (6eq), NMP (0.2M); d) 20% Piperidine in DMF (0.1M); e) PhCHO (2eq); NaH_3BCN (2eq); DMF (0.1M); f) Boc-Amino Acid (3eq); HATU (3eq), DIPEA (6eq); NMP (0.2M); g) TFA.

In order to synthesize these, an alternative solid phase synthesis had to be devised to assemble the tetra and penta substituted DKP rings shown in Scheme 2. The bis-amino acid derivative [83] **25** was attached to an isobutyl amine modified formyl resin via HATU promoted acylation. The pyrollidine Alloc group was removed using Palladium catalyst in the presence of a scavenger and then acylated with the t-butyl protected 4-hydroxy benzoic acid. The C-4 amino acid protecting group was then removed followed by reductive alkylation to the C-4 nitrogen with benzaldehyde to form **26**. The carboxy-phenylalanine derivative was introduced via HATU promoted acylation to form **27**. Treatment of the resin with neat TFA was used to cleave the intermediate from the resin, which led to spontaneous diketopiperazine formation and concomitant removal of all protecting groups

to yield **19k-m**. Purification with reverse phase HPLC yielded the pure catalysts in 75-80% yields relative to solid support loading.

Kinetic studies of catalysts **19a**, **19h**, and **19k-m** are shown in figure 2. Improvement in catalytic rate was observed over the course of each catalyst generation with **19m** (k_{rel} = 58) providing the largest rate enhancement relative to the background reaction.

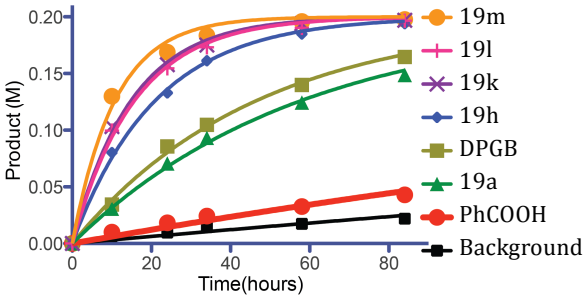

Figure 3-2. Claisen rearrangement product formation as a function of time and catalyst (0.2 M substrate in dichloroethane, 60ºC, 0.02M catalyst).

The catalyst **19a** was crystallized from water/acetonitrile 1:1 at room temperature and its crystal structure was determined (Figure 3). In the crystal structure the tyrosine side chain is observed to fold back over the diketopiperazine and pyrrolidine rings in the conformation that was proposed for bifunctional hydrogen bonded catalysis. The terephthalic acid is rotated away from the tyrosine in one of the two available amide rotamers. The preference of this rotamer of the terephthalic acid in the crystal structure can be understood in terms of crystal packing forces and an intermolecular hydrogen bond between the amide carbonyl of the terephthalic acid and the tyrosine alcohol of another molecule of **19a**. The X-ray crystal structure is very similar to the predicted conformation **19a'** in Figure 4b.

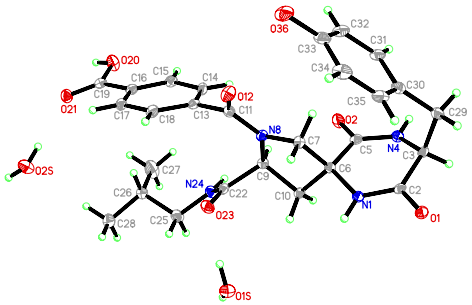

Figure 3-3. X-ray crystal structure of 19a illustrates the proposed catalytically active conformation of the tyrosine side-chain and one of the two possible amide rotamers of the terphthalic acid. This X-ray observed conformation is very similar to 19a' (Figure 4b), one of the lowest energy predicted structures of 19a.

We have explored the catalysis by **19a**, **19h** and **19k-m** using Molecular Dynamics (MD) to explore the conformational space of each catalyst and used quantum mechanics (QM) to evaluate transition states. We performed a conformational analysis of **19a**, **19h** and **19k-m** using the Monte Carlo (MCMM) method and the OPLS-AA force field as implemented in the MacroModel computational package (see SI for a detailed description of the computational methods used).[85,86] In each case, 20 or more lower energy conformers were further re-optimized using the hybrid meta exchange-correlation DFT functional M06-2X,[87,88] which includes medium-range correlation, with the standard 6-31G(d) basis set.[89,90] Solvent effects were included with the Conductor-like Polarizable Continuum Model (CPCM)[91] with dichloroethane as the solvent. M06-2X/6-31G(d) energies indicated that the lowest energy conformer for **19h** is from 6.5 up to 18.6 kcal/mol more stable than the rest of the computed conformers. The situation for **19a** is slightly different as the lowest energy conformer (BPC1a) is only 0.6 kcal/mol more stable than **19a"**, with the rest of the computed conformers being from 4 up to 15 kcal/mol higher in energy (see Figure 4). **19h** and **19a"** both present close approaching, preorganized

carboxylic acid and phenol groups for catalysis, while **19a'** has these two functional groups far separated (see Figure 4).

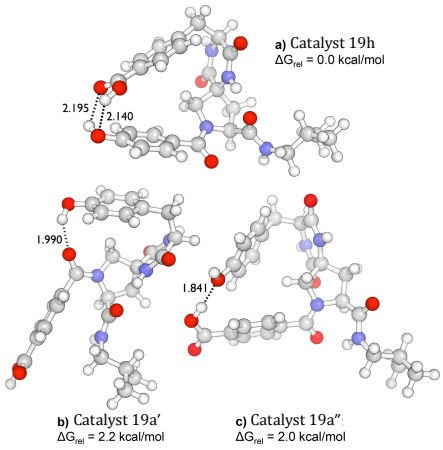

Figure 3-4. M06-2X/6-31G(d) optimized structures for the lowest energy conformers for **19h**, **19a'** and **19a"**. M06-2X/6-311+G(d,p)//M06-2X/6-31G(d) relative Gibbs free energies have been computed using the thermal corrections at M06-2X/6-31G(d) level (all distances are represented in Å).

The optimized transition state structures with catalytic conformations of **19h**, **19a'** and **19a"** are shown in Figure 6. The computed activation barrier for the Claisen rearrangement catalyzed by **19h** is 26.0 kcal/mol with respect to isolated reactants (i.e. **19h** and the coumarin reactant). As a reference, the computed activation barrier in terms of free Gibbs energy for the background reaction is 29.9 kcal/mol at the M06-2X/6-311+G(d,p)//M06-2X/6-31G(d) level of theory in CPCM dichloroethane (see Figure 5). The catalyzed reaction is bimolecular, and the rate of rearrangement is considerably faster than the background, but there is unfavorable entropy of association of the substrate and catalyst. The reactant complex between **19h** and the 1,1-dimethylallyl coumarin ether is 2.1 kcal/mol higher in Gibbs free energy than isolated reactants; that is, the nearly 10 kcal/mol binding is counteracted by $-T\Delta S$ for the bimolecular association. In the transition

state, both hydroxyl groups of **19h** are stabilizing the partial negative charge on the ether oxygen and are approximately 1.7 Å away (see Figure 6). The breaking O-C and the forming C-C bond distances are 2.274, 2.416 Å, respectively.

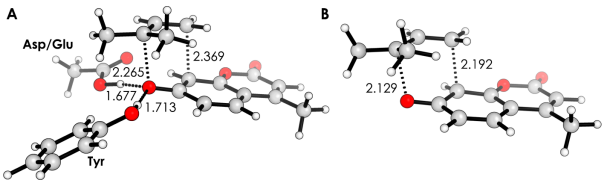

Figure 3-5. M06-2X/6-31G(d) optimized structures for the a) theozyme with the Asp/Glu and Tyr motif and b) the uncatalyzed reaction (all distances are represented in Å).

For **19a'**, the catalysis of the aromatic Claisen rearrangement could be assessed considering two different approaches. The phenol group and the benzoic acid moiety are not in close contact. Instead, the hydroxyl group of the phenol is interacting with a carbonyl group of the bis-peptide backbone (see Figures 4b and 6b). Therefore, the **19a'** catalyzed reaction was studied using either the phenol or the carboxylic group individually hydrogen bonded to the ether oxygen of the coumarin transition state. A lower energy transition state was found for the phenol-mediated catalysis. This single hydrogen-bonding TS has a computed Gibbs free activation barrier of 28.6 kcal/mol relative to isolated reactants, **19a'** and the coumarin ether. At the TS, the hydrogen bond distance between the ether oxygen and the hydrogen of the phenol is 1.743 Å, and the C-O breaking and C-C forming bond are 2.159, and 2.279 Å, respectively. The coumarin analogue is nicely π-stacked to the benzoic acid moiety (the distance between the center of mass of the benzene rings is approximately 3.3 Å). An enantiomer bound to the same catalyst was also found, but was 0.2 kcal/mol higher in energy. The transition state involving **19a"**, which has both hydroxyl groups in a closer disposition, presents an activation barrier that is 0.1 kcal/mol higher than the

previous TS for **19a'** (the Gibbs free activation barrier compared to isolated reactants is 28.7 kcal/mol, see Figure 6c). This slightly higher activation barrier is mainly attributed to the fact that only the hydroxyl group of the phenol moiety is stabilizing the negative charge of the ether oxygen, and more importantly the favorable π-stacking interaction between the coumarin derivative and the benzoic acid moiety is lost (see Figure 6c).

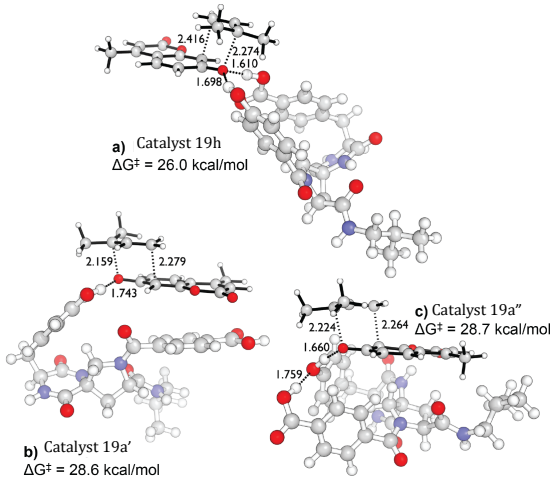

Figure 3-6. M06-2X/6-311+G(d,p)//M06-2X/6-31G(d) optimized transtition state structures for the Claisen rearrangement catalyzed by (a) **19h**, (b) **19a'**, (c) **19a"** in dichloroethane using CPCM implicit solvation model. The uncatalyzed reaction has a Gibbs free activation barrier of 29.9 kcal/mol. All distances are represented in Å.

We have also studied the more active catalysts **19k-m**. The conformational analysis and the subsequent optimization at M06-2X/6-31G(d) level indicated that the lowest energy conformers for all three cases present the proper arrangement for catalysis with the carboxyl and the phenol group in close proximity (see Figure 7).

We have studied the spiroligozyme catalyzed Claisen rearrangement of the lowest energy conformers of the catalysts (i.e. 4 for **19k**, 4 for **19l**, and 4 for **19m**). It should be emphasized here that the main differences between the 4 different conformers studied for each case, arise mainly from different conformations of the benzyl and isopropyl

substituents. The difference in energy between the different conformers is less than 4 kcal/mol in all cases.

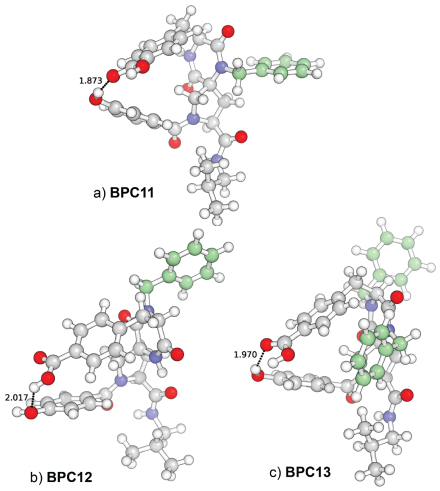

Figure 3-7. M06-2X/6-31G(d) optimized structures for the lowest energy conformers for a) **19k**, b) **19l** and b) **19m**. The benzyl substituents have been marked in light green for clarity. All distances are represented in Å.

Molecular Dynamics (MD) simulations using AMBER11[92] and a 10 Å truncated octahedral box with explicit chloroform molecules were performed in order to determine the relative free energies of catalytic and non-catalytic conformers of the catalyst. In Figure 8, the average distances between both oxygen atoms of the phenol and benzoic acid moieties of the spiroligozymes (dist OOH-OOH) along the 1 microsecond MD simulation are represented. In Figure 9, the histograms for the OOH-OOH distance are provided. The standard deviation is also shown using a shaded area and has been computed every 20 ps. For each catalyst analyzed in this way (i.e **19h** and **19k-m**), 250 superimposed MD snapshots have also been included where both the open and closed conformations have been marked using two different colors. The ideal arrangement

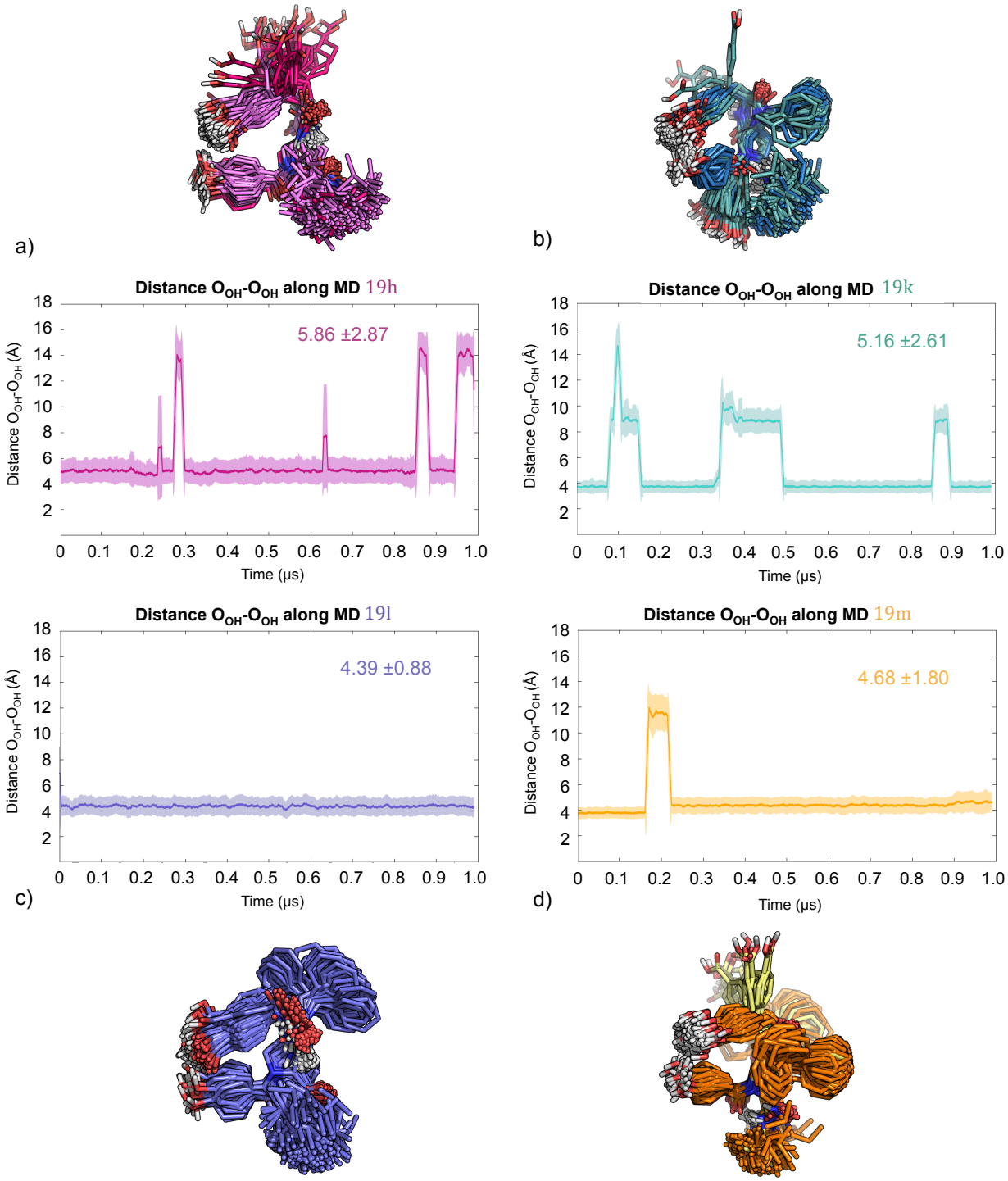

Figure 3-8. Representation of 250 superimposed MD snapshots for (a) **19h**, (b) **19k**, (c) **19l** and (d) **19m**. The plots monitoring the O_{OH}-O_{OH} distance along the 1 microsecond MD trajectory for these catalysts are also included. The computed QM distance at M06-2X/6-31G(d) is ca. 2.836 Å. The standard deviation is also represented using a shaded area and has been calculated every 10 steps of the simulation (i.e. 20 ps) (all distances are expressed in Å).

for catalysis is substantially altered along the simulation for **19h**, **19k** and **19m** catalysts (see Figure 8 and 10). The distance between the hydroxyl groups of both the phenol and benzoic acid moieties (d(O_{OH}-O_{OH})) along the MD trajectory for **19h** and **19k-m** are 5.86±2.87, 5.16±2.61, 4.39±0.88, 4.677±1.80 Å, respectively. These distances are substantially longer than the optimized QM value of 2.84 Å, especially for **19h** and **19k** cases. The higher distance and deviation found for **19h** and **19k** is due to a conformational change that leads to an arrangement where both benzoic acid and phenol moieties are not interacting (see snapshots in Figure 8, and histograms in Figure 9). Interestingly, in most cases more than 100 ns of simulation is needed to observe the latter conformational change (see plots in Figure 8). MD simulations indicate that the correct arrangement for catalysis is present 68.5% of the simulation time for **19h**. In this suitable arrangement, the averaged O_{OH}-O_{OH} distance is 4.41±0.79 Å, which is still substantially longer than the QM value of 2.84 Å. The distance between hydroxyl groups is less than 3 Å 14.5% of the simulation time. The introduction of a benzyl substituent on the amide backbone leads to a substantial improvement. **19k** adopts the proper conformation for catalysis ca. 74% of the simulation time, and the averaged O_{OH}-O_{OH} distance for this arrangement is 3.73±0.51 Å. The arrangement stays close to the QM value (i.e. less than 3 Å) 55.5% of the time. The benzoic acid moiety in **19l** stays in the proper orientation ca. 99% of the time, however the O_{OH}-O_{OH} distance is close to the QM value 32.1% of the simulation time. **19m**, which have benzyl substituents on both amide backbone nitrogens, adopt the correct arrangement ca. 94% of the time during the MD trajectory. The averaged O_{OH}-O_{OH} distance for the **19m** suitable arrangement for catalysis is 4.41±0.79 Å; the O_{OH}-O_{OH} distance is less than 3 Å

31.9% of the time. The MD simulations performed on the free catalysts have shown that the ideal arrangement for catalysis is substantially modified, especially in the case of **19h**. In the case of **19k**, **19l** and **19m**, those conformers with the suitable arrangement for catalysis present averaged O_{OH}-O_{OH} distances closer to the optimized QM value. These simulations indicate the fraction of conformers that have the catalytic groups properly preorganized for catalysis.

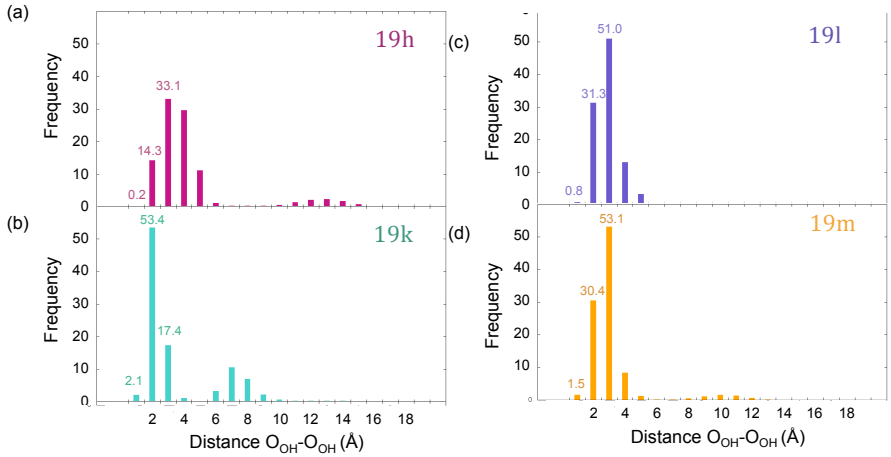

Figure 3-9. Distribution of the O_{OH}-O_{OH} distance during the 1 microsecond MD trajectory for (a) **19h** (purple), (b) **19k** (green), (c) **19l** (blue) and (d) **19m** (orange). All distances are expressed in Å.

We have also computed the Gibbs free activation energies for the spiroligozyme catalyzed Claisen rearrangement involving **19k**, **19l** and **19m**. In Figure 10, the M06-2X/6-31G(d) optimized transition state structures for the lowest activation barrier with each catalyst are shown. The computed activation barriers for **19k**, **19l** and **19m** are 26.6, 27.2 and 23.5 kcal/mol referred to the reactants, isolated spiroligozyme and the coumarin ether. Minor differences are observed among the computed activation barriers, especially in the case of **19k** and **19l**. As mentioned earlier for **19a** and **19h**, the optimized reactant

complexes are ca. 5-6 kcal/mol higher in Gibbs-free energy than isolated reactants in the case of **19k** and **19l**, and ca. 3 kcal/mol in **19m**. In all cases, the breaking O-C and the forming C-C bond distances are approximately 2.260 and 2.390 Å (see Figure 10). The hydrogen bonds formed between the ether oxygen and the phenol and benzoic acid moieties to stabilize the partial negative charge are 1.710 and 1.692, and 1.734 and 1.640 Å in **19k** and **19l**, respectively. Interestingly, **19m** presents slightly shorter hydrogen bond distances of 1.620 and 1.718 Å.

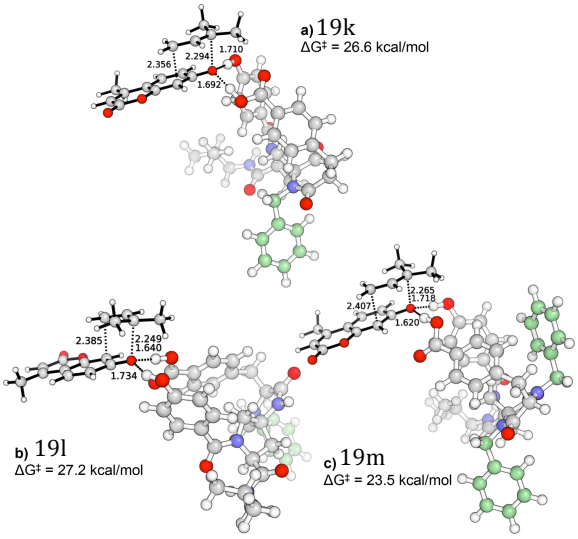

Figure 3-10. M06-2X/6-311+G(d,p)//M06-2X/6-31G(d) optimized transition state structures for the Claisen rearrangement catalyzed by (a) **19k**, (b) **19l** and (c) **19m** in dichloroethane using CPCM implicit solvation model. The uncatalyzed reaction has a Gibbs free activation barrier of 29.9 kcal/mol. All distances are represented in Å.

The computed activation barriers for the uncatalyzed, **19a**, **19h** and **19k-m** catalyzed Claisen rearrangements are 29.9, 28.7, 26.0, 26.6, 27.2 and 23.5 kcal/mol, respectively. MD simulations have shown that **19h** and **19k-m** adopt the appropriate conformation for catalysis (the hydroxyl distance is less than 3 Å) 14.5%, 55.5%, 32.1%

and 31.9% of the simulation time, respectively. The latter fraction of conformers (f) in the catalytic conformation can be used to estimate the experimental rate constant (k_{cat} = f•k_{cat},computed). This leads to a computed k_{cat}/k_{uncat} of ca. 100 and 15,800 for **19h** and **19m** with respect to the background reaction, respectively. Although the fraction of active conformers from the MD has been included, the predicted values are substantially overestimated compared to the experimentally observed k_{rel} values.

3.3 Conclusions

We have developed a series of bifunctional hydrogen-bond donor catalysts for the aromatic Claisen rearrangement modeled on the active site of Ketosteroid Isomerase. These catalysts are designed to present a carboxylic acid and a phenol alcohol that each simultaneously donates one hydrogen bond donor to a single ether oxygen of the 1,1-dimethylallyl coumarin substrate to stabilize the developing negative charge on the ether oxygen in the transition state of the Claisen rearrangement. The catalysts provide increasing reactivity as they better organize their hydrogen bonding groups and more closely approximate the functional group display observed in Ketosteroid Isomerase and as they are better able to stabilize the transition state as determined by transition state modeling. The first designed catalyst **19a** accelerates the reaction 11-fold relative to background while the best catalyst **19m**, accelerates the reaction 58-fold. The combined QM and MD computational study of these systems established that **19m** gives a higher acceleration of the reaction due to an optimal disposition of the hydroxyl groups of both the phenol and benzoic acid moieties in both the TS and the reactant complex. This optimal arrangement is induced by the benzyl substituents of the amide backbone, which limit the movement of the benzoic acid and

phenol moieties. MD simulations have determined that this arrangement is better conserved in the case of **19m** and **19k** cases. The higher efficiency of **19m** compared to **19h**, **19k** and **19l** is due to the combination of a lower activation barrier and a better pre-organization of the catalyst, which maintains both hydrogen donors in close proximity ca. 94% of the time during the 1 microsecond MD simulation. Comparison of the experimentally determined activation barrier lowering to calculated values demonstrates that calculations overestimate the catalytic power of the two hydrogen bond catalysis by two-fold.

These catalysts represent the first examples of synthetic Claisen rearrangement catalysts that utilize O-H hydrogen bond donors as found in the Ketosteroid Isomerase enzyme rather than N-H hydrogen bond donors observed in urea-, thiourea-, guanidinium-, and bisimidazolium-based catalysts of the Claisen rearrangement.

3.4 Experimental

General Methods

All Bis amino acid starting materials were synthesized according to literature procedure.[22] Diphenylguandidinium BARF catalyst was synthesized according to literature procedure.[23] Anhydrous N-methylpyrrolidinone, anhydrous dimethylformamide, anhydrous dichloromethane were purchased from Acros. HATU was purchased from Genscript. PyAOP was purchased from Oakwood. MSNT and solid phase resins were purchased from Novabiochem. All amino acids were purchased from Bachem. Redistilled diisopropylethylamine, tetrakis(triphenylphosphine) palladium0 ,borane: dimethyl-amine complex, diisopropylcarbodiimide, and all other reagents were purchased from Aldrich. Flash Chromatography was perfored on an ISCO CombiFlash Companion with cartridges filled with Bodman 32-63 D (60.) grade silica gel. Analytical HPLC-MS analysis was performed on a Hewlett-Packard Series 1200 with a Waters Xterra MS C18 column (3.5um packing, 4.6 mm x 100mm) with a solvent system of water/acetonitrile with 0.1% formic acid at a flow rate of 0.8mL/min. Preparatory Scale HPLC purification was performed on a Varian Prostar Prep HPLC with a Waters Xterra column (5um packing, 19mm x 100mm) with a solvent system of water/acetonitrile with 0.1% formic acid at a flow rate of 12mL/min. NMR experiments were performed on a Bruker 500mHz NMR with a chemical shifts (δ) reported relative to DMSO-d6 or CDCl3 residual solvent peaks. HRESIQTOFMS analysis was performed by Ohio State University.

Synthesis of Claisen substrate 24

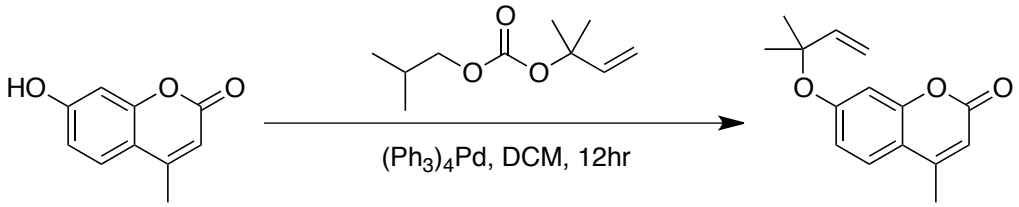

To a solution of 4-methylumbelliferone (880.9mg, 5 mmoles) and 1,1-dimethylallyl isobutyl carbonate (1.86g, 10 mmoles) in 90mL dichloromethane (DCM) was added tetrakis(triphenyl-phosphine)palladium0 (1.1g, 1 mmole) in 10mL of DCM. The reaction was allowed to stir at room temperature for 12 hours then concentrated on celite and purified by silica gel chromatography (gradient elution from 10% ethyl acetate in hexanes to 100% ethyl acetate. The product containing fractions were combined and concentrated under reduced pressure to yield the product as a white powder (86%, 1g). ^{1}H NMR (500MHz, $CDCl_3$, 273K, δ) 7.4 (d, 1H, *J*=8.8), 7.0 (s, 1H), 6.9 (m, 1H), 6.1 (m, 2H), 5.2 (dd, 2H, *J*=15.8,1.8), 2.4 (s, 3H), 1.5 (s, 6H). 13C NMR (125MHz, $CDCl_3$, 273K, δ) 161.3, 159.8, 154.5, 152.4, 143.4, 124.8, 117.0, 114.4, 112.1, 107.1, 80.8, 27.1, 18.5. Purity was assessed with analytical HPLC; mobile phase 5-95% acetonitrile in water modified with 0.1% formic acid, UV detection at 320nm, tR = 23.0.

Solid Phase Assembly of 19a-j

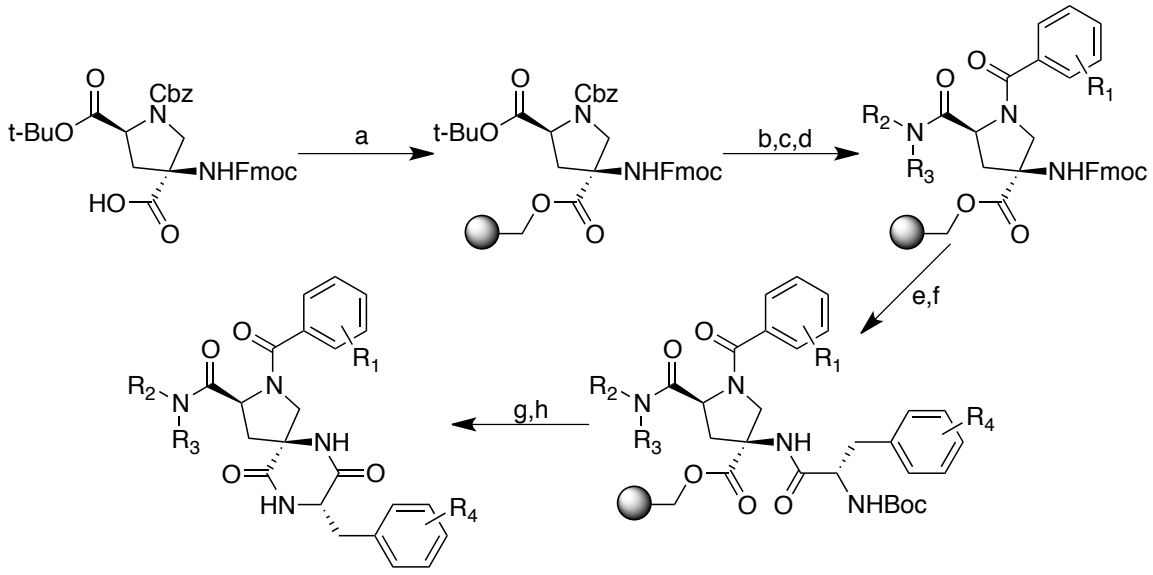

a) HMBA Resin (1.1eq), MSNT (2eq), NMI (2eq), DCM (0.1M); b) 33% HBr in AcOH/DCM (1:1, 0.1M); c) Benzoic Acid Derivative (3eq), HATU (3eq), DIPEA (6eq), NMP (0.2M); d) Substituted Amine (6eq), PyAOP (3eq), NMP (0.2M); (e) 20% Piperidine in DMF (0.1M); f)Boc-Amino Acid (3eq), HATU (3eq), DIPEA (6eq), NMP (0.2M); g) TFA/DCM (1:1, 0.1M); h) 10% DIPEA in MeCN (0.05M).

General Procedure (A): Attachment to HMBA Resin

To a the bis amino acid (1 equivalents) in dichloromethane (DCM) (10mL/mmole) was added N-methyl imidazole (NMI) (2 equivalents) followed by 1-(Mesitylene-2-sulfonyl)-3-nitro-1H-1,2,4-triazole (MSNT) (2 equivalents). The reaction mixture was allowed to stir

for 30 minutes then added to a pre-swelled portion of HMBA resin (1.1 equivalents). The reaction was stirred overnight and filtered and washed with DMF, DCM, and DMF.

General Procedure (B): tBu and Cbz Deprotection

A solution of 33% Hydrogen Bromide in Acetic Acid was mixed 1:1 volumetrically with dichloromethane (DCM) (10mL/mmole based on resin loading) was added to the resin and stirred for 30 minutes, filtered and washed with DMF, DCM, DMF.

General Procedure (C,F): HATU Coupling

To a solution of the acid (3 equivalents based on resin loading) and HATU (3 equivalents based on resin loading in N-methylpyrrolidine (NMP) (5mL/mmole of acid) was added diiso-propylethylamine (DIPEA) (6 equivalents based on resin loading). The reaction mixture was added to a pre-swelled (in dimethylformamide) portion of resin in a solid phase reactor and stirred for 45 minutes. The resin was filtered and washed with DMF, DCM, DMF.

General Procedure (D): PyAOP Coupling

To a solution of the amine (3 equivalents based on resin loading) and PyAOP (3 equivalents based on resin loading in N-methylpyrrolidine (NMP) (5mL/mmole of amine) was added diiso-propylethylamine (DIPEA) (6 equivalents based on resin loading). The reaction

mixture was added to a pre-swelled (in dimethylformamide) portion of resin in a solid phase reactor and stirred for 45 minutes. The resin was filtered and washed with DMF, DCM, DMF.

General Procedure (E): Fmoc Deprotection

A solution of of piperidine was mixed 1:4 volumetrically with dimethylformamide (DMF) (15mL/mmole based on resin loading) was added to a pre-swelled (in DMF) portion of resin in a solid phase reactor and stirred for 15 minutes. The resin was filtered and washed with DFM, DCM, DMF.

General Procedure (G): Boc Deprotection

A solution of Trifluoroacetic acid was mixed 1:1 volumetrically with dichloromethane (DCM) (10mL/mmole based on resin loading) was added to the resin and stirred for 2 hours, filtered and washed with DMF, DCM, DMF.

General Procedure (H): Liberation from HMBA resin and DKP Formation

A solution of diisopropylethylamine (DIPEA) was mixed 1:9 volumetrically with acetonitrile (MeCN) was added to the resin and stirred overnight, filtered, and the filtrated was acidified with with a 10% Formic acid solution in water and freeze-dried.

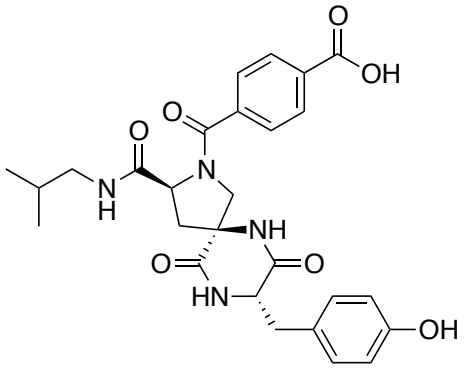

19a

HMBA Resin (220mg, 200umoles loading) was placed in a 8 mL solid phase reactor. The bis amino acid was attached according to general procedure (A) and modified according to the above scheme to yield BPC1 as a white powder (72%, 75mg) after purification by reverse-phase chromatography (gradient elution over 30 minutes from 5-95% acetonitrile in water modified with 0.1% formic acid. ^{1}H NMR (500MHz, DMSO-*d*6, 333K, δ) 8.2 (d, 2H, *J*=8.3), 8.1 (d, 2H, *J*=8.2), 7.0 (d, 2H, *J*=8.5), 6.8 (d, 2H, *J*=8.5), 4.5 (t, 1H, *J*=8.3,7.9), 4.3 (t, 1H, *J*=4.7,4.9), 3.1 (d, 1H, *J*=13.8), 2.8 (m, 2H), 2.6 (d, 1H, *J*=7.0), 2.5 (d, 2H, *J*=12.2), 2.1 (m, 2H), 1.5 (m, 1H), 0.8 (d, 6H, *J*=6.7). 13C NMR (125MHz, DMSO-*d*6, 333K, δ) 171.0, 169.7, 163.5, 163.1, 152.5, 135.0, 131.0, 130.1, 129.6, 128.4, 128.3, 127.9, 127.8, 123.6, 120.4, 64.7, 56.9, 48.6, 47.7, 46.3, 32.5, 29.9, 26.4, 18.3. Purity was assessed with analytical HPLC; mobile phase 5-95% acetonitrile in water modified with 0.1% formic acid, UV detection at 274nm, tR = 15.5. HRESIQTOFMS calculated for $C_{27}H_{31}N_4O_7$ ($M + H^+$) 523.2114 measured 523.2120 (1.1ppm).

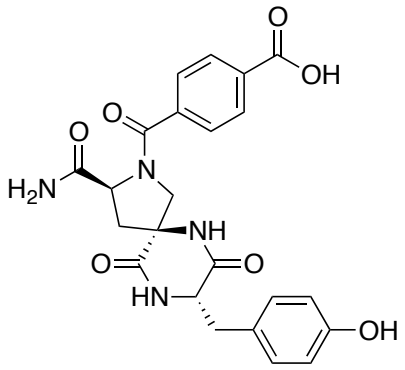

19b

HMBA Resin (220mg, 200umoles loading) was placed in a 8 mL solid phase reactor. The bis amino acid was attached according to general procedure (A) and modified according to the above scheme to yield BPC1 as a white powder (79%, 74mg) after purification by reverse-phase chromatography (gradient elution over 30 minutes from 5-95% acetonitrile in water modified with 0.1% formic acid. ^{1}H NMR (500MHz, DMSO-*d*6, 333K, δ) 8.2 (d, 2H, *J*=8.3), 8.2 (d, 2H, *J*=8.2), 7.0 (d, 2H, *J*=8.5), 6.9 (d, 2H, *J*=8.5), 4.5 (t, 1H, *J*=8.3,7.9), 4.3 (t, 1H, *J*=4.7,4.9), 3.1 (d, 1H, *J*=13.8), 2.9 (m, 2H), 2.5 (d, 2H, *J*=12.2), 2.1 (m, 2H). 13C NMR (125MHz, DMSO-*d*6, 333K, δ) 172.5, 171.2, 165.1, 164.6, 154.0, 136.5, 132.5, 132.4, 131.2, 129.8, 129.3, 125.1, 121.9, 66.2, 58.2, 49.2, 47.8, 34.0, 27.7. Purity was assessed with analytical HPLC; mobile phase 5-95% acetonitrile in water modified with 0.1% formic acid, UV detection at 274nm, tR = 13.9. HRESIQTOFMS calculated for $C_{23}H_{23}N_4O_7$ ($M + H^+$) 467.1488 measured 467.1492 (0.9ppm).

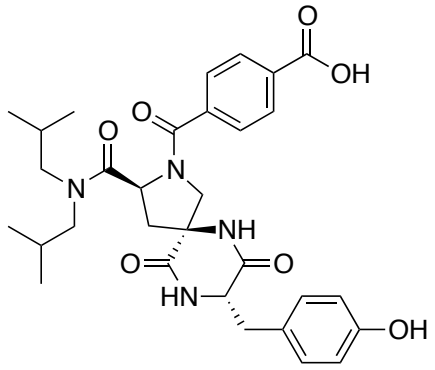

19c

HMBA Resin (220mg, 200umoles loading) was placed in a 8 mL solid phase reactor. The bis amino acid was attached according to general procedure (A) and modified according to the above scheme to yield BPC1 as a white powder (70%, 73mg) after purification by reverse-phase chromatography (gradient elution over 30 minutes from 5-95% acetonitrile in water modified with 0.1% formic acid. ^{1}H NMR (500MHz, DMSO-*d*6, 333K, δ) 8.2 (d, 2H, *J*=8.3), 8.1 (d, 2H, *J*=8.2), 7.0 (d, 2H, *J*=8.5), 6.8 (d, 2H, *J*=8.5), 4.5 (t, 1H, *J*=8.3,7.9), 4.3 (t, 1H, *J*=4.7,4.9), 3.1 (d, 1H, *J*=13.8), 2.8 (m, 2H), 2.6 (d, 1H, *J*=7.0), 2.5 (d, 2H, *J*=12.2), 2.4 (d, 2H, *J*=6.55), 2.1 (m, 2H), 1.5 (m, 1H), 0.8 (d, 6H, *J*=6.7). 13C NMR (125MHz, DMSO-*d*6, 333K, δ)171.0, 169.7, 163.5, 163.1, 152.5, 135.0, 131.0, 130.9, 129.6, 128.3, 127.8, 123.6, 120.4, 64.7, 56.9, 49.4, 48.6, 47.7, 46.3, 32.5, 30.8, 29.9, 26.4, 19.1, 18.3. Purity was assessed with analytical HPLC; mobile phase 5-95% acetonitrile in water modified with 0.1% formic acid, UV detection at 274nm, tR = 17.1. HRESIQTOFMS calculated for $C_{31}H_{39}N_4O_7$ ($M + H^+$) 579.2740 measured 579.2760 (3.4ppm).

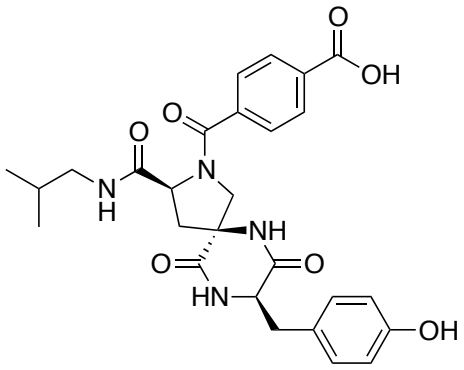

19d

HMBA Resin (220mg, 200umoles loading) was placed in a 8 mL solid phase reactor. The bis amino acid was attached according to general procedure (A) and modified according to the above scheme to yield BPC1 as a white powder (70%, 73mg) after purification by reverse-phase chromatography (gradient elution over 30 minutes from 5-95% acetonitrile in water modified with 0.1% formic acid. ^{1}H NMR (500MHz, DMSO-*d*6, 333K, δ) 8.2 (d, 2H, *J*=8.3), 8.1 (d, 2H, *J*=8.2), 7.0 (d, 2H, *J*=8.5), 6.7 (d, 2H, *J*=8.5), 4.5 (t, 1H, *J*=8.3,7.9), 4.3 (t, 1H, *J*=4.7,4.9), 3.1 (d, 1H, *J*=13.8), 2.9 (m, 2H), 2.6 (d, 1H, *J*=7.0), 2.5 (d, 2H, *J*=12.2), 2.1 (m, 2H), 1.5 (m, 1H), 0.8 (d, 6H, *J*=6.7). 13C NMR (125MHz, DMSO-*d*6, 333K, δ) 171.0, 169.7, 163.5, 163.1, 152.5, 135.0, 131.0, 130.1, 129.6, 128.4, 128.3, 127.9, 127.8, 123.6, 120.4, 64.7, 56.9, 48.6, 47.7, 46.3, 32.5, 29.9, 26.4, 18.3. Purity was assessed with analytical HPLC; mobile phase 5-95% acetonitrile in water modified with 0.1% formic acid, UV detection at 274nm, tR = 14.2. HRESIQTOFMS calculated for $C_{27}H_{31}N_4O_7$ ($M + H^+$) 523.2114 measured 523.2130 (3.1ppm).

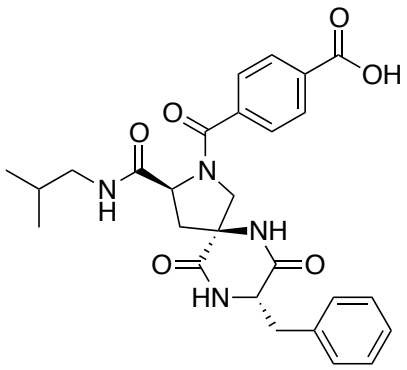

19e

HMBA Resin (220mg, 200umoles loading) was placed in a 8 mL solid phase reactor. The bis amino acid was attached according to general procedure (A) and modified according to the above scheme to yield BPC1 as a white powder (75%, 76mg) after purification by reverse-phase chromatography (gradient elution over 30 minutes from 5-95% acetonitrile in water modified with 0.1% formic acid. ^{1}H NMR (500MHz, DMSO-*d*6, 333K, δ) 7.3 (m, 5H), 7.0 (d, 2H, *J*=8.5), 6.8 (d, 2H, *J*=8.5), 4.5 (t, 1H, *J*=8.3,7.9), 4.3 (t, 1H, *J*=4.7,4.9), 3.1 (d, 1H, *J*=13.8), 2.8 (m, 2H), 2.6 (d, 1H, *J*=7.0), 2.5 (d, 2H, *J*=12.2), 2.1 (m, 2H), 1.5 (m, 1H), 0.8 (d, 6H, *J*=6.7). 13C NMR (125MHz, DMSO-*d*6, 333K, δ) 173.3, 171.0, 163.5, 152.5, 137.8, 131.0, 129.6, 128.8, 127.8, 126.0, 123.6, 120.4, 64.7, 56.9, 48.6, 47.7, 46.3, 32.4, 27.9, 26.2, 18.3. Purity was assessed with analytical HPLC; mobile phase 5-95% acetonitrile in water modified with 0.1% formic acid, UV detection at 274nm, tR = 16.6. HRESIQTOFMS calculated for $C_{27}H_{31}N_4O_6$ ($M + H^+$) 507.2165 measured 507.2176 (2.1ppm).

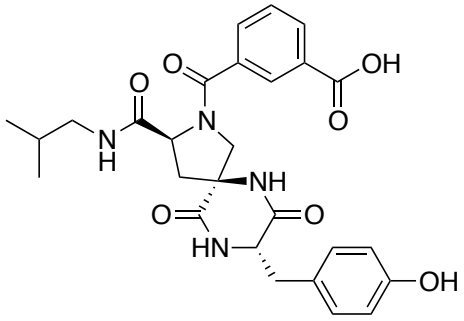

19f

HMBA Resin (220mg, 200umoles loading) was placed in a 8 mL solid phase reactor. The bis amino acid was attached according to general procedure (A) and modified according to the above scheme to yield BPC1 as a white powder (69%, 72mg) after purification by reverse-phase chromatography (gradient elution over 30 minutes from 5-95% acetonitrile in water modified with 0.1% formic acid. ^{1}H NMR (500MHz, DMSO-*d*6, 333K, δ) 8.7 (s, 1H), 8.2 (m, 2H), 7.5 (t, 1H, *J*=7.8,7.8), 7.0 (d, 2H, *J*=8.5), 6.8 (d, 2H, *J*=8.5), 4.5 (t, 1H, *J*=8.3,7.9), 4.3 (t, 1H, *J*=4.7,4.9), 3.1 (d, 1H, *J*=13.8), 2.8 (m, 2H), 2.6 (d, 1H, *J*=7.0), 2.5 (d, 2H, *J*=12.2), 2.1 (m, 2H), 1.5 (m, 1H), 0.8 (d, 6H, *J*=6.7). 13C NMR (125MHz, DMSO-*d*6, 333K, δ) 171.4, 171.0, 164.7, 163.5, 152.5, 134.5, 133.8, 132.7, 131.2, 131.0, 129.6, 129.5, 128.5, 123.6, 120.4, 64.7, 56.9, 48.6, 47.7, 46.3, 32.5, 29.9, 26.2, 18.3. Purity was assessed with analytical HPLC; mobile phase 5-95% acetonitrile in water modified with 0.1% formic acid, UV detection at 274nm, tR = 15.4. HRESIQTOFMS calculated for $C_{27}H_{31}N_4O_7$ ($M + H^+$) 523.2114 measured 523.2123 (1.7ppm).

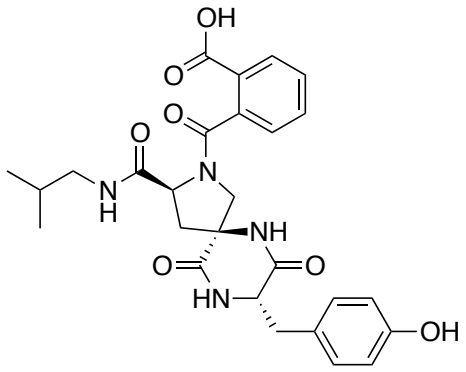

19g

HMBA Resin (220mg, 200umoles loading) was placed in a 8 mL solid phase reactor. The bis amino acid was attached according to general procedure (A) and modified according to the above scheme to yield BPC1 as a white powder (65%, 68mg) after purification by reverse-phase chromatography (gradient elution over 30 minutes from 5-95% acetonitrile in water modified with 0.1% formic acid. ^{1}H NMR (500MHz, DMSO-*d*6, 333K, δ) 7.9 (d, 1H, *J*=7.5), 7.8 (d, 1H, *J*=7.5), 7.7 (m, 2H), 7.0 (d, 2H, *J*=8.5), 6.8 (d, 2H, *J*=8.5), 4.5 (t, 1H, *J*=8.3,7.9), 4.3 (t, 1H, *J*=4.7,4.9), 3.1 (d, 1H, *J*=13.8), 2.8 (m, 2H), 2.6 (d, 1H, *J*=7.0), 2.5 (d, 2H, *J*=12.2), 2.1 (m, 2H), 1.5 (m, 1H), 0.8 (d, 6H, *J*=6.7). 13C NMR (125MHz, DMSO-*d*6, 333K, δ) 173.0, 171.0, 167.0, 163.5, 152.5, 134.7, 131.9, 131.0, 130.4, 130.0, 129.6, 129.5, 128.8, 123.6, 120.4, 64.7, 56.9, 48.6, 47.7, 46.3, 32.5, 30.0, 26.2, 18.3. Purity was assessed with analytical HPLC; mobile phase 5-95% acetonitrile in water modified with 0.1% formic acid, UV detection at 274nm, tR = 14.9. HRESIQTOFMS calculated for $C_{27}H_{31}N_4O_7$ ($M + H^+$) 523.2114 measured 523.2127 (2.4ppm).

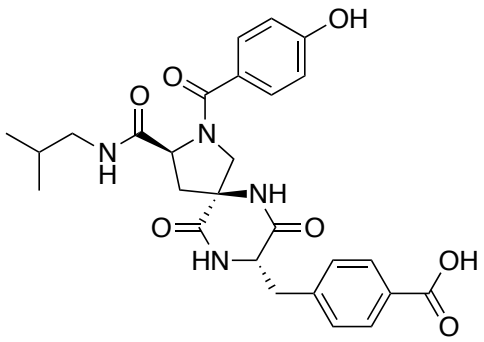

19h

HMBA Resin (220mg, 200umoles loading) was placed in a 8 mL solid phase reactor. The bis amino acid was attached according to general procedure (A) and modified according to the above scheme to yield BPC1 as a white powder (74%, 77mg) after purification by reverse-phase chromatography (gradient elution over 30 minutes from 5-95% acetonitrile in water modified with 0.1% formic acid. ^{1}H NMR (500MHz, DMSO-*d*6, 333K, δ) 8.2 (d, 2H, *J*=8.3), 8.1 (m, 6H), 6.8 (d, 2H, *J*=8.5), 4.5 (t, 1H, *J*=8.3,7.9), 4.3 (t, 1H, *J*=4.7,4.9), 3.1 (d, 1H, *J*=13.8), 2.8 (m, 2H), 2.6 (d, 1H, *J*=7.0), 2.5 (d, 2H, *J*=12.2), 2.1 (m, 2H), 1.5 (m, 1H), 0.8 (d, 6H, *J*=6.7). 13C NMR (125MHz, DMSO-*d*6, 333K, δ) 172.5, 171.2, 165.1, 164.6, 154.0, 136.5, 132.4, 131.2, 130.0, 129.8, 129.3, 125.1, 121.9, 66.2, 58.4, 49.2, 47.8, 34.0, 28.0, 20.0. Purity was assessed with analytical HPLC; mobile phase 5-95% acetonitrile in water modified with 0.1% formic acid, UV detection at 274nm, tR = 15.8. HRESIQTOFMS calculated for $C_{27}H_{31}N_4O_7$ (M + H^+) 523.2114 measured 523.2133 (3.6ppm).

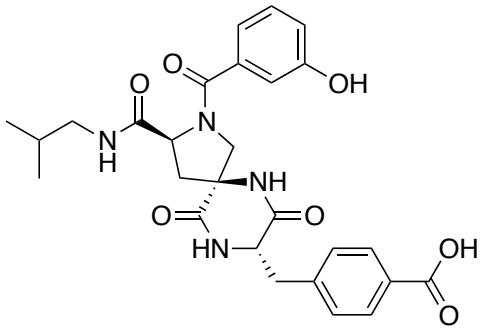

19i

HMBA Resin (220mg, 200umoles loading) was placed in a 8 mL solid phase reactor. The bis amino acid was attached according to general procedure (A) and modified according to the above scheme to yield BPC1 as a white powder (71%, 74mg) after purification by reverse-phase chromatography (gradient elution over 30 minutes from 5-95% acetonitrile in water modified with 0.1% formic acid. ^{1}H NMR (500MHz, DMSO-*d*6, 333K, δ) 8.0 (m, 6H), 7.5 (m, 2), 4.6 (t, 1H, *J*=8.3,7.9), 4.3 (t, 1H, *J*=4.7,4.9), 3.1 (d, 1H, *J*=13.8), 2.8 (m, 2H), 2.6 (d, 1H, *J*=7.0), 2.5 (d, 2H, *J*=12.2), 2.1 (m, 2H), 1.5 (m, 1H), 0.8 (d, 6H, *J*=6.7). 13C NMR (125MHz, DMSO-*d*6, 333K, δ) 172.5, 171.1, 165.1, 154.0, 151.2, 132.5, 131.2, 130.8, 129.5, 127.5, 126.8, 125.1, 123.1, 121.9, 66.2, 58.4, 50.1, 49.2, 47.8, 34.0, 31.5, 27.7, 19.8. Purity was assessed with analytical HPLC; mobile phase 5-95% acetonitrile in water modified with 0.1% formic acid, UV detection at 274nm, tR = 15.6. HRESIQTOFMS calculated for $C_{27}H_{31}N_4O_7$ ($M + H^+$) 523.2114 measured 523.2126 (2.3ppm).

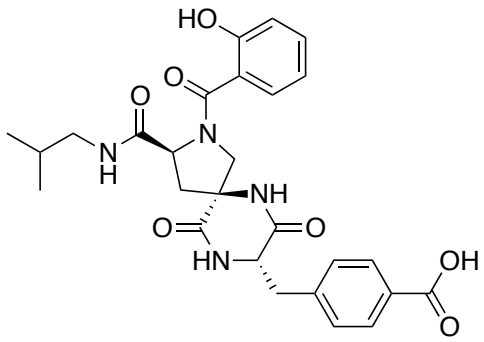

19j

HMBA Resin (220mg, 200umoles loading) was placed in a 8 mL solid phase reactor. The bis amino acid was attached according to general procedure (A) and modified according to the above scheme to yield BPC1 as a white powder (63%, 66mg) after purification by reverse-phase chromatography (gradient elution over 30 minutes from 5-95% acetonitrile in water modified with 0.1% formic acid. ^{1}H NMR (500MHz, DMSO-*d*6, 333K, δ) 8.0 (m, 5H), 7.6 (m, 1H), 7.3 (m, 2H), 4.5 (t, 1H, *J*=8.3,7.9), 4.3 (t, 1H, *J*=4.7,4.9), 3.1 (d, 1H, *J*=13.8), 2.8 (m, 2H), 2.6 (d, 1H, *J*=7.0), 2.5 (d, 2H, *J*=12.2), 2.1 (m, 2H), 1.5 (m, 1H), 0.8 (d, 6H, *J*=6.7). 13C NMR (125MHz, DMSO-*d*6, 333K, δ)172.5, 170.2, 165.1, 154.0, 151.4, 134.8, 132.5, 132.4, 131.2, 126.1, 125.1, 123.7, 122.6, 121.9, 66.2, 58.4, 50.1, 49.2, 47.8, 34.0, 31.5, 27.7, 19.9. Purity was assessed with analytical HPLC; mobile phase 5-95% acetonitrile in water modified with 0.1% formic acid, UV detection at 274nm, tR = 15.3. HRESIQTOFMS calculated for $C_{27}H_{31}N_4O_7$ ($M + H^+$) 523.2114 measured 523.2124 (1.9ppm).

Solid Phase Assembly of 19k-m

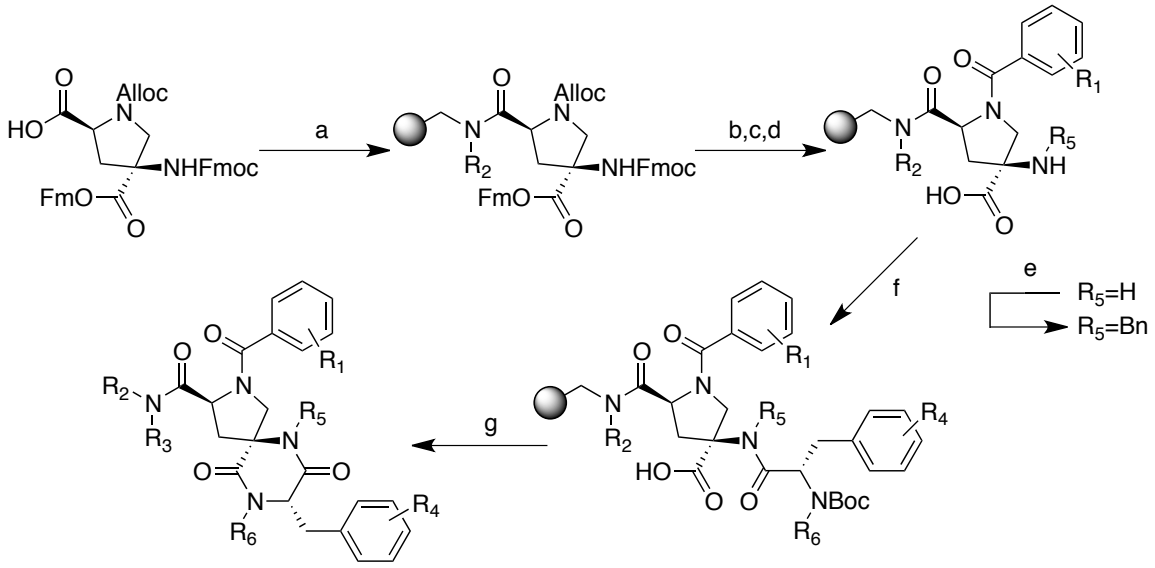

a) Substituted Amino Resin (1 eq), HATU (1eq) DIPEA (2eq), NMP (0.2M); b) (P(Ph3)4)Pd(0) (0.3eq), BH3:DMA (6eq), DCM (0.1M); c) Benzoic Acid Derivative (3eq), HATU (3eq), DIPEA (6eq), NMP (0.2M); d) 20% Piperidine in DMF (0.1M); e) PhCHO (2eq); NaH3BCN (2eq); DMF (0.1M); f) Boc-Amino Acid (3eq); HATU (3eq), DIPEA (6eq); NMP (0.2M); g) TFA

General Procedure (A): Attachment to Isobutyl Amino Resin

To the bis amino acid (1 equivalents) N-methylpyrrolidine (NMP) (5mL/mmole of acid) was added HATU (1 equivalents) followed by diisopropylethylamine (DIPEA) (2 equivalents). The reaction mixture was allowed to stir for 30 minutes then added to a pre-swelled portion of resin (1.1 equivalents). The reaction was stirred overnight and filtered

and washed with DMF, DCM, DMF.

General Procedure (B): Alloc Cleavage

A solution of borane:dimethylamine complex (6 equivalents based on resin loading) in dichloromethane (DCM) (10mL/mmole based on resin loading) was added to a pre-swelled (in DMF) portion of resin in a solid phase reactor and stirred for 5 minutes. To this solution was added a solution of tetrakis(triphenylphosphine)palladium0 (0.1 equivalents based on resin loading) in DCM (10mL/mmole based on resin loading). The reaction mixture was stirred for 2 hour. The resin was filtered and washed with DMF, DCM, DMF

General Procedure (C,F): HATU Coupling

To a solution of the acid (3 equivalents based on resin loading) and HATU (3 equivalents based on resin loading in N-methylpyrrolidine (NMP) (5mL/mmole of acid) was added diiso-propylethylamine (DIPEA) (6 equivalents based on resin loading). The reaction mixture was added to a pre-swelled (in dimethylformamide) portion of resin in a solid phase reactor and stirred for 45 minutes. The resin was filtered and washed with DMF, DCM, DMF.

General Procedure (D): Fmoc and OFm Cleavage

A solution of of piperidine was mixed 1:4 volumetrically with dimethylformamide (DMF)

(15mL/mmole based on resin loading) was added to a pre-swelled (in DMF) portion of resin in a solid phase reactor and stirred for 2 hours. The resin was filtered and washed with DFM, DCM, DMF.

General Procedure (E): Reductive Alkylation

A solution of aldehyde (2 equivalents based on resin loading) in dimethylformamide (DMF) (5mL/mmole based on resin loading) was added to a pre-swelled (in DMF) portion of resin in a solid phase reactor and stirred for 2 hours. To this solution was added a solution of sodium cyanoborohydride (2 equivalents based on resin loading) in DMF (5mL/mmole based on resin loading). The reaction mixture was stirred overnight. The resin was filtered and washed with DMF, DCM, DMF

General Procedure (G): Liberation from Resin and DKP Formation

A solution of 5% triisopropylsilane and 5% water in trifluoroacetic acid (25 mL/mmole based on resin loading was added to a portion of resin (successively washed with dichloromethane and methanol, and thoroughly dried under vacuum) and stirred overnight. The resin was filtered and washed with trifluoroacetic acid. The filtrate was concentrated, reconstituted in 75% acetonitrile in water (0.05% formic acid) and freeze-dried.

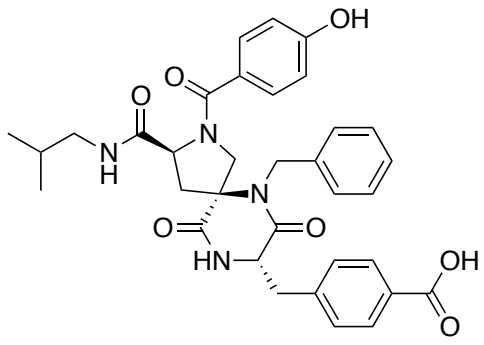

19k

HMBA Resin (220mg, 200umoles loading) was placed in a 8 mL solid phase reactor. The bis amino acid was attached according to general procedure (A) and modified according to the above scheme to yield BPC1 as a white powder (61%, 75mg) after purification by reverse-phase chromatography (gradient elution over 30 minutes from 5-95% acetonitrile in water modified with 0.1% formic acid. ^{1}H NMR (500MHz, DMSO-*d*6, 333K, δ) 8.1 (m, 6H), 7.3 (m, 7H), 4.5 (t, 1H, *J*=8.3,7.9), 4.3 (t, 1H, *J*=4.7,4.9), 3.8 (s, 2H), 3.1 (d, 1H, *J*=13.8), 2.8 (m, 2H), 2.6 (d, 1H, *J*=7.0), 2.5 (d, 2H, *J*=12.2), 2.1 (m, 2H), 1.5 (m, 1H), 0.8 (d, 6H, *J*=6.7). 13C NMR (125MHz, DMSO-*d*6, 333K, δ) 172.5, 171.1, 165.1, 154.0, 151.5, 151.3, 143.4, 132.5, 131.2, 130.8, 129.5, 128.5, 127.5, 127.1, 126.8, 126.7, 125.1, 123.1, 121.9, 66.2, 58.4, 50.1, 49.2, 47.8, 46.5, 33.9, 31.5, 27.6, 19.9. Purity was assessed with analytical HPLC; mobile phase 5-95% acetonitrile in water modified with 0.1% formic acid, UV detection at 274nm, tR = 18.3. HRESIQTOFMS calculated for $C_{34}H_{37}N_4O_7$ ($M + H^+$) 613.2584 measured 613.2607 (3.8ppm).

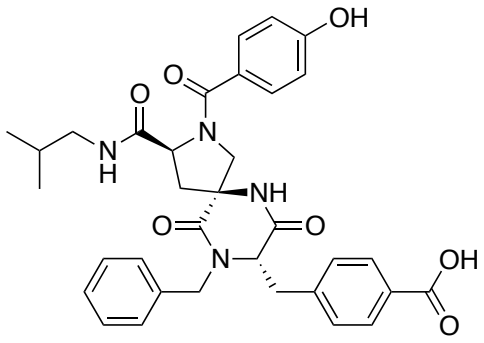

19l

HMBA Resin (220mg, 200umoles loading) was placed in a 8 mL solid phase reactor. The bis amino acid was attached according to general procedure (A) and modified according to the above scheme to yield BPC1 as a white powder (64%, 79mg) after purification by reverse-phase chromatography (gradient elution over 30 minutes from 5-95% acetonitrile in water modified with 0.1% formic acid. ^{1}H NMR (500MHz, DMSO-*d*6, 333K, δ) 8.2 (m, 6H), 7.4 (m, 7H), 4.5 (t, 1H, *J*=8.3,7.9), 4.3 (t, 1H, *J*=4.7,4.9), 3.9 (s, 2H), 3.1 (d, 1H, *J*=13.8), 2.8 (m, 2H), 2.6 (d, 1H, *J*=7.0), 2.5 (d, 2H, *J*=12.2), 2.1 (m, 2H), 1.5 (m, 1H), 0.8 (d, 6H, *J*=6.7). 13C NMR (125MHz, DMSO-*d*6, 333K, δ) 172.6, 171.0, 165.0, 153.9, 151.5, 151.1, 142.7, 132.5, 131.2, 130.8, 129.5, 127.7, 127.4, 126.8, 126.3, 125.9, 125.1, 123.1, 121.9, 66.1, 58.4, 50.1, 49.3, 47.8, 45.8, 33.9, 31.5, 27.8, 19.7. Purity was assessed with analytical HPLC; mobile phase 5-95% acetonitrile in water modified with 0.1% formic acid, UV detection at 274nm, tR = 18.2. HRESIQTOFMS calculated for $C_{34}H_{37}N_4O_7$ ($M + H^+$) 613.2584 measured 613.2610 (4.3ppm).

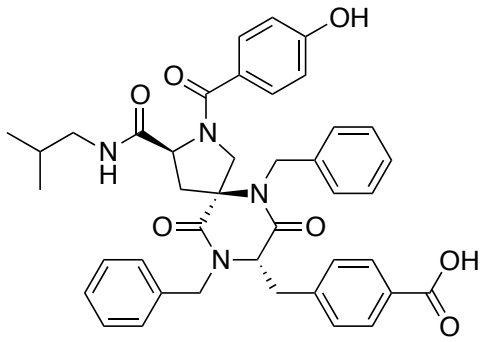

19m

HMBA Resin (220mg, 200umoles loading) was placed in a 8 mL solid phase reactor. The bis amino acid was attached according to general procedure (A) and modified according to the above scheme to yield BPC1 as a white powder (66%, 93mg) after purification by reverse-phase chromatography (gradient elution over 30 minutes from 5-95% acetonitrile in water modified with 0.1% formic acid. ^{1}H NMR (500MHz, DMSO-*d*6, 333K, δ) 8.2 (m, 6H), 7.3 (m, 12H), 4.5 (t, 1H, *J*=8.3,7.9), 4.3 (t, 1H, *J*=4.7,4.9), 3.9 (s, 2H), 3.8 (s, 2H), 3.1 (d, 1H, *J*=13.8), 2.8 (m, 2H), 2.6 (d, 1H, *J*=7.0), 2.5 (d, 2H, *J*=12.2), 2.1 (m, 2H), 1.5 (m, 1H), 0.8 (d, 6H, *J*=6.7). 13C NMR (125MHz, DMSO-*d*6, 333K, δ) 172.6, 171.1, 165.1, 153.9, 151.6, 151.2, 143.5, 142.7, 132.5, 131.2, 130.8, 129.5, 128.5, 127.8, 127.5, 127.1, 126.8, 126.7, 126.3, 126.1, 125.1, 123.1, 121.9, 66.3, 58.2, 50.3, 49.4, 47.8, 46.4, 45.7, 33.7, 31.5, 27.7, 19.3. Purity was assessed with analytical HPLC; mobile phase 5-95% acetonitrile in water modified with 0.1% formic acid, UV detection at 274nm, tR = 21.5. HRESIQTOFMS calculated for $C_{41}H_{43}N_4O_7$ ($M + H^+$) 703.3053 measured 703.3073 (2.9ppm).

Kinetic Measurements

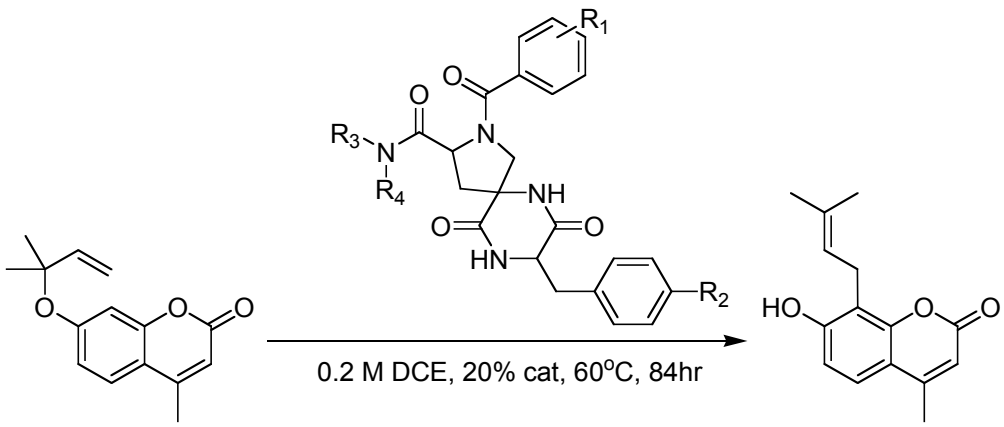

General Procedure:

The Clasien substrate (24.2mg, 100 umoles) and the catalyst (20 umoles) were dissolved in 500uL of 1,2-Dichloroethane in a HDPE sealed vial inside a glass pressure vessel. The reaction mixture was heated to 60°C and monitored by HPLC analysis. The peaks areas were extracted and used for determining concentrations of both starting material and product.

Substrate	244.3	g/mole			24.2	mg			99.05853	umoles			0.198117	Molar								
Solvent					500	uL																
Catalysis									20	umoles			0.04	Molar								
	Background				Benzoic Acid				BPC 1				BPC 4				BPC 5					
	0	g/mole			122.1	g/mole			522.5	g/mole			522.5	g/mole			506.6	g/mole				
	0.0	mg			2.4	mg			10.5	mg			10.5	mg			10.1	mg				
Time	% Comp	[Sub]	[Pro]		% Comp	[Sub]	[Pro]		% Comp	[Sub]	[Pro]		% Comp	[Sub]	[Pro]		% Comp	[Sub]	[Pro]			
0	0.0	0.198117	0		0.0	0.198117	0		0.0	0.198117	0		0.0	0.198117	0		0.0	0.198117	0			
10	3.3	0.191579	0.006538		5.1	0.188013	0.010104		15.5	0.167409	0.030708		5.4	0.187419	0.010698		4.8	0.188607	0.00951			
24	4.9	0.188409	0.009708		9.2	0.17989	0.018227		35.6	0.127587	0.07053		8.6	0.181079	0.017038		10.4	0.177513	0.020604			
34	7.3	0.183655	0.014463		12.2	0.173947	0.02417		47.0	0.105002	0.093115		12.3	0.173749	0.024368		11.6	0.175135	0.022982			
58	8.8	0.180683	0.017434		16.5	0.165428	0.032689		62.8	0.0737	0.124418		17.2	0.164041	0.034076		16.1	0.16622	0.031897			
84	11.1	0.176126	0.021991		21.7	0.155126	0.042991		75.0	0.049529	0.148588		21.7	0.155126	0.042991		22.5	0.153541	0.044576			
	BPC 8				Diphenylguandidinium BARF				BPC 11				BPC 12				BPC 13					
	522.5	g/mole			1075.5	g/mole			612.7	g/mole			612.7	g/mole			702.8	g/mole				
	10.5	mg			21.5	mg			12.3	mg			12.3	mg			14.1	mg				
Time	% Comp	[Sub]	[Pro]		% Comp	[Sub]	[Pro]		% Comp	[Sub]	[Pro]		% Comp	[Sub]	[Pro]		% Comp	[Sub]	[Pro]			
0	0.0	0.198117	0		0.0	0.198117	0		0.0	0.198117	0		0.0	0.198117	0		0.0	0.198117	0			
10	40.5	0.11788	0.080237		17.4	0.163645	0.034472		52.1	0.094898	0.103219		50.3	0.098464	0.099653		65.6	0.068152	0.129965			
24	67.1	0.065181	0.132937		43.2	0.11253	0.085587		79.6	0.040416	0.157701		78.0	0.043586	0.154531		85.2	0.029321	0.168796			
34	81.4	0.03685	0.161267		52.9	0.093313	0.104804		88.4	0.022982	0.175135		87.4	0.024963	0.173154		92.6	0.014661	0.183456			
58	93.3	0.013274	0.184843		70.6	0.058246	0.139871		97.9	0.00416	0.193957		96.1	0.007727	0.190391		98.9	0.002179	0.195938			
84	97.9	0.00416	0.193957		83.1	0.033482	0.164635		99.4	0.001189	0.196928		99.2	0.001585	0.196532		99.8	0.000396	0.197721			

Table 3-2. Kinetic Raw Data

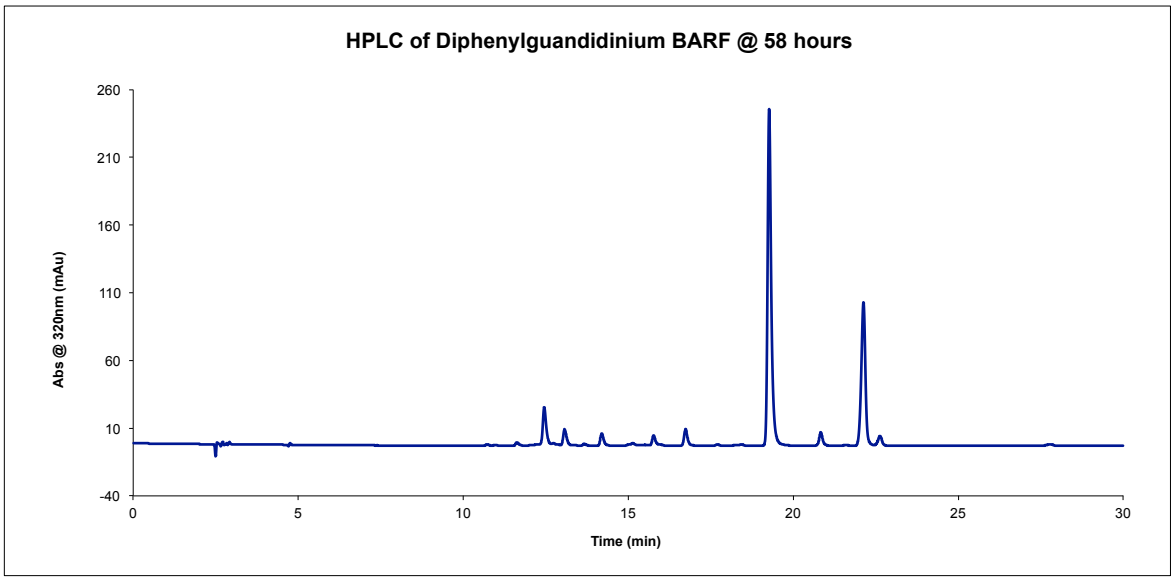

Figure 3-11. HPLC of Diphenylguandidinium BARF @ 58 hours

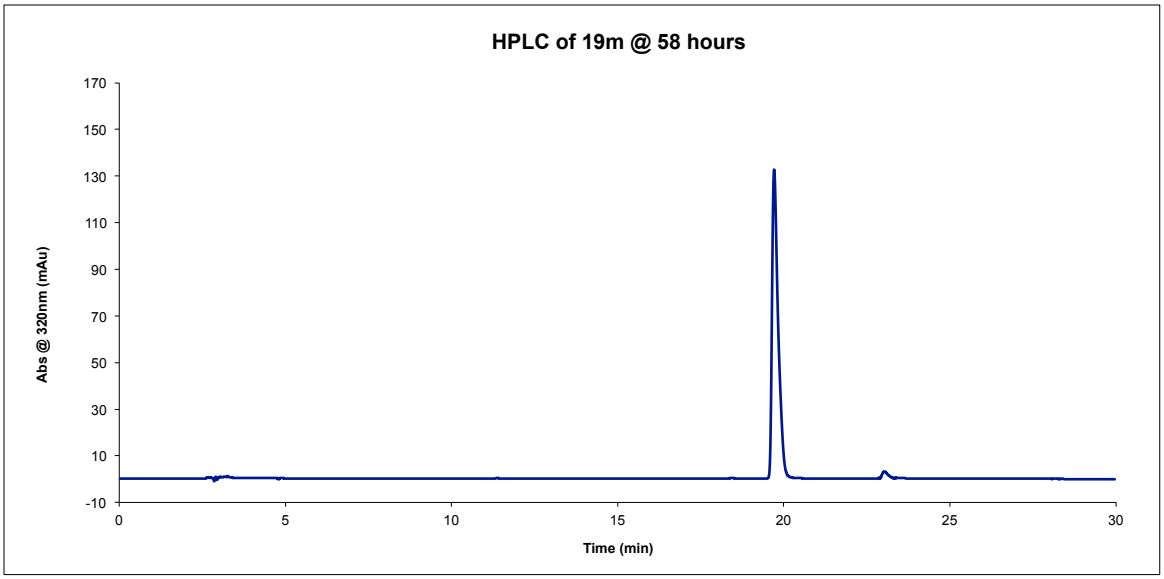

Figure 3-12. HPLC of **19m** @ 58 hours

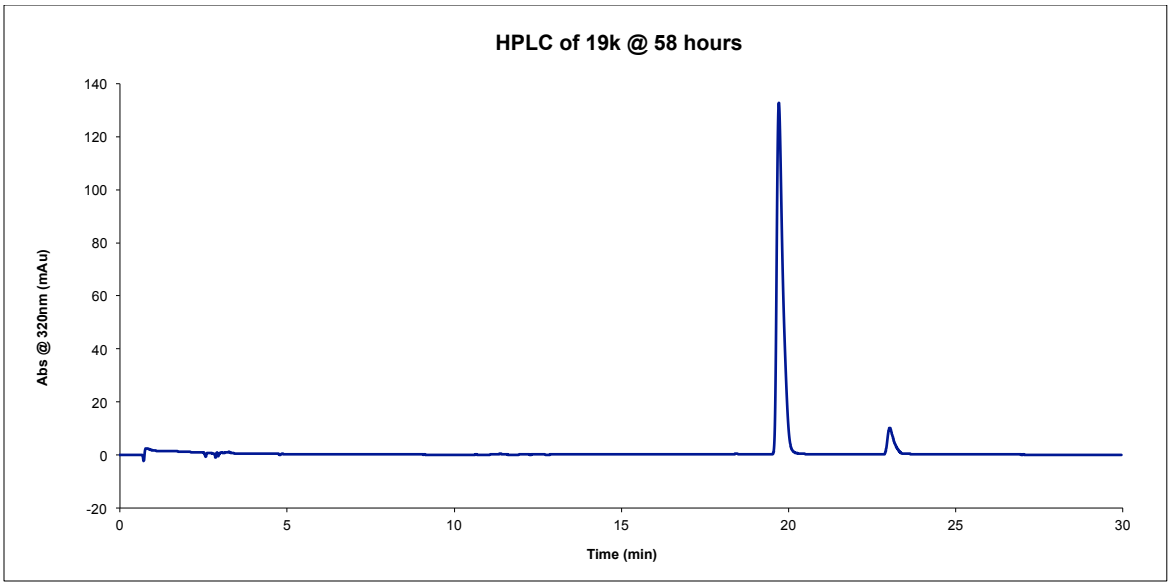

Figure 3-13: HPLC of **19k** @ 58 hours

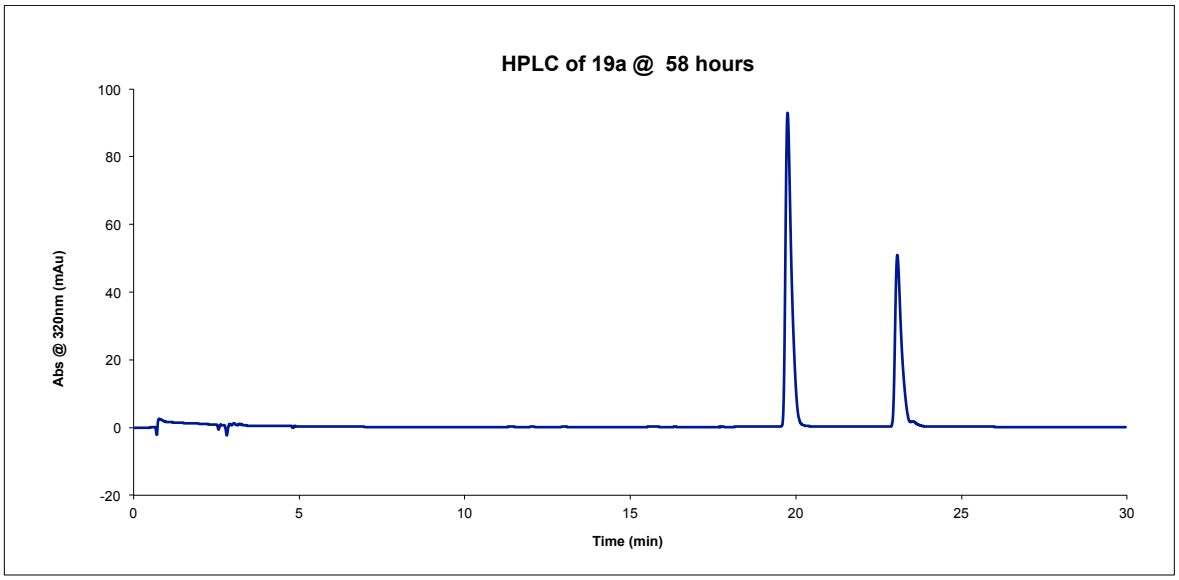

Figure 3-14: HPLC of **19a** @ 58 hours

3.5 References

[1] Fafarman, A. T.; Sigala, P. A.; Schwans, J. P.; Fenn, T. D.; Herschlag, D.; Boxer, S. G. *Proc. Natl. Acad. Sci. U.S.A.* **2012**, *109*, E299.

[2] Claisen, L. *Chem. Ber.* **1912**, *43*, 3157.

[3] Martín Castro, A. M. *Chem. Rev.* **2004**, *104*, 2939.

[4] Ziegler, F. E. *Chem. Rev* **1988**, *88*, 1423.

[5] Majumdar, K. C.; Alam, S.; Chattopadhyay, B. *Tetrahedron* **2008**, *64*, 597.

[6] Knowles, R. R.; Jacobsen, E. N. *Proc. Natl. Acad. Sci. U.S.A.* **2010**, *107*, 20678.

[7] Warshel, A.; Sharma, P. K.; Kato, M.; Xiang, Y.; Liu, H.; Olsson, M. H. M. *Chem. Rev* **2006**, *106*, 3210.

[8] Annamalai, V. R.; Linton, E. C.; Kozlowski, M. C. *Org. Lett.* **2008**, *11*, 621.

[9] Curran, D. P.; Lung, H. K. *Tetrahedron Lett.* **1995**, *36*, 6647.

[10] Rodriguez, A. A.; Yoo, H.; Ziller, J. W.; Shea, K. J. *Tetrahedron Lett.* **2009**, *50*, 6830.

[11] Uyeda, C.; Jacobsen, E. N. *J. Am. Chem. Soc.* **2008**, *130*, 9228.

[12] Uyeda, C.; Jacobsen, E. N. *J. Am. Chem. Soc.* **2011**, *133*, 5062.

[13] Uyeda, C.; Rötheli, A. R.; Jacobsen, E. N. *Angew. Chem., Int. Ed.* **2010**, *49*, 9753.

[14] Aemissegger, A.; Jaun, B.; Hilvert, D. *J. Org. Chem.* **2002**, *67*, 6725.

[15] Andrews, P. R.; Smith, G. D.; Young, I. G. *Biochemistry* **1973**, *12*, 3492.

[16] McIntosh, J. A.; Donia, M. S.; Nair, S. K.; Schmidt, E. W. *J. Am. Chem. Soc.* **2011**, *133*, 13698.

[17] Osuna, S.; Kim, S.; Bollot, G.; Houk, K. N. *Eur. J. Org. Chem.* **2013**, *2013*, 2823.

[18] Zhao, Q.; Lam, Y. H.; Kheirabadi, M.; Xu, C.; Houk, K. N.; Schafmeister, C. E. *J. Org. Chem.* **2012**, *77*, 4784.

[19] Claisen, L. *Chem. Ber.* **1912**, *43*, 3157.

[20] Cramer, C. J.; Truhlar, D. G. *J. Am. Chem. Soc.* **1992**, *114*, 8794.

[21] Severance, D. L.; Jorgensen, W. L. *J. Am. Chem. Soc.* **1992**, *114*, 10966.

[22] White, W. N.; Wolfarth, E. F. *J. Org. Chem.* **1970**, *35*, 2196.

[23] Coates, R. M.; Rogers, B. D.; Hobbs, S. J.; Curran, D. P.; Peck, D. R. *J. Am. Chem. Soc.* **1987**, *109*, 1160.

[24] Grieco, P. A.; Brandes, E. B.; McCann, S.; Clark, J. D. *J. Org. Chem.* **1989**, *54*, 5849.

[25] Brandes, E.; Grieco, P. A.; Gajewski, J. J. *J. Org. Chem.* **1989**, *54*, 515.

[26] Gajewski, J. J. *Acc. Chem. Res* **1997**, *30*, 219.

[27] Sehgal, A.; Shao, L.; Gao, J. *J. Am. Chem. Soc.* **1995**, *117*, 11337.

[28] Gajewski, J. J.; Jurayj, J.; Kimbrough, D. R.; Gande, M. E.; Ganem, B.; Carpenter, B. K. *J. Am. Chem. Soc.* **1987**, *109*, 1170.

[29] Pawlak, J. L.; Padykula, R. E.; Kronis, J. D.; Aleksejczyk, R. A.; Berchtold, G. A. *J. Am. Chem. Soc.* **1989**, *111*, 3374.

[30] Guilford, W. J.; Copley, S. D.; Knowles, J. R. *J. Am. Chem. Soc.* **1987**, *109*, 5013.

[31] Stewart, J.; Wilson, D. B.; Ganem, B. *J. Am. Chem. Soc.* **1990**, *112*, 4582.

[32] Bartlett, P. A.; Johnson, C. R. *J. Am. Chem. Soc.* **1985**, *107*, 7792.

[33] Ganem, B. *Tetrahedron* **1978**, *34*, 3353.

[34] Hilvert, D.; Nared, K. D. *J. Am. Chem. Soc.* **1988**, *110*, 5593.

[35] Jackson, D. Y.; Jacobs, J. W.; Sugasawara, R.; Reich, S. H.; Bartlett, P. A.; Schultz, P. G. *J. Am. Chem. Soc.* **1988**, *110*, 4841.

[36] Hilvert, D.; Carpenter, S. H.; Nared, K. D.; Auditor, M. T. *Proc. Natl. Acad. Sci. U.S.A.* **1988**, *14*, 4953.

[37] Acevedo, O.; Armacost, K. *J. Am. Chem. Soc.* **2010**, *132*, 1966.

[38] Repasky, M. P.; Guimaraes, C. R. W.; Chandrasekhar, J.; Tirado-Rives, J.; Jorgensen, W. L. *J. Am. Chem. Soc.* **2003**, *125*, 6663.

[39] Kincaid, J. F.; Tarbell, D. S. *J. Am. Chem. Soc.* **1939**, *61*, 3085.

[40] Chanda, A.; Fokin, V. V. *Chem. Rev* **2009**, *109*, 725.

[41] Narayan, S.; Muldoon, J.; Finn, M. G.; Fokin, V. V.; Kolb, H. C.; Sharpless, K. B. *Angew. Chem., Int. Ed.* **2005**, *44*, 3275.

[42] Ganem, B. *Angew. Chem., Int. Ed.* **1996**, *35*, 936.

[43] Copley, S. D.; Knowles, J. R. *J. Am. Chem. Soc.* **1987**, *109*, 5008.

[44] Guest, J. M.; Craw, J. S.; Vincent, M. A.; Hillier, I. H. *J. Chem. Soc., Perkin Trans. 2* **1997**, *2*, 71.

[45] Paton, R. S.; Mackey, J. L.; Kim, W. H.; Lee, J. H.; Danishefsky, S. J.; Houk, K. N. *J. Am. Chem. Soc.* **2010**, *132*, 9335.

[46] Ganesh, M.; Seidel, D. *J. Am. Chem. Soc.* **2008**, *130*, 16464.

[47] Huang, J.; Corey, E. J. *Org. Lett.* **2004**, *6*, 5027.

[48] Vance, R. L.; Rondan, N. G.; Houk, K. N.; Jensen, F.; Borden, W. T.; Komornicki, A.; Wimmer, E. *J. Am. Chem. Soc.* **1988**, *110*, 2314.

[49] Marti, S.; Andres, J.; Moliner, V.; Silla, E.; Tunon, I.; Bertran, J. *J. Am. Chem. Soc.* **2003**, *126*, 311.

[50] Claeyssens, F.; Ranaghan, K. E.; Lawan, N.; Macrae, S. J.; Manby, F. R.; Harvey, J. N.; Mulholland, A. J. *Org. Biomol. Chem.* **2011**, *9*, 1578.

[51] Rothlisberger, D.; Khersonsky, O.; Wollacott, A. M.; Jiang, L.; DeChancie, J.; Betker, J.; Gallaher, J. L.; Althoff, E. A.; Zanghellini, A.; Dym, O.; Albeck, S.; Houk, K. N.; Tawfik, D. S.; Baker, D. *Nature* **2008**, *453*, 190.

[52] Rothlisberger, D.; Khersonsky, O.; Wollacott, A. M.; Jiang, L.; Dechancie, J.; Betker, J.; Gallaher, J. L.; Althoff, E. A.; Zanghellini, A.; Dym, O.; Albeck, S.; Houk, K. N.; Tawfik, D. S.; Baker, D. *Nature* **2008**, *453*, 190.

[53] Jiang, L.; Althoff, E. A.; Clemente, F. R.; Doyle, L.; Rothlisberger, D.; Zanghellini, A.; Gallaher, J. L.; Betker, J. L.; Tanaka, F.; Barbas, C. F., III; Hilvert, D.; Houk, K. N.; Stoddard, B. L.; Baker, D. *Science* **2008**, *319*, 1387.

[54] Siegel, J. B.; Zanghellini, A.; Lovick, H. M.; Kiss, G.; Lambert, A. R.; St.Clair, J. L.; Gallaher, J. L.; Hilvert, D.; Gelb, M. H.; Stoddard, B. L.; Houk, K. N.; Michael, F. E.; Baker, D. *Science* **2010**, *329*, 309.

[55] DeChancie, J.; Clemente, F. R.; Gunaydin, H.; Smith, A. J. T.; Zhang, X.; Zhao, Y.-L.; Houk, K. N. *J. Org. Chem.* **2007**, *16*, 1851.

[56] Tantillo, D. J.; Jiangang, C.; Houk, K. N. *Curr. Opin. Chem. Biol.* **1998**, *2*, 743.

[57] Ujaque, G.; Tantillo, D. J.; Hu, Y.; Houk, K. N.; Hotta, K.; Hilvert, D. *J. Comput. Chem.* **2003**, *24*, 98.

[58] Berman, H.; Henrick, K.; Nakamura, H. *Nat. Struct. Mol. Biol.* **2003**, *10*, 980.

[59] Zanghellini, A.; Jiang, L.; Wollacott, A. M.; Cheng, G.; Meiler, J.; Althoff, E. A.; Röthlisberger, D.; Baker, D. *Protein Sci.* **2006**, *15*, 2785.

[60] Das, R.; Baker, D. *Annu. Rev. Biochem.* **2008**, *77*, 363.

[61] Richter, F.; Leaver-Fay, A.; Khare, S. D.; Bjelic, S.; Baker, D. *PLoS ONE* **2011**, *6*, e19230.

[62] Zhang, X.; Houk, K. N. *Acc. Chem. Res* **2005**, *38*, 379.

[63] Breslow, R.; Dong, S. D. *Chem. Rev* **1998**, *98*, 1997.

[64] Cram, D. J. *Angew. Chem., Int. Ed.* **1988**, *27*, 1009.

[65] Rebek, J. *Science* **1987**, *235*, 1478.

[66] Wiester, M. J.; Ulmann, P. A.; Mirkin, C. A. *Angew. Chem., Int. Ed.* **2011**, *50*, 114.

[67] Meeuwissen, J.; Reek, J. N. H. *Nat. Chem.* **2010**, *2*, 615.

[68] Dalko, P. I.; Moisan, L. *Angew. Chem., Int. Ed.* **2001**, *40*, 3726.

[69] Hastings, C. J.; Pluth, M. D.; Bergman, R. G.; Raymond, K. N. *J. Am. Chem. Soc.* **2010**, *132*, 6938.

[70] Kheirabadi, M.; Çelebi-Ölçüm, N.; Parker, M. F. L.; Zhao, Q.; Kiss, G.; Houk, K. N.; Schafmeister, C. E. *J. Am. Chem. Soc.* **2012**, *134*, 18345.

[71] Brown, Z. Z.; Schafmeister, C. E. *J. Am. Chem. Soc.* **2008**, *130*, 14382.

[72] Gupta, S.; Schafmeister, C. E. *J. Org. Chem.* **2009**, *74*, 3652.

[73] Brown, Z. Z.; Schafmeister, C. E. *Org. Lett.* **2010**, *12*, 1436.

[74] Sigala, P. A.; Kraut, D. A.; Caaveiro, J. M. M.; Pybus, B.; Ruben, E. A.; Ringe, D.; Petsko, G. A.; Herschlag, D. *J. Am. Chem. Soc.* **2008**, *130*, 13696.

[75] Schwans, J. P.; Sunden, F.; Gonzalez, A.; Tsai, Y.; Herschlag, D. *J. Am. Chem. Soc.* **2011**, *133*, 20052.

[76] Gerlt, J. A.; Gassman, P. G. *Biochemistry* **1993**, *32*, 11943.

[77] Gerlt, J. A.; Gassman, P. G. *J. Am. Chem. Soc.* **1993**, *115*, 11552.

[78] Guthrie, J. P. *Chem. Biol.* **1996**, *3*, 163.

[79] Warshel, A.; Papazyan, A.; Kollman, P. A.; Cleland, W. W.; Kreevoy, M. M.; Frey, P. A. *Science* **1995**, *269*, 102.

[80] Cornell, W. D.; Cieplak, P.; Bayly, C. I.; Gould, I. R.; Merz, K. M.; Ferguson, D. M.; Spellmeyer, D. C.; Fox, T.; Caldwell, J. W.; Kollman, P. A. *J. Am. Chem. Soc.* **1995**, *117*, 5179.

[81] Chakrabarti, S.; Parker, M. F. L.; Morgan, C. W.; Schafmeister, C. E.; Waldeck, D. H. *J. Am. Chem. Soc.* **2009**, *131*, 2044.

[82] Brown, Z. Z.; Alleva, J.; Schafmeister, C. E. *Biopolymers* **2011**, *96*, 578.

[83] Schafmeister, C. E.; Brown, Z. Z.; Gupta, S. *Acc. Chem. Res.* **2008**, *41*, 1387.

[84] Palacin, S.; Chin, D. N.; Simanek, E. E.; MacDonald, J. C.; Whitesides, G. M. *J. Am. Chem. Soc.* **1997**, *119*, 11807.

[85] Maestro *Ligprep, Macromodel, Glide and QikProp; Schrodinger, LLC, New York, NY. 2011.* http://www.schrodinger.comLigprep.

[86] Jorgensen, W. L.; Maxwell, D. S.; Tirado-Rives, J. *J. Am. Chem. Soc.* **1996**, *118*, 11225.

[87] Zhao, Y.; Truhlar, D. G. *Acc. Chem. Res.* **2008**, *41*, 157.

[88] Zhao, Y.; Truhlar, D. G. *Theor. Chem. Acc.* **2008**, *120*, 215.

[89] Hehre, W. J.; Ditchfield, R.; Pople, J. A. *J. Chem. Phys.* **1972**, *56*, 2257.

[90] Hariharan, P. C.; Pople, J. A. *Theoret. Chim. Acta (Berl.)* **1973**, *28*, 213.

[91] Barone, V.; Cossi, M. *J. Phys. Chem. A* **1998**, *102*, 1995.

[92] Case, D. A.; Darden, T. A.; Cheatham, T. E.; Simmerling, C. L.; Wang, J.; Duke, R. E.; Luo, R.; Crowley, M.; Walker, R. C.; Zhang, W.; Merz, K. M.; Wang, B.; Hayik, S.; Roitberg, A.; Seabra, G.; Kolossváry, I.; Wong, K. F.; Paesani, F.; Vanicek, J.; Wu, X.; Brozell, S. R.; Steinbrecher, T.; Gohlke, H.; Yang, L.; Tan, C.; Mongan, J.; Hornak, V.; Cui, G.; Mathews, D. H.; Seetin, M. G.; Sagui, C.; Babin, V.; Kollman, P. A. *AMBER 11, Universtiy of California, San Francisco, 2011.*

4.0 Synthesis of Fauxteins, covalent molecular assemblies of spiroligomers

Chapter 4 details our use of spiroligomers as intermediate building blocks to create larger 3-dimensional assemblies that possess a "tertiary" structure. Highlights of this work are the first synthesis of a 3-oligomer bundled Fauxtein. Methods were developed to synthesize spiroligomers on solid support using cheap, more conventional resins. Methods were also developed to introduce ^{15}N into the Fauxtein at every internal DKP, which will aid in structural determination.

4.1 Introduction

A common goal among scientists across a diverse of fields is the design of materials that approach the capabilities of proteins. [1,2,3] One possible way to achieve this grand endeavor is the use of molecular scaffolding as a skeleton to direct functional groups into specific 3-dimensional orientations. [4,5] Borrowing from protein design, a hierarchal build up of well-defined and predictable structures that are both rich with functionality and chirality would be ideally suited. However, effiecient methods to execute this are limited.

Chapters 2 and 3 demonstrate that spiroligomers can position 2-4 functional residues in a localized area, which is the maximum a single oligomer can possess. A longstanding challenge is how to bring 5 or more groups into proximity. Modeling of the rigid structures show that all combinations of Pro4 building block of all stereochemistries result in rods and gentle turns. With this limited building capacity, the alternative strategy is the use of crosslinks to assemble multiple spiroligomers together.

Spiroligomers can be viewed as "secondary" structural units not unlike a single alpha-helix or beta-strand. The assembly and covalent crosslinking or 2 or 3 oligomers would create a "tertiary" structural unit where functional groups from different oligomers can work synergistically to perform a desired function. Multiple oligomers can potentially form larger external surfaces with unique functional topographies for binding proteins and other surfaces. Conversely, multiple oligomers can potentially form a shallow internal pocket for small molecule recognition or catalysis.

4.2 Results and Discussion

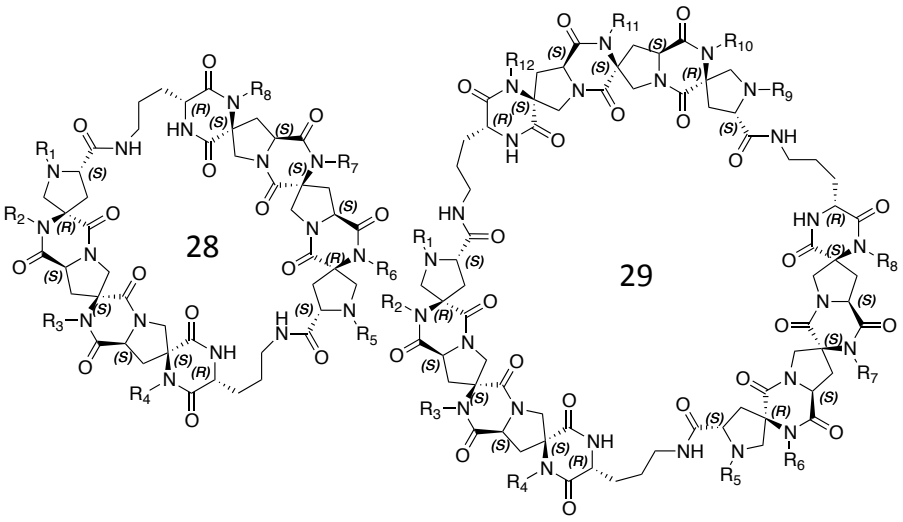

Figure 4-1. Structures of Spiroligomer macrocycles. Macrocycle **28** is derived from 2 oligomers and macrocycle **29** is derived from 3 oligomres.

From a retrosynthetic analysis, it is quite intuitive how to assemble multiple spiroligomers into macrocycles (**28** and **29**) by attaching the spiroligomers through amide bond from end to end. (Figure 4-1) Spiroligomers, in a reduced sense, can be viewed as essentially Fmoc amino acids and can be handled in similar manners in solution, but more appropriately, on solid phase synthesis. This is analogous to the synthesis of cyclic peptides.

Figure 4-2 outlines a more ambitious goal. Three spiroligomers cross-linked a total of 4 times, drawing them together in a bundle **31**. We envision this architecture to take on a variety of morphologies based on the length and stereochemistry of the spiroligomers, including bowl shapes that present a shallow pocket for binding of small molecules and catalysis. Furthermore, the shallow pocket will be made up of many chiral units and

surrounded with functionality. These two factors are very protein-like in essence and are uncommon features in other synthetic materials. For this reasons, this class of molecules are called “Fauxteins”.

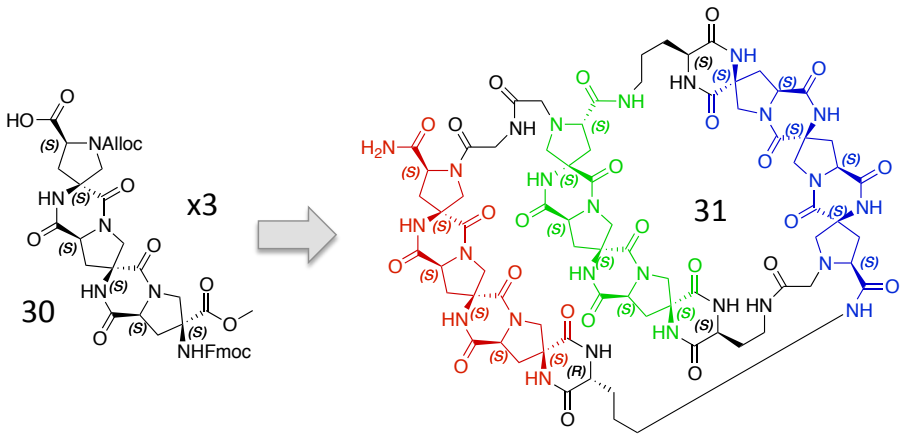

Figure 4-2. Structure of a spiroligomer bundle (called a “Fauxtein”) derived from 3 segments

To begin our pursuit of these molecular assemblies, we used a spiroligomer without any functional groups compound **30**. This would allow for the testing of whether 3 rigid bodies can undergo the crosslinking without the added bulk and possible clashes from the functional groups. To make Fauxtein **31** from 3 of spiroligomer **30**, the red oligomer can be attached to resin via its C-2 acid. From the C-4 Fmoc amino acid methyl ester on the other end can be modified with a linker in the form of a diamino acid residue. The second (blue) oligomer can then be attached, again form the C-2 acid and the process repeated until all 3 oligomers are attached. This leaves two crosslinks to be made either one at a time using orthogonal chemistries or both connected simultaneously under controlled conditions. (Figure 4-3) The length and the rigidity of the spiroligomers make it possible to introduce 2 sets of the same A-B ligation. For instance careful placement of two nucleophiles

(pyrrolidine nitrogens of the green and blue oligomers) and two electrophiles (bromoacetates on the red and green oligomers) onto the open form will result in only one possible reaction outcome. The two electrophiles won't cross-react nor will the two nucleophiles. With the right set up, as shown in Figure 4-3, the green oligomer nucleophile can only attack the electrophile on the red oligomer (bromine atom is highlighted in green). The green oligomer cannot physically reach the other electrophile (bromine atom is highlighted in blue). The rigidity of the spiroligomers prevents the blue electrophile to come in contact. The same argument can be made for the second nucleophile on the blue oligomer. Like with other macrocyclization and ligations, polymerization is a very real concern.

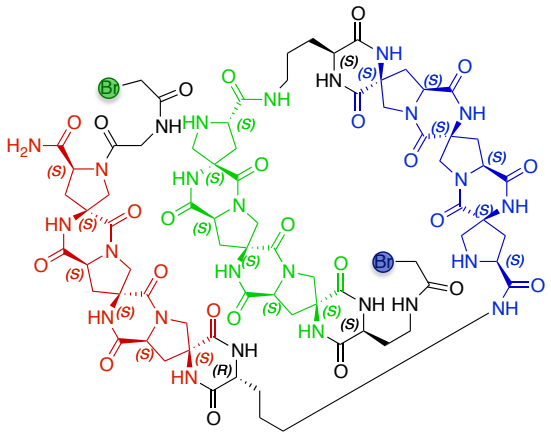

Figure 4-3. Crosslinking strategy for Fauxtein **31**

The synthesis of Fauxtein **31** starts on rink amide resin. (Scheme 4-1) Fmoc-1-naphthalanine is added to the resin to lend as a chromophore handle to monitor the chemistry by LCMS. This is accomplished by standard peptide solid phase chemistry using HATU and DIPEA in NMP. The Fmoc is removed with 20% piperidine in DMF solution and

the first oligomer **30** is coupled using PYAOP as a coupling agent with DIPEA in NMP. First the Alloc on the pyrrolidine nitrogen is removed with palladium catalyst and scavenger in DCM. Boc-Gly-OH is coupled using HATU and DIPEA in NMP. The Fmoc of the oligomer is removed with 20% piperidine in DMF. Fmoc-DAB(IvDde)-OH is coupled using HATU and DIPEA in NMP. Treatment with 20% piperidine in DMF removes the FMOC as well as closes the DKP. The IvDde group is removed with Hydrazine DMF solution. The second oligomer **30** is coupled using PYAOP and DIPEA in NMP. The Fmoc of the oligomer is removed with 20% piperidine in DMF. Fmoc-DAB(IvDde)-OH is coupled using HATU and DIPEA in NMP. Treatment with 20% piperidine in DMF removes the FMOC as well as closes the DKP. The IvDde group is removed with Hydrazine DMF solution. The third oligomer **30** is coupled using PYAOP and DIPEA in NMP. The Fmoc of the oligomer is removed with 20% piperidine in DMF. Fmoc-DAB(Boc)-OH is coupled using HATU and DIPEA in NMP. Treatment with 20% piperidine in DMF removes the FMOC as well as closes the DKP. The two Alloc groups on the pyrrolidine nitrogens of oligomer 2 and 3are removed with palladium catalyst and scavenger in DCM. Fmoc-Gly-OH is coupled using HATU and DIPEA in NMP. 20% piperidine in DMF is used to remove the two FMOC groups and the molecule is treated with bromoacetic anhydride and DIPEA in NMP.

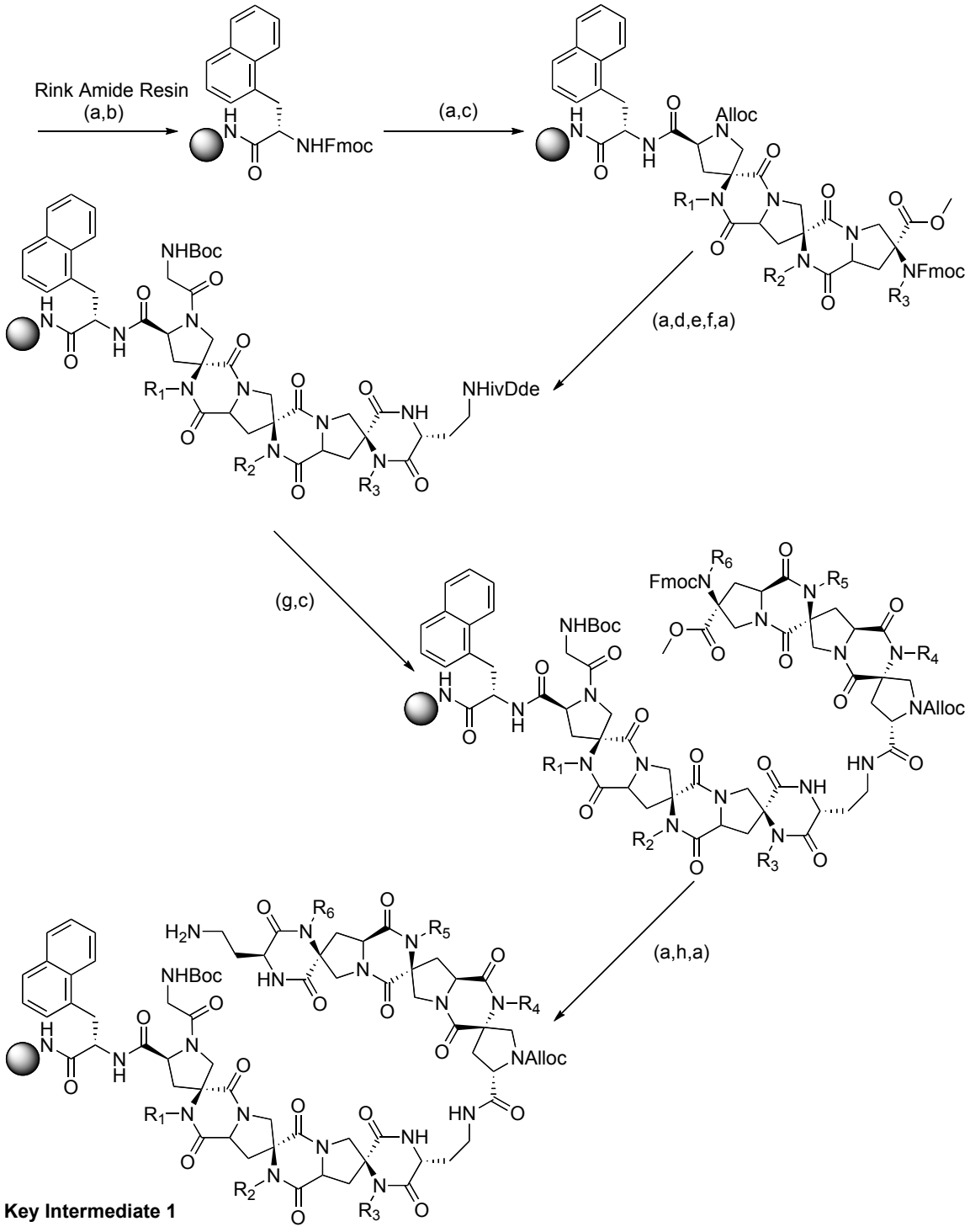

Key Intermediate 1

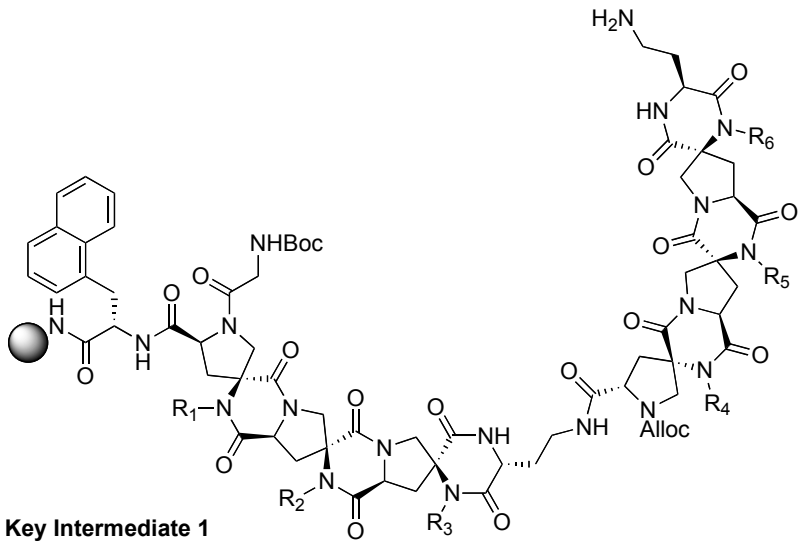

Key Intermediate 1

(c)

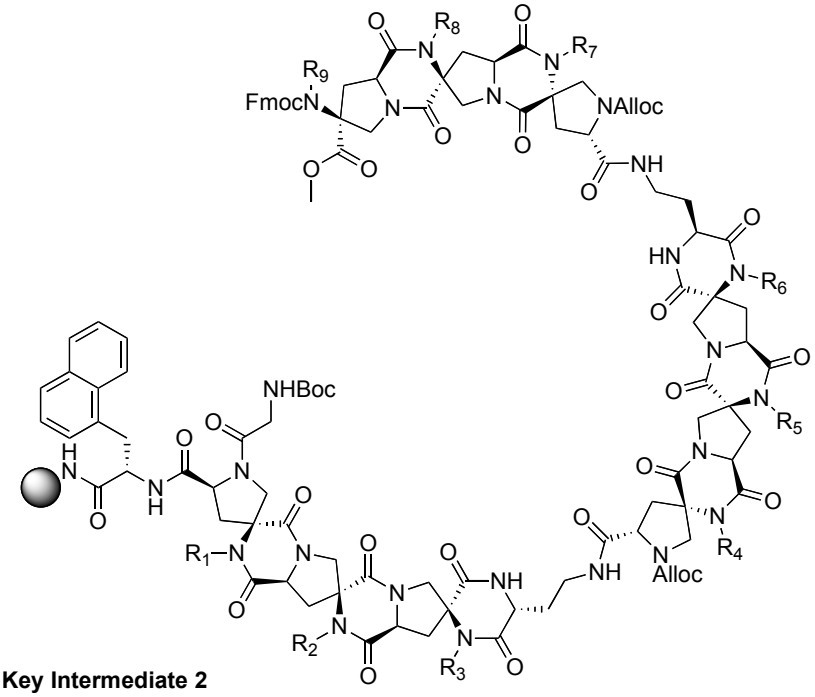

Key Intermediate 2

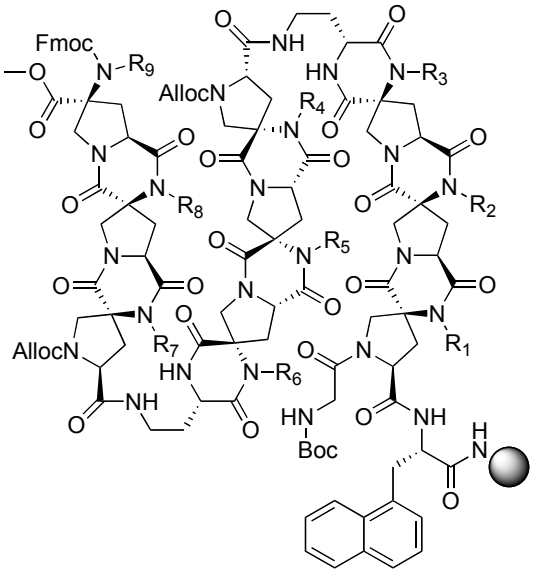

Key Intermediate 2

(n,a)

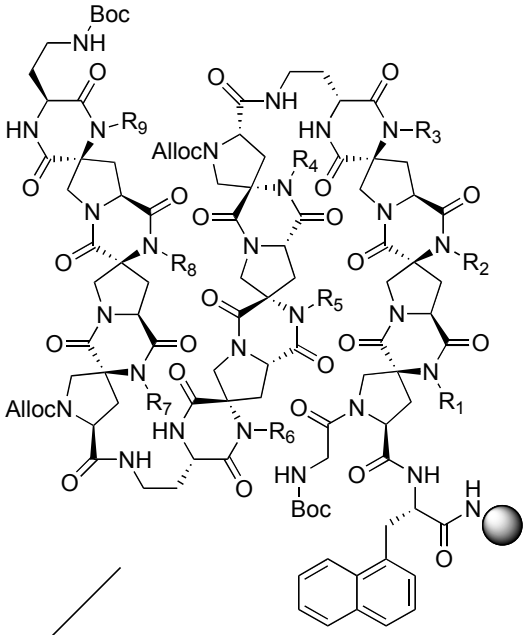

(e,o)

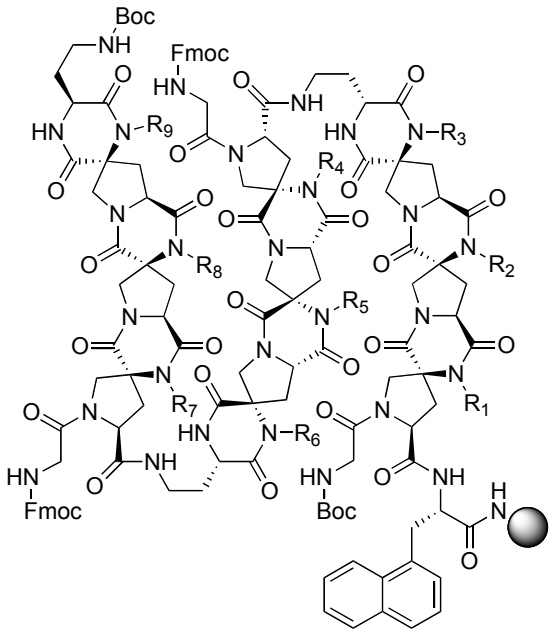

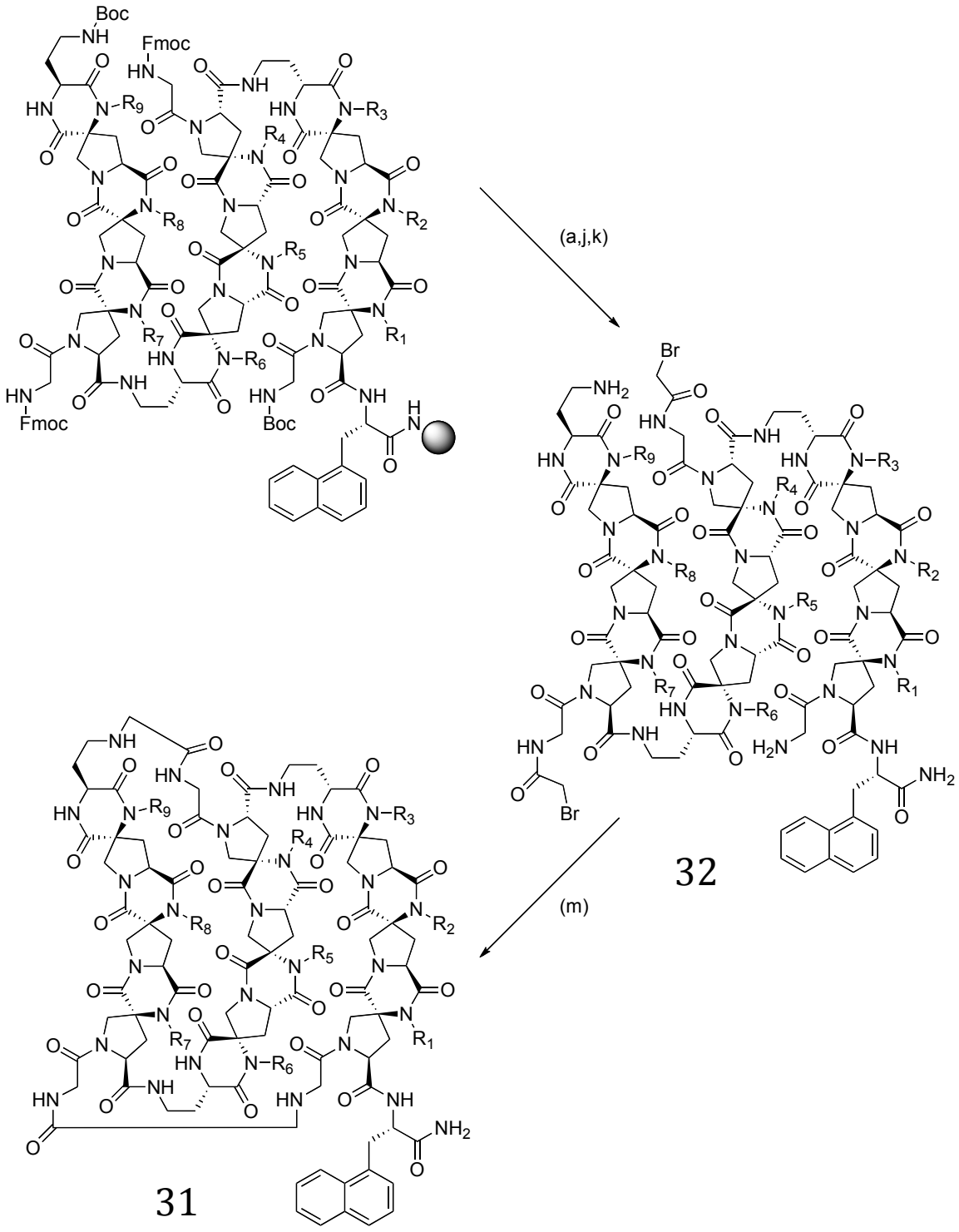

Scheme 4-1. Synthesis of Fauxtein **31**. (R=H) a) 1:4 Piperidine/DMF; b) Fmoc-Nal-OH, HATU, DIPEA, NMP; c) Spiroligomer, PyAOP, DIPEA, NMP; d) Fmoc-D-Dab(ivDde)-OH; e) $(PPh_3)_4Pd$, BH_3:DMA, DCM; f) Boc-Gly-OH, HATU, DIPEA, NMP; g) 1:49 Hydrazine/DMF; h) Fmoc-Dab(Fmoc)-OH, HATU, DIPEA, NMP; j) Bromoacetic Anhydride, DIPEA, NMP; k) 38:1:1 TFA/H_2O/TIPS; m) 1:99 TEA/DMF (0.0015M); n) Fmoc-Dab(Boc)-OH, HATU, DIPEA, NMP; o) Fmoc-Gly-OH, HATU, DIPEA, NM

Treatment with TFA soln removed all the BOC groups and cleaves the molecule from the resin to yield the open form **32**. The additional crosslinks can be formed by treatment with 1:99 TEA/DMF mixture (0.0015M) to provide **31**.

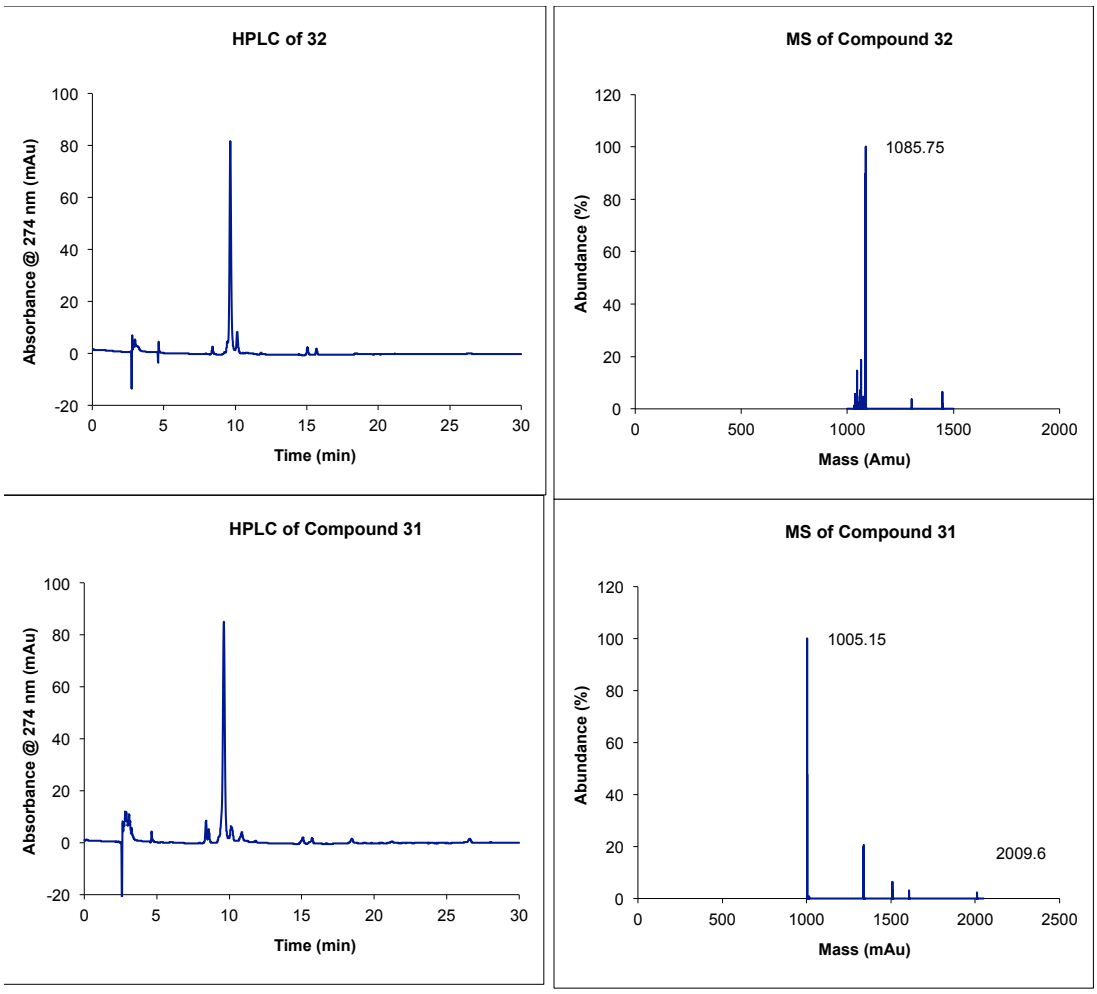

Figure 4-4. HPLC and MS traces for **32** and **31**.

The HPLC and MS traces for the **31** and **32** show only a slight change in the retention time but the crosslinking reaction can be followed by mass. (Figure 4-4) Encouraged by this result a new Fauxtein was designed. The new Fauxtein **33** design is shown in Figure 4-5. Every aspect of it has been maticulously optimized for solution characterization by NMR. It is fully functional. It is made of tetramers instead of trimers so that each spiroligomer can

carry three functional groups at the internal DKPs. The stereochemistry was modeled using AMBER 94 force field to come up with a design that create as many inter-oligomer functional group interactions as possible. Additonally the functional groups in proximity are as different as possible. Every aspect of it has been maticulously optimized for solution characterization by NMR. Lastly and most importantly, the building blocks will be ^{15}N labelled at the C-4 position. [6] This will bring an additional dimensionality for solution characterization.

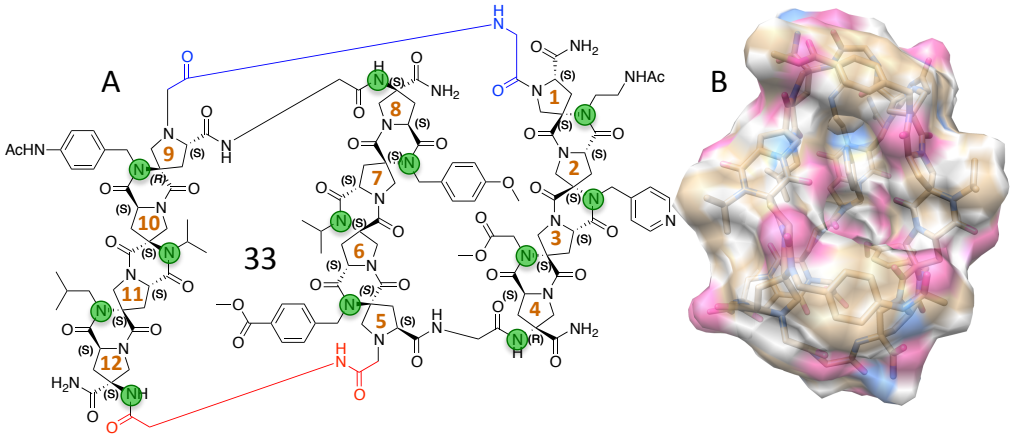

Figure 4-5 Structure of Fauxtein 33. (a) breakdown of structural features (b) AMBER 94 minimized structure with hydrophobic surface displayed.

Beyond modeling for characterization success, the model also possesses a useful structure. Based on our model, the bundle creates a shallow pocket with a unique topography. As designed, a nucleophilic catalyst is at the center of the shallow pocket by design. The crosslinking, stereochemistry, and functional group placement are all playing key role to define the ultimate shape. If the model is accurate, it should be a useful architecture for catalysis moving forward. The synthesis of Fauxtein **33** is much like that of Fauxtein **31** but will require 100s of milligrams of three different tetramers fully

functionalized and ^{15}N labeled. Both of these synthetic hurdles will need to be addressed.

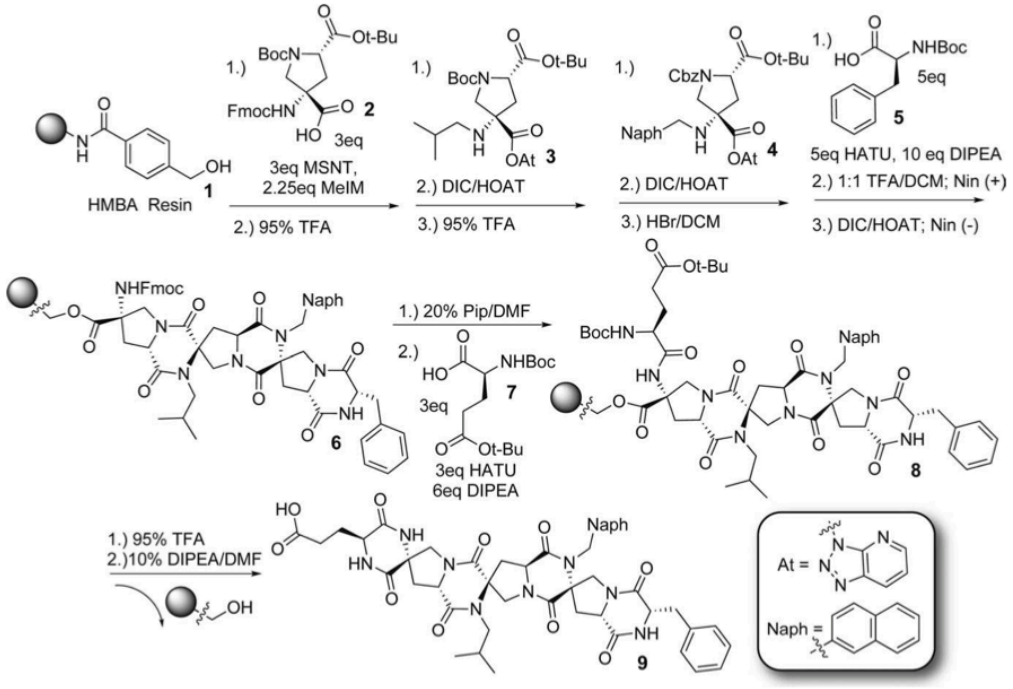

Scheme 4-2. Solid Phase Synthesis of Functionalized Spiroligomers [7]

The previous synthesis of functionized oligomers is shown in Scheme 4-2. [7] A summary of the approach is that it assembles the Pro4 monomers together with both amide bonds at once forming a DKP after each coupling step. It requires strong acid at regular intervals to remove the pyrrolidine nitrogen and C-2 acid protecting groups. The use of strong acid limits the the scope of solid phase synthesis techniques and resin options. Previous mechanistic insight into the coupling reaction has elucidated a possible way to improve the synthesis. [8]

Figure 4-6 shows a competition experiment of one of the activated Pro4 building blocks (**B**) which is the activatied ester of Pro4 building block (**A**). (**B**) is reacted with an

excess of (**C**) and (**D**) to form two different products. (**C**) reacts with (**B**) via an acyl transfer reaction forming product (**E**). (**D**) reacts with (**B**) via a direct acylation reaction forming product (**F**). Monitoring of this complex reaction mixture by HPLC analysis show that Direct acylation is ~8 times more efficient than Acyl Transfer. Product (**F**) is completely stable to further attack by any nucleophiles. The C-4 nitrogen group is too hindered to be a competent nucleophile to react with anything and spontaneous DKP formation does not occur under any conditions as long as the C-2 acid is protected as an ester. However, as an acid it can react in the presence of dehydration reagents to form the DKP. The favorable and abundant formation of product (**F**) validates that with the appropriate pyrrolidine protecting group, the spiroligomer can be assembled with one amide bond followed by a rigidification step at the end as shown in Chapter 1.

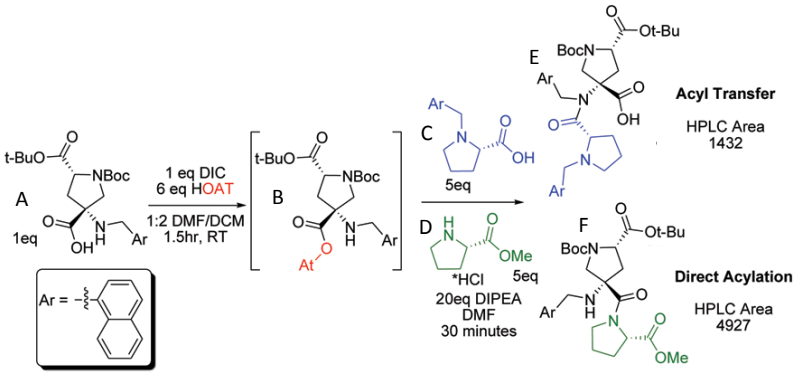

Figure 4-6. Functionalized bis-amino acid coupling competition reaction. [8]

The new protecting group selected was para-Nitrobenzylcarbamate (pNZ). [9, 10, 11] It can be installed via the chloroformate, which is commercially available. It is a great chromophore, which is helpful for monitoring reactions by HPLC. It possesses al the same orthogonality of the Cbz group and it has a very selective cleavage mechanism. The direct

target for deprotection is the reduction of the aryl nitro group down to the aniline. The aniline performs a spontaneous [1,6] elimination liberating a carboxylate that also eliminates to yield CO_2 furnishing the free amine. (Figure 4-7)

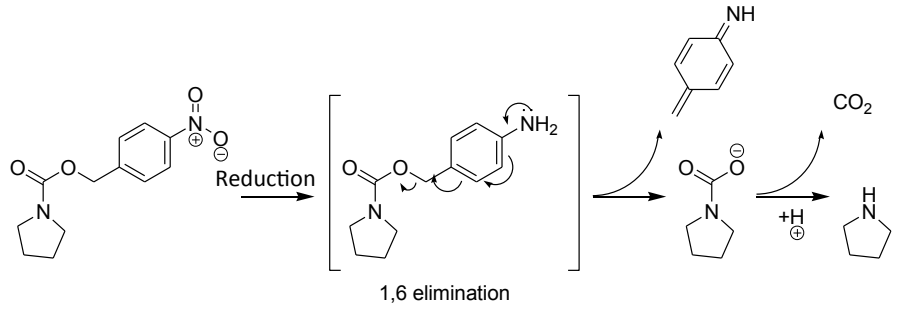

Figure 4-7. pNZ protecting group deprotection mechanism via nitro reduction.

The pNZ protecting group can be installed at the hydantoin stage of Pro4 synthesis (See Chapter 1). The Cbz protecting group on compound **7a** can be removed with Pd/C and H_2(g) in THF. After sparging the reaction with Ar(g), pNC-Cl and TEA can be added to make compound **34**. The hydantoin can be hydrolyzed by first reaction with Boc_2O and DMAP in THF followed by a dropwise addition of 2M KOH. The resulting amino acid can be reductively alkylated with any aldehyde and sodium cyanoborohydride in MeOH. The functionalized amino acid can then be activated with a mixture of HOAT and DIC in a DCM/DMF mixture to yield compound **35**. (Scheme 4-3)

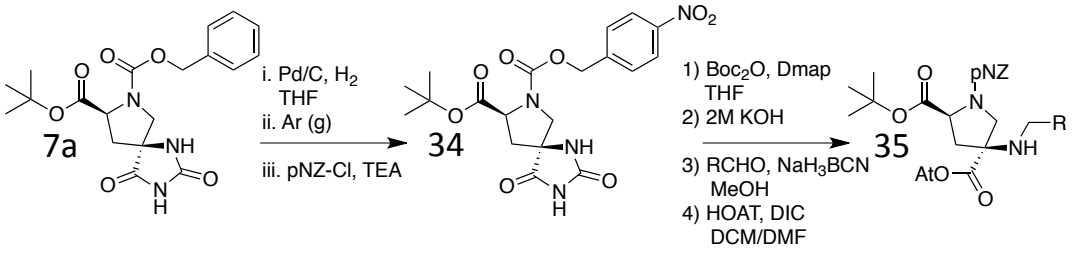

Scheme 4-3. Synthesis of Functionalized pNZ Pro4 building blocks.

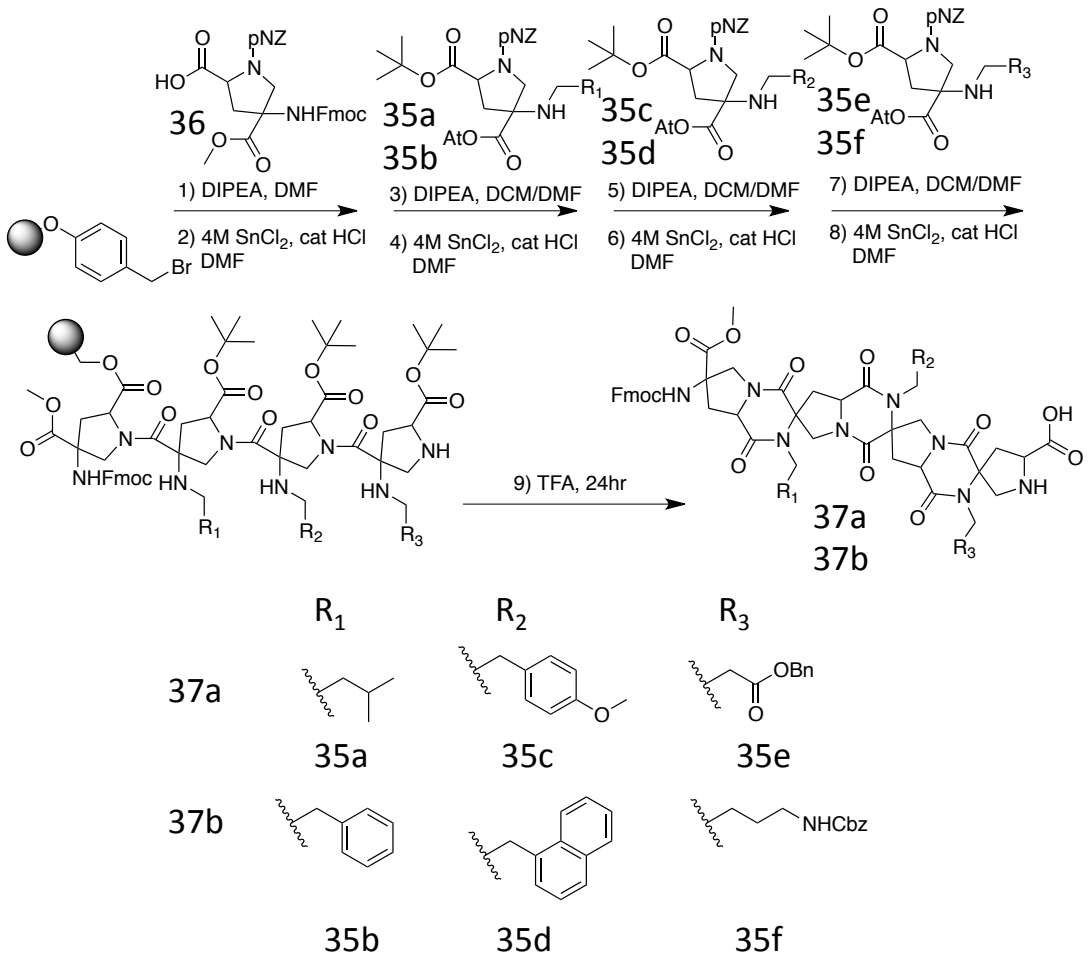

Scheme 4-4 Solid Phase Spiroligomer Synthesis using pNZ protecting group and direct acylation.

With the new protection scheme, spiroligomers can be assembled using more conventional resins for solid phase peptide synthesis like Rink amide and Wang resin which are cleavable by TFA. The addition of TFA will also cleave all of the tert-butyl esters liberating amino acid pair that can be dehydrated in a rigidification step. Scheme 4-4 outlines the oligomer synthesis. The first building block **36** is attached to the resin

followed by removal of the pNZ group using a 4M tin (II) chloride solution with catalytic acid. Each successive building block (**35a**, **35c**, **35e** to yield **37a** or **35b**, **35d**, **35f** to yield 37b) is attached followed by pNZ removal. Treatment with TFA provided a mixture of product by mass were identified as products with various combinations of open and closed DKPs. The TFA treatment and was extended to 24 hours to yield the fully closed product in 50-60% yield. Although, this initially surprised us, DKPs have been known to form under general acid catalysis mechanism. [12,13,14]. The scope and limitations of the spontaneous DKP formation for rigidifying the oligomers is still unknown. However, this has been a viable strategy to make a variety of oligomers on cheap, conventional resins in larger quantities in moderate yields.

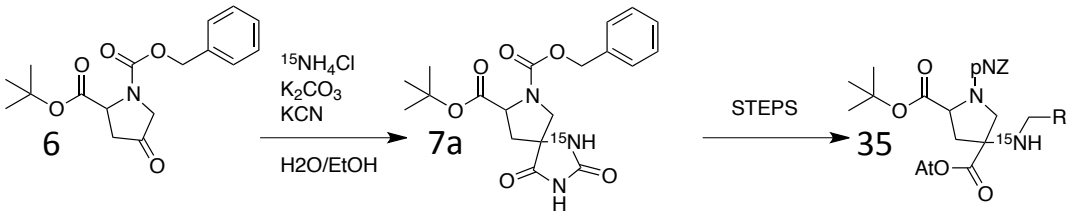

Scheme 4-5. Synthesis of ^{15}N label Pro4 building blocks for oligomer assembly

The Pro4 building block was labeled with ^{15}N with slight modification to the already existing building block synthesis. The amino acid is formed during the Bucherer Berg step, which uses a mixture of ammonium carbonate and potassium cyanide. The C-4 nitrogen comes from the ammonia. The commercially available source of ^{15}N comes from ammonium chloride. To make the ^{15}N labeled building block, a mixture of potassium cyanide, ^{15}N ammonium chloride, and potassium carbonate are used in a water/Ethanol mixture. (Scheme 4-5)

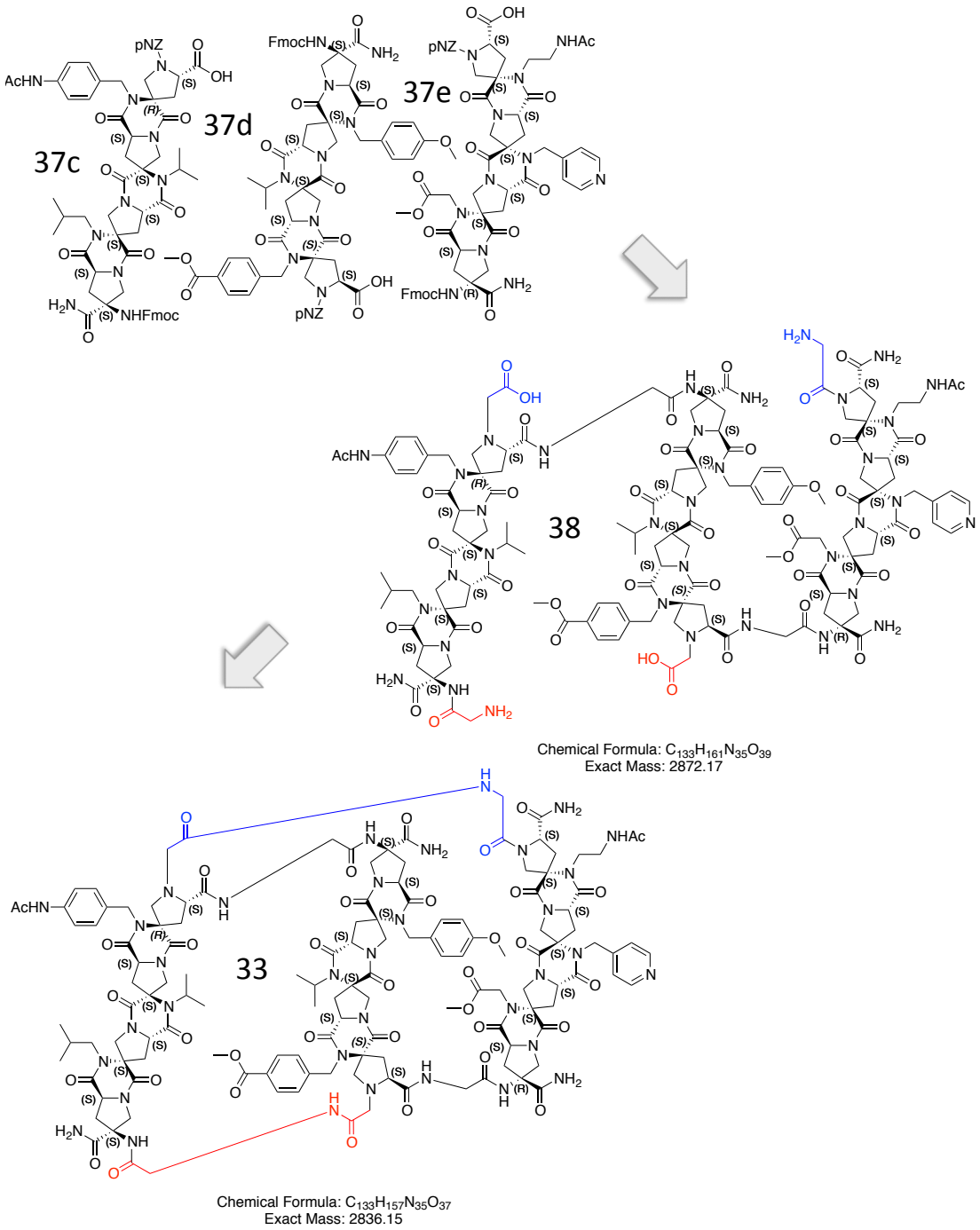

Figure 4-8. Assembly of Fauxtein **33** from oligomers **37c**, **37d**, and **37e** as shown in Scheme 4-1 to obtain intermediate **38**. Fauxtein 33 was afforded after dropwise addition of intermediate **38** to a rapidly stirring solution of PyAOP and DIPEA In DCM under dilute conditions.

With ^{15}N labeled building blocks and a means to assemble them into oligomers, the 3 oligomers need to assemble Fauxtein **33** were synthesized. (Figure 4-8, Oligomers **37c**, **37d**, **37e**) Following the methods outlined for Fauxtein **31**, Fauxtein **33** was assembled. The setup for crosslinking here is different than that of Fauxtein **31** where bromoacetates and amines were used. For Fauxtein **33**, acylation is the reaction for crosslinking. Intermediate **38** possess 2 carboxylic acids and 2 amines. As with before, the acids and amines are positioned to offer only one competent reaction pathway (Figure 4-8, colored red and blue). The length and rigidity of the spiroligomer prevents the blue acid and red amine, and the red acid and blue amine from reacting with one another respectively. Intermediate **38** was dissolved in a DCM to a concentration of 6 mM. This solution was added dropwise at a rate of 12.5 uL/min from a syringe pump to a stirring DCM solution of equal volume of PyAOP and DIPEA. Figure 4-8 shows the HPLC and MS traces for the intermediate **38** and Fauxtein **33**. A very large change of retention time is observed which is consistent with lose of two free acids and two free amines. (Figure 4-9, peaks are highlighted in yellow) The observed change in mass is consistent with the loss of two water molecules. The (m+2)/2 masses are observed for both compounds. The recovery of Fauxtein **33** on small scale was encouraging, however, scale up attempts did not provide sufficient quantities. Efforts to increase the quantity of Fauxtein **33** are currently under way.

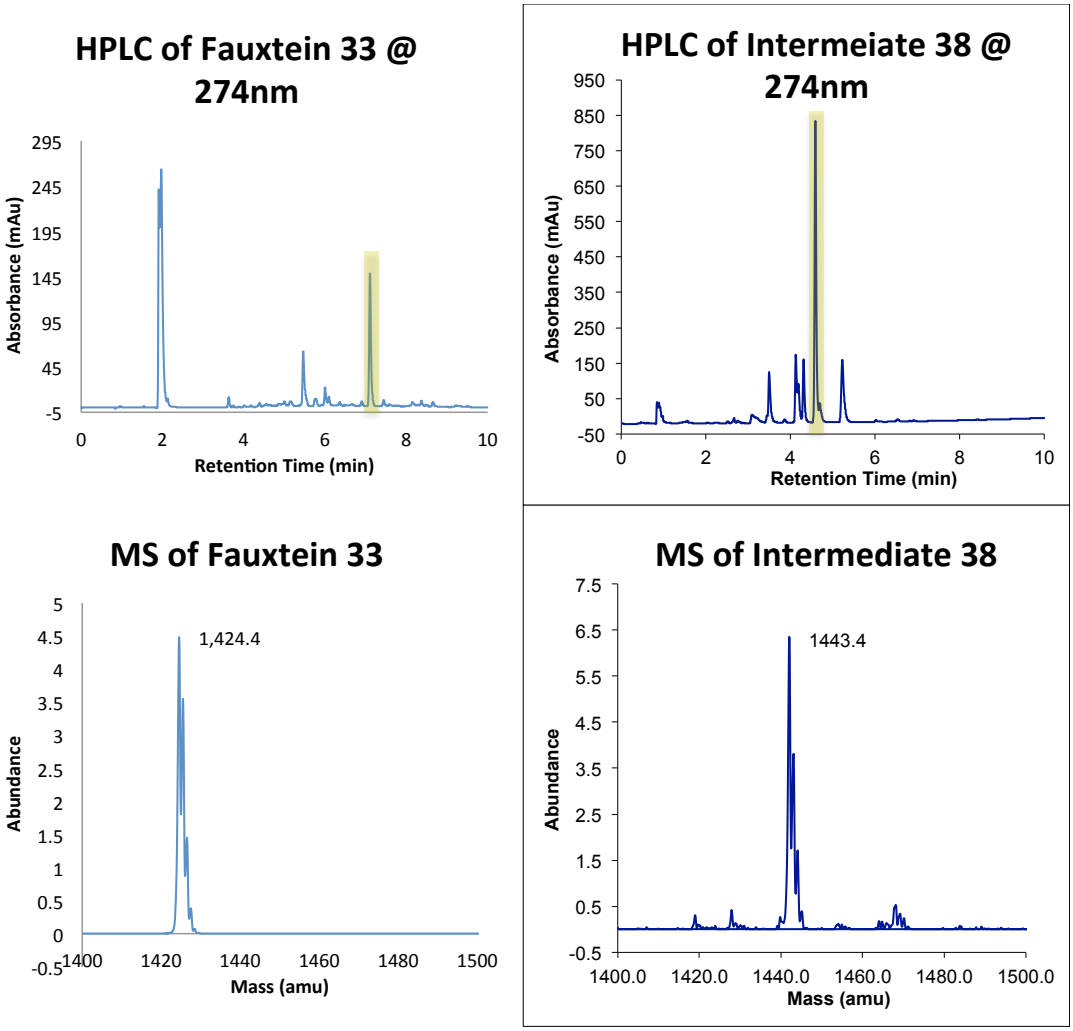

Figure 4-9. HPLC and MS traces for Fauxtein **33** and Intermediate **38**.

4.3 Conclusion

Progress has been made towards the realization of Fauxteins with the first evidence of the formation of a fully functionalized assembly. Along the path to this molecule, several advances in the building block chemistry and oligomer chemistry has been realized. These advances are of general interest and have impact other current ongoing research. Much work still remains not only to routinely making these complex systems but also to characterize and fully understand them.

4.4 Experimental Details

General Methods:

All Bis-amino acids were synthesized according to established literature procedure. All amino acids including diamines were purchased from either Novabiochem or Bachem. O-(7-Azabenzotriazole-1-yl)-N, N,N'N'-tetramethyluronium hexafluorophosphate (HATU) and 1-Hydroxy-7-azabenzotriazole (HOAT) were purchased from Genscript. All other reagent were purchased from Aldirch. Flash Chromatography was performed on an ISCO CombiFlash Rf with ISCO prepackaged silica gel or C 18 columns. Analytical HPLC-MS analysis was performed on a Agilent Series 1200 HPLC attached to an Agilent Single Quadrole ESI Mass Spec with a Waters Xterra MS C18 column (3.5um packing, 4.6 mm x 150mm) with a solvent system of water/acetonitrile with 0.1% formic acid at a flow rate of 0.8mL/min. Preparatory Scale HPLC purification was performed on a Agilent Series 1100 HPLC with a Waters Xterra column (5um packing, 7.8mm x 150mm) with a solvent system of water/acetonitrile with 0.1% formic acid at a flow rate of 3mL/min.

General procedure (A): Attachment to Trityl Resin

To a solution of trityl resin and the amino acid (0.9 equivalents based on resin loading) in DCM (10mL/g of resin) was added DIPEA (4 equivalents based on resin loading). The reaction mixture was stirred overnight. The solution was poured through a solid phase reactor to remove the resin from solution and washed with DMF, DCM, DMF, IPA, DMF, DCM and DMF.

General Procedure (B): Attachment to Brominated Wang Resin

To a solution of brominated Wang resin and the amino acid (0.9 equivalents based on resin loading) in DCM (10mL/g of resin) was added DIPEA (4 equivalents based on resin loading). The reaction mixture was stirred overnight. The solution was poured through a solid phase reactor to remove the resin from solution and washed with DMF, DCM, DMF, IPA, DMF, DCM and DMF.

General procedure (C): Attachment to NovaPEG Rink Amide Resin

To a solution of amino acid (3 equivalents based on resin loading) and HATU (3 equivalents based on resin loading in NMP (5mL/mmole of amino acid) was added DIPEA (6 equivalents based on resin loading). The reaction mixture was agitated for 5 minutes then added to a pre-swelled (with DMF) portion of resin in a solid phase reactor and stirred for 4 hours. The resin was filtered and washed with DMF, DCM, DMF, IPA, DMF, DCM and DMF.

General Procedure (D): Coupling of Functionalized Bis-amino acid

To a solution of the functionalized bis-amino acid (3 equivalents relative to resin loading) and HOAT (6 equivalents relative to bis-amino acid) in 1:2 DMF/DCM (18mL/mmole) was added DIC (1equivalent relative to bis-amino acid). The reaction was stirred for 90 minutes then added to a pre-swelled (with DMF) portion of resin in a solid phase reactor. A solution of DIPEA (2 equivalents based on resin loading) in DMF (6mL/mmole) and stirred for 3 hours. An additional aliquiot of DIC (3 equivalents relative to resin loading) was added and stirred for 1 hour. The resin was filtered and washed with DMF, DCM, DMF, IPA, DMF, DCM and DMF.

General Procedure (E): Solution Coupling of Functionalized Bis-amino acid

To a solution of the functionalized bis-amino acid (1 equivalent) and HOAT (6 equivalents) in 1:2 DMF/DCM (18mL/mmole) was added DIC (1equivalent). The reaction was stirred for 90 minutes then added to a second bis-amino acid (0.8 equivalents) and DIPEA (1.6 equivalents) in DMF (6mL/mmole). The reaction was stirred for 7.5 hours and an additional aliquiot of DIC (2 equivalents was added and stirred overnight. The reaction was diluted with EtOAc then washed with sat. NH_4Cl (aq) x 3, sat. NaCl (aq) x 1, sat. $NaHCO_3$ (aq) x 3, NaCl (aq) x 2, dried over Na_2SO_4, filtered, and concentrated under reduced pressure.

General procedure (F): HATU Coupling

To a solution of amino acid (3 equivalents based on resin loading) and HATU (3 equivalents based on resin loading in NMP (5mL/mmole of amino acid) was added DIPEA (6 equivalents based on resin loading). The reaction mixture was agitated for 5 minutes then added to a pre-swelled (with DMF) portion of resin in a solid phase reactor and stirred for 4 hours. The resin was filtered and washed with DMF, DCM, DMF, IPA, DMF, DCM and DMF.

General procedure (G): PyAOP Coupling

To a solution of amino acid (3 equivalents based on resin loading) and PyAOP (3 equivalents based on resin loading in NMP (5mL/mmole of amino acid) was added DIPEA (6 equivalents based on resin loading). The reaction mixture was agitated for 5 minutes then added to a pre-swelled (with DMF) portion of resin in a solid phase reactor and stirred

for 12 hours. The resin was filtered and washed with DMF, DCM, DMF, IPA, DMF, DCM and DMF.

General Procedure (H): Boc and *tert*-Butyl Ester Deprotection

A solution of 5% TIPS in TFA (10mL/mmole based on resin loading) was added to a pre-swelled (with DMF) portion of resin in a solid phase reactor and stirred for 30 minutes. The resin was filtered and washed with DMF, DCM, DMF, IPA, DMF, DCM and DMF. This process was repeated in duplicate to ensure complete deprotection.

General Procedure (I): Cbz and *tert*-Butyl Ester Deprotection

A solution of the Spiroligomer and 1:2 HBr/AcOH (5mL/mmole) in DCM (5mL/mmole) was stirred for 4 hours. The reaction mixture was concentrated under reduced pressure.

General procedure (J): Fmoc Deprotection

A solution of 20% of piperidine in DMF (10mL/mmole based on resin loading) was added to a pre-swelled (with DMF) portion of resin in a solid phase reactor and stirred for 15 minutes. The resin was filtered and washed with DMF, DCM, DMF, IPA, DMF, DCM and DMF. This process was repeated in duplicate to ensure complete deprotection.

General procedure (K): Alloc Deprotection

A solution of borane:dimethylamine complex (6 equivalents based on resin loading) in DCM (10mL/mmole based on resin loading) was added to a pre-swelled (with DMF) portion of resin in a solid phase reactor and stirred for 5 minutes. To this solution was

added a solution of tetrakis(triphenylphosphine)palladium(0) (0.1 equivalents based on resin loading) in DCM (10mL/mmole based on resin loading). The reaction mixture was stirred for 2 hour. The resin was filtered and washed with DMF, DCM, DMF, IPA, DMF, DCM and DMF.

General procedure (L): IvDde Deprotection

A solution of 2% of hydrazine in DMF (10mL/mmole based on resin loading) was added to a pre-swelled (with DMF) portion of resin in a solid phase reactor and stirred for 20 minutes. The resin was filtered and washed with DMF, DCM, DMF, IPA, DMF, DCM and DMF. This process was repeated in triplicate to ensure complete deprotection.

General procedure (M): Bromoacetate Acylation

To a solution of bromoacetic anhydride (3 equivalents based on resin loading) in NMP (5mL/mmole of amino acid) was added DIPEA (6 equivalents based on resin loading). The reaction mixture was agitated for 5 minutes then added to a pre-swelled (with DMF) portion of resin in a solid phase reactor and stirred for 4 hours. The resin was filtered and washed with DMF, DCM, DMF, DCM, DMF, DCM and DMF

General Procedure (N): Alloc Protection

To a solution of the oligomer (1 equivalent) and Alloc-Cl (1.1 equivalents) in DCM (10mL/mmole) was added DIPEA (3 equivalents). The reaction mixture was stirred overnight then diluted with EtOAc. The solution was washed with sat. NH_4Cl (aq) x 3, sat. NaCl (aq) x 2, dried over Na_2SO_4, filtered, and concentrated under reduced pressure.

General Procedure (O): Safety Catch Cleavage from HMBA resin

A solution of 10% DIPEA in DMF (10 mL/mmole based on resin loading was added to a portion of resin and stirred overnight. The resin was filtered. The filtrate was concentrated, reconstituted in 50% MeCN in water (0.1% formic acid) and freeze-dried.

General procedure (P): Liberation from Trityl or Rink Amide Solid Phase Resins

A solution of 5% TIPS and 5% water in TFA (20 mL/mmole based on resin loading was added to a portion of resin (successively washed with DCM and MeOH, and thoroughly dried under vacuum) and stirred for 4 hours. The resin was filtered and rinsed with TFA. The filtrate was concentrated, reconstituted in 50% MeCN in water (0.1% formic acid) and freeze-dried.

General Procedure (Q): Rigidification of Spiroligomers:

A solution of the spiroligomer in 0.5 M NH_4OAc in MeCN/water 1:1 (20mL/umole) was heated to 60^{o}C and stirred overnight and freeze-dried.

General Procedure (R): Cross-linking in Aqueous Solution:

A solution of the spiroligomer linear assembly in 50% MeCN in water (22mL/umole) was added dropwise to a solution of 0.05M pH 7 Phosphate Buffer (44ml/umole) and stirred for 60 hours and freeze-dried.

General Procedure (S): Cross-linking in Organic Solution:

A solution of the spiroligomer linear assembly in DMF (22mL/umole) was added dropwise to a solution of 1.5% TEA in DMF (44mL/umole) and stirred overnight. The solution was added dropwise to a solution of diethyl ether (666mL/umole, chilled to –20^{o}C) and centrifuged. The solvent was decanted and the pellet was reconstituted in 50% MeCN in water (0.1% formic acid) and freeze-dried.

General procedure (T): pNZ Deprotection

A 4M solution of tin (II) chloride with 64 uM HCl in DMF (10mL/mmole based on resin loading) was added to a pre-swelled (with DMF) portion of resin in a solid phase reactor and stirred for 30 minutes. The resin was filtered and washed with DMF, DCM, DMF, IPA, DMF, DCM and DMF. This process was repeated in triplicate to ensure complete deprotection.

General procedure (U): Rigidification with deprotection from Wang resin

A solution of TFA (20 mL/mmole based on resin loading was added to a portion of resin (successively washed with DCM and MeOH, and thoroughly dried under vacuum) and stirred for 24 hours. The resin was filtered and rinsed with TFA. The filtrate was concentrated, reconstituted in 50% MeCN in water (0.1% formic acid) and freeze-dried.

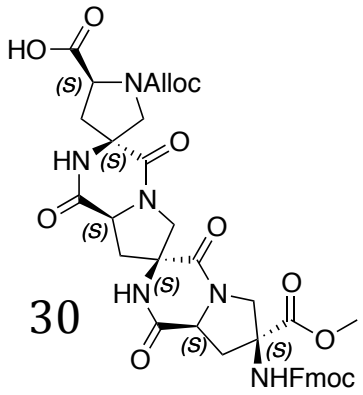

30

Spiroligomer 30:

Pro4ssAHFM (494.5mg, 1mmole) was attached to Trityl resin (1g, 1.1mmole) according to general procedure (A) using DCM (10mL) and DIPEA (696.8uL, 4mmoles). The terminal Fmoc group was removed according to general procedure (J) using 20% piperidine in DMF (900uL).

Pro4ssBHFM (1.53g, 3mmole) was coupled according to general procedure (F) using HATU (1.14g, 3mmoles), NMP (15mL), and DIPEA (1.05mL, 6mmoles). The terminal Fmoc group was removed according to general procedure (J) using 20% piperidine in DMF (900uL). The residue was reconstituted in 50% MeCN in water (0.1% formic acid) and purified by reverse-phase chromatography (gradient elution over 30 minutes from water (0.1% formic acid) to 50% MeCN in water (0.1% formic acid). Desired fractions were combined and freeze-dried to yield a white powder.

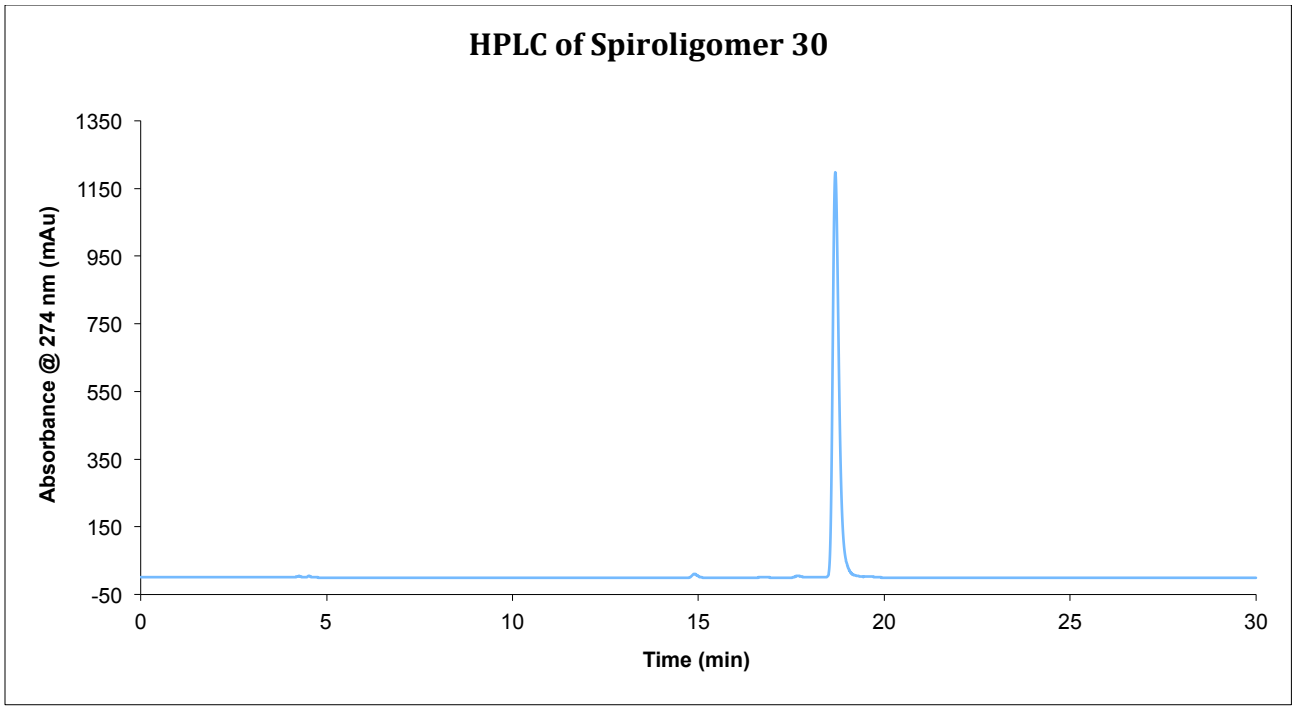

Figure 4-10. HPLC of Spiroligomer **30**

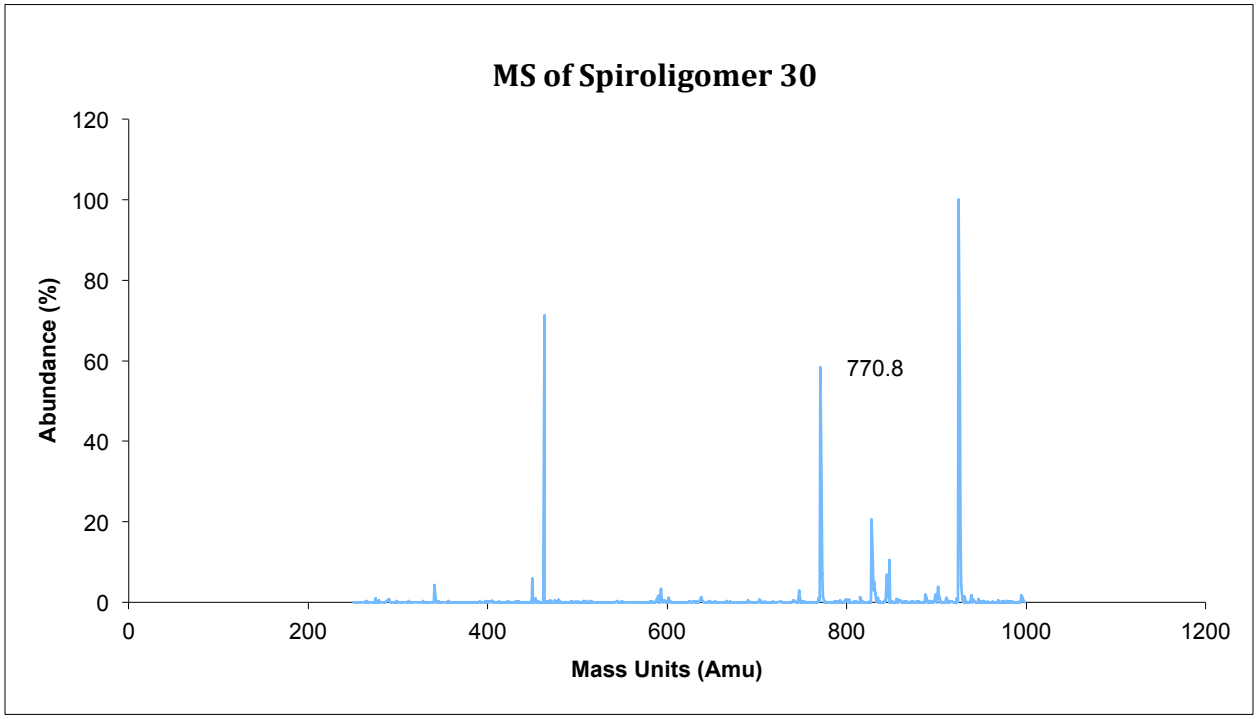

Figure 4-11. MS of Spiroligomer **30**

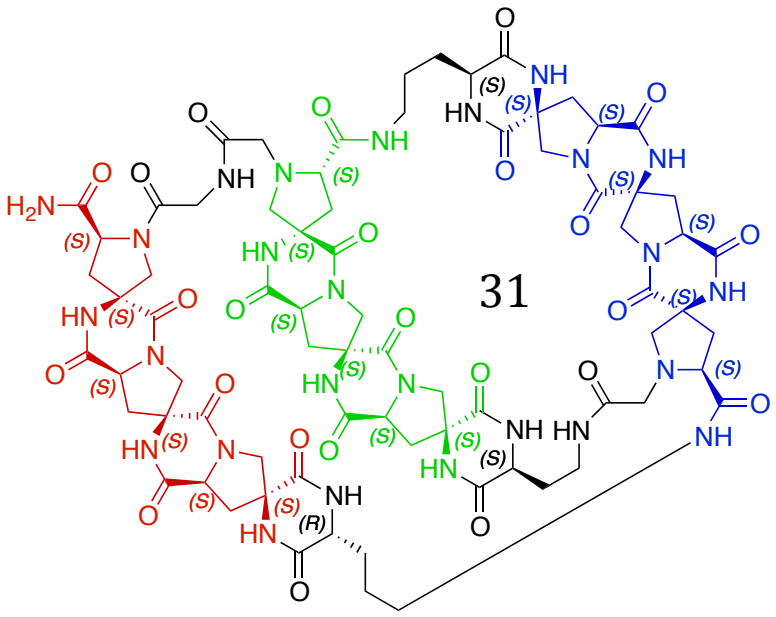

Fauxtein 31:

NovaPEG Rink Amide Resin (81.1mg, 30umoles loading) was placed in an 8mL solid phase reactor. (S)-N-Fmoc-1-Naphthylalanine-OH (39.4mg, 90umoles) was attached according to general procedure (C) using HATU (34.2mg, 90umoles), NMP (450uL) and DIPEA (31.4uL, 180umoles). The terminal Fmoc group was removed according to general procedure (J) using 20% piperidine in DMF (900uL).

Oligomer **30** (69.4mg, 90umoles) was coupled according to general procedure (G) using PyAOP (46.9mg, 90umoles), NMP (450uL), and DIPEA (31.4uL, 180umoles). The terminal Fmoc group was removed according to general procedure (J) using 20% piperidine in DMF (900uL).

Fmoc-D-Dab(IvDde)-OH (49.2mg, 90umoles) was coupled according to general procedure (F) using HATU (34.2mg, 90umoles), NMP (450uL) and DIPEA (31.4uL, 180umoles). The terminal Fmoc group was removed according to general procedure (J) using 20%

piperidine in DMF (900uL). Exposure to the deprotection solution was extended to 2 hours to enable complete diketopiperazine closure.

The Alloc group was removed according to general procedure (K) using borane:dimethylamine complex (10.6mg, 180umoles) in DCM (450uL) and tetrakis(triphenylphosiphine)palladium(0) (10.4mg, 9umoles) in DCM (450uL). Boc-Gly-OH (15.8mg, 450umoles) was coupled according to general procedure (F) using HATU (34.2mg, 90umoles), NMP (450uL), and DIPEA (31.4uL, 180umoles). The terminal IvDde group was removed according to general procedure (L) using 2% Hydrazine in DMF (900uL).

Oligomer **30** (69.4mg, 90umoles) was coupled according to general procedure (G) using PyAOP (46.9mg, 90umoles), NMP (450uL), and DIPEA (31.4uL, 180umoles). The terminal Fmoc group was removed according to general procedure (J) using 20% piperidine in DMF (900uL).

Fmoc-L-Dab(Fmoc)-OH (50.6mg, 90umoles) was coupled according to general procedure (F) using HATU (34.2mg, 90umoles), NMP (450uL) and DIPEA (31.4uL, 180umoles). The terminal Fmoc group was removed according to general procedure (J) using 20% piperidine in DMF (900uL). Exposure to the deprotection solution was extended to 2 hours to enable complete diketopiperazine closure.

Oligomer 30 (69.4mg, 90umoles) was coupled according to general procedure (G) using PyAOP (46.9mg, 90umoles), NMP (450uL), and DIPEA (31.4uL, 180umoles). The terminal Fmoc group was removed according to general procedure (J) using 20% piperidine in DMF (900uL).

Fmoc-L-Dab(Boc)-OH (39.6mg, 90umoles) was coupled according to general procedure (F) using HATU (34.2mg, 90umoles), NMP (450uL) and DIPEA (31.4uL, 180umoles). The terminal Fmoc group was removed according to general procedure (J) using 20% piperidine in DMF (900uL). Exposure to the deprotection solution was extended to 2 hours to enable complete diketopiperazine closure.

The Alloc group was removed according to general procedure (K) using borane:dimethylamine complex (10.6mg, 180umoles) in DCM (450uL) and tetrakis(triphenylphosiphine)palladium(0) (10.4mg, 9umoles) in DCM (450uL). Fmoc-Gly-OH (53.5mg, 180umoles) was coupled according to general procedure (F) using HATU (68.4mg, 180umoles), NMP (900uL) and DIPEA (62.8uL, 360umoles).

Bromoacetates were introduced according to general procedure (M) using bromoacetic anhydride (46.8mg, 180umoles), NMP (900uL), and DIPEA (62.8uL, 360umoles). The linear assembly of spiroligomer was liberated from the resin according to general procedure (P) using 95% TFA/2.5% Tips/2.5% Water (1.8mL) to **32**.

32 (4.1mg, 2umoles) was cross-linked according to general procedure [R] or [S] using DMF (44mL) and 1.5% TEA in DMF (88mL/umole) or 50% MeCN in water (44mL) and 0.05M pH7 Phosphate Buffer (88mL). The residue was reconstituted in 50% MeCN in water (0.1% formic acid) and purified by reverse-phase chromatography (gradient elution over 30 minutes from water (0.1% formic acid) to 50% MeCN in water (0.1% formic acid). Desired fractions were combined and freeze-dried to yield **31** as a white powder.

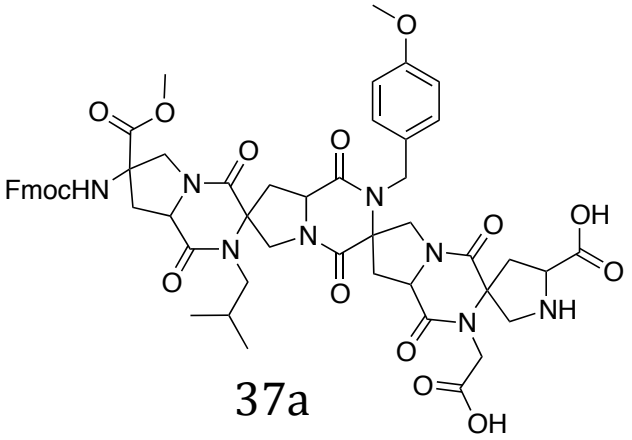

37a

Spiroligomer 37a

Pro4ssNHFM (1.65g, 1mmoles) was attached to brominated Wang resin (1.1, 1.1 mmoles) according to general procedure (B) using DMF (10mL) and DIPEA (696.8uL, 4mmoles). The terminal pNZ group was removed according to general procedure (T) using the 4M tin (II) chloride solution (10mL).

Compound **36a** (3 mmoles) was coupled according to general procedure (D) using HOAT (2.45g , 18 mmoles), 1:2 DMF/DCM (54mL), and DIC (468uL, 3mmoles) followed by DIPEA (3.48uL, 20mmoles) in DMF (18 mL). The terminal pNZ group was removed according to general procedure (T) using the 4M tin (II) chloride solution (10mL).

Compound **36c** (3mmoles) was coupled according to general procedure (D) using HOAT (2.45g , 18 mmoles), 1:2 DMF/DCM (54mL), and DIC (468uL, 3mmoles) followed by DIPEA (3.48uL, 20mmoles) in DMF (18 mL). The terminal pNZ group was removed according to general procedure (T) using the 4M tin (II) chloride solution (10mL).

Compound **36e** (3mmoles) was coupled according to general procedure (D) using HOAT (2.45g , 18 mmoles), 1:2 DMF/DCM (54mL), and DIC (468uL, 3mmoles) followed by DIPEA (3.48uL, 20mmoles) in DMF (18 mL). The terminal pNZ group was removed according to general procedure (T) using the 4M tin (II) chloride solution (10mL). The spiroligomer

was liberated from the resin according to general procedure (U) using 20mL of TFA. The residue was reconstituted in 50% MeCN in water (0.1% formic acid) and purified by reverse-phase chromatography (gradient elution over 30 minutes from water (0.1% formic acid) to 50% MeCN in water (0.1% formic acid). Desired fractions were combined and freeze-dried to yield **37a** as a white powder.

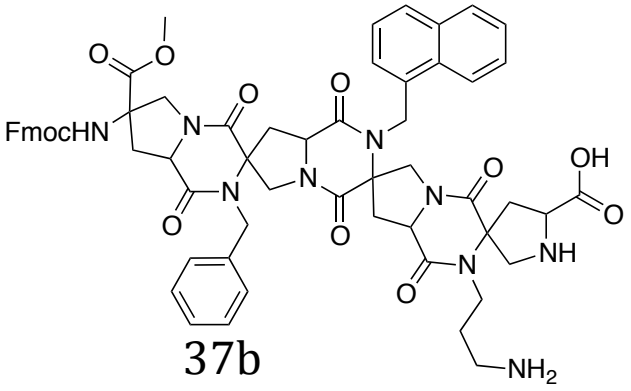

37b

Spiroligomer 37b

Pro4ssNHFM (1.65g, 1mmoles) was attached to brominated Wang resin (1.1, 1.1 mmoles) according to general procedure (B) using DMF (10mL) and DIPEA (696.8uL, 4mmoles). The terminal pNZ group was removed according to general procedure (T) using the 4M tin (II) chloride solution (10mL).

Compound **36b** (3 mmoles) was coupled according to general procedure (D) using HOAT (2.45g , 18 mmoles), 1:2 DMF/DCM (54mL), and DIC (468uL, 3mmoles) followed by DIPEA (3.48uL, 20mmoles) in DMF (18 mL). The terminal pNZ group was removed according to general procedure (T) using the 4M tin (II) chloride solution (10mL).

Compound **36d** (3mmoles) was coupled according to general procedure (D) using HOAT (2.45g , 18 mmoles), 1:2 DMF/DCM (54mL), and DIC (468uL, 3mmoles) followed by DIPEA

(3.48uL, 20mmoles) in DMF (18 mL). The terminal pNZ group was removed according to general procedure (T) using the 4M tin (II) chloride solution (10mL).

Compound **36f** (3mmoles) was coupled according to general procedure (D) using HOAT (2.45g , 18 mmoles), 1:2 DMF/DCM (54mL), and DIC (468uL, 3mmoles) followed by DIPEA (3.48uL, 20mmoles) in DMF (18 mL). The terminal pNZ group was removed according to general procedure (T) using the 4M tin (II) chloride solution (10mL). The spiroligomer was liberated from the resin according to general procedure (U) using 20mL of TFA. The residue was reconstituted in 50% MeCN in water (0.1% formic acid) and purified by reverse-phase chromatography (gradient elution over 30 minutes from water (0.1% formic acid) to 50% MeCN in water (0.1% formic acid). Desired fractions were combined and freeze-dried to yield **37b** as a white powder.

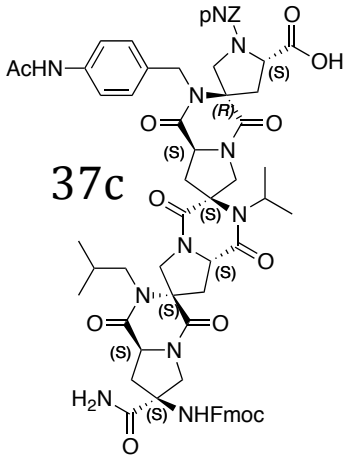

Spiroligomer 37c

Synthesized according to the same strategy as for Spiroligomer **37a** and **37b** using ^{15}N Pro4 building block.

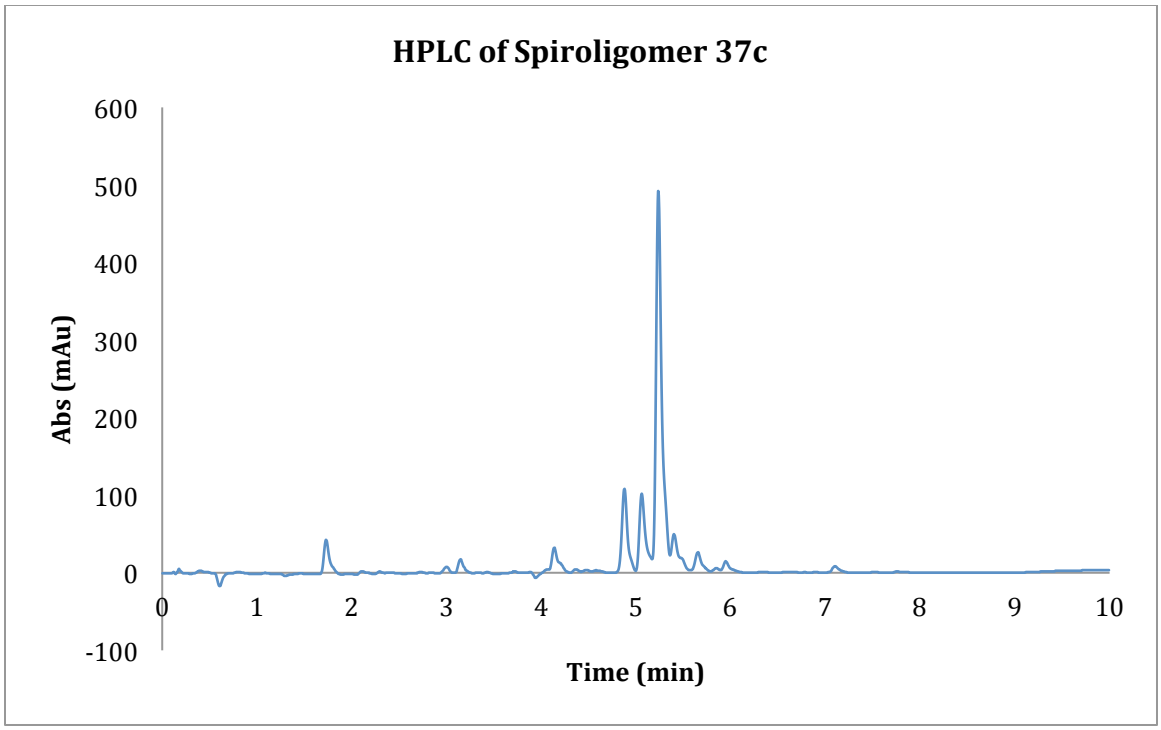

Figure 4-12. HPLC of Spiroligomer **37c**

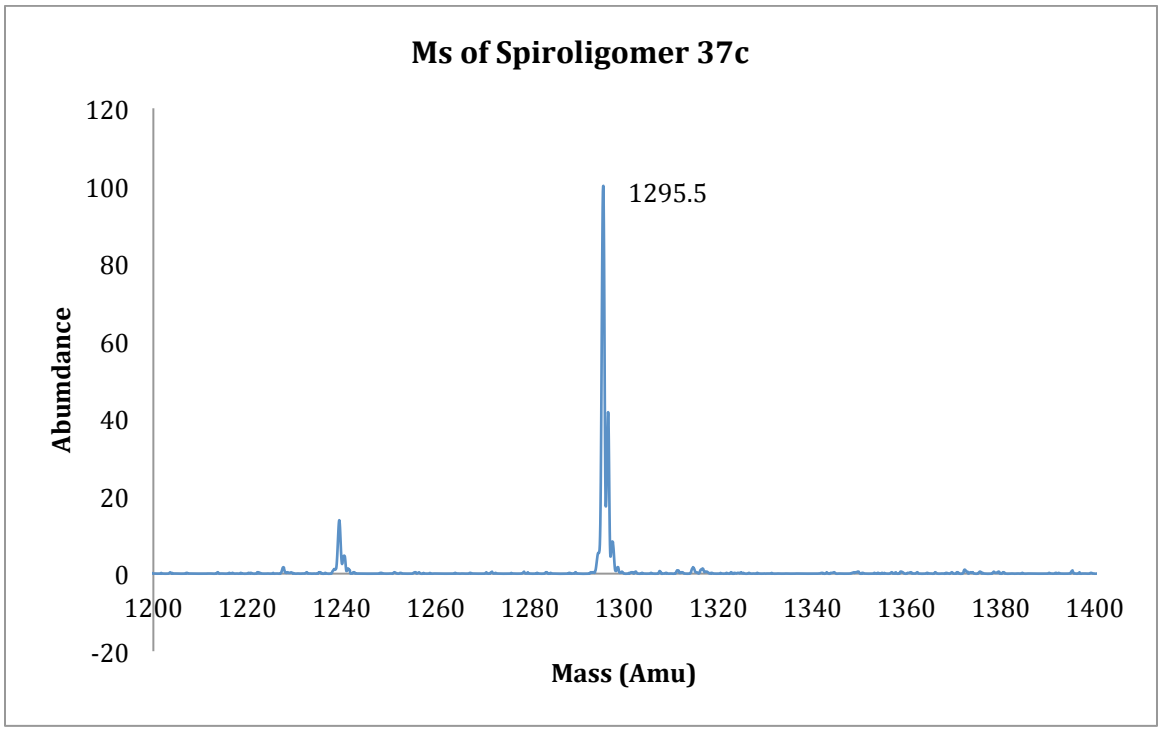

Figure 4-13. MS of Spiroligomer **37c**

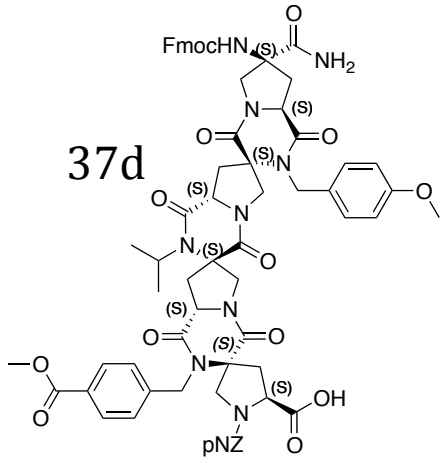

Spiroligomer 37d

Synthesized according to the same strategy as for Spiroligomer **37a** and **37b** using ^{15}N Pro4 building block.

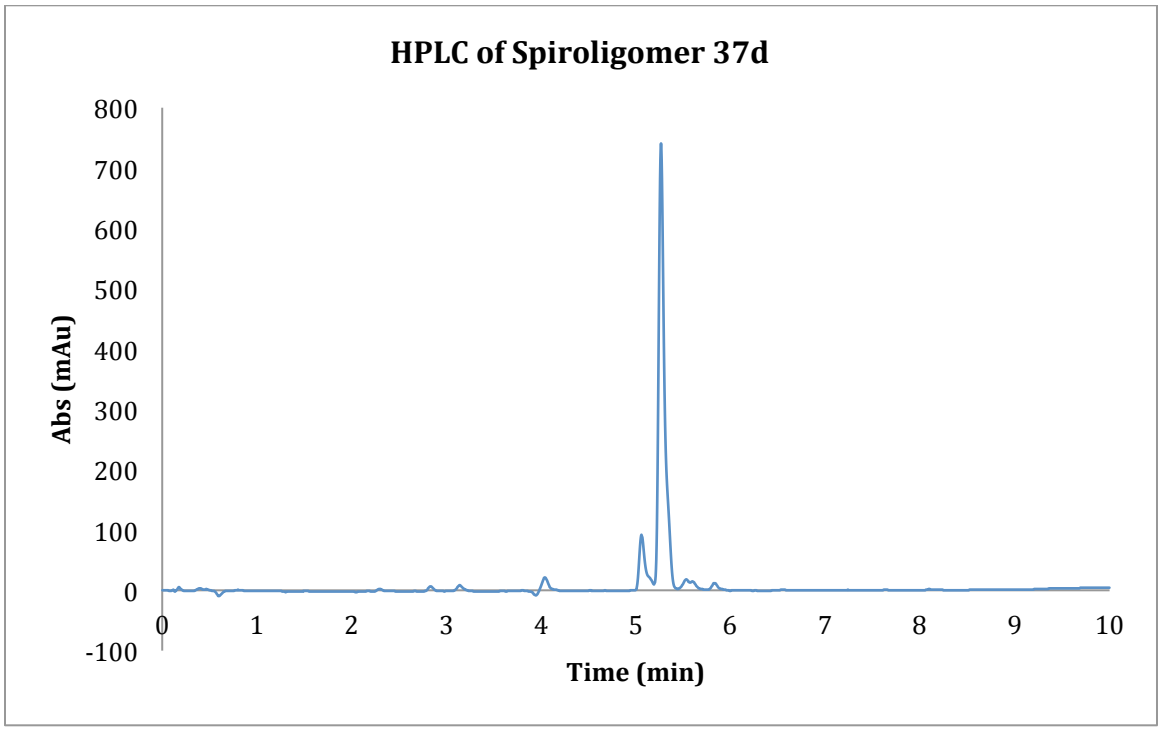

Figure 4-14. HPLC of Oligomer **37d**

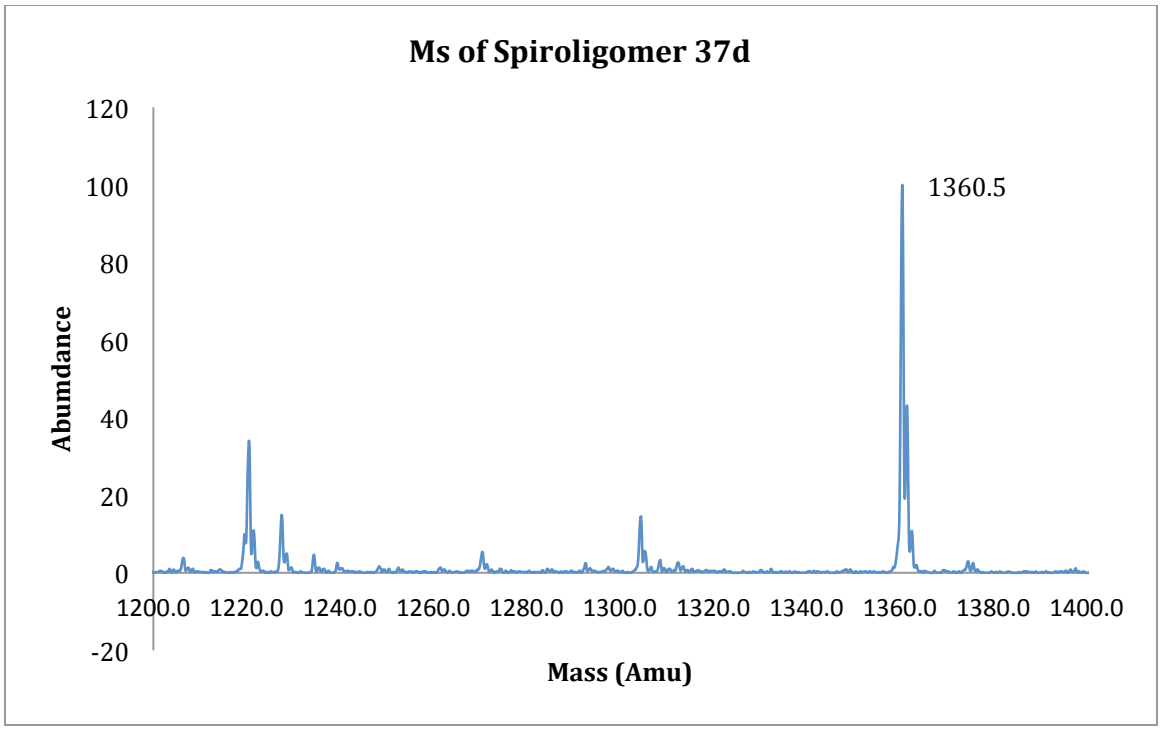

Figure 4-15. MS of Spiroligomer **37d**

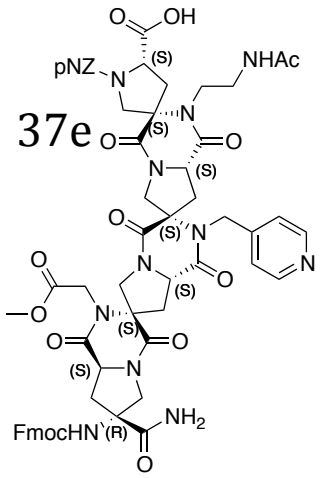

Spiroligomer 37e

Synthesized according to the same strategy as for Spiroligomer **37a** and **37b** using ^{15}N Pro4 building block.

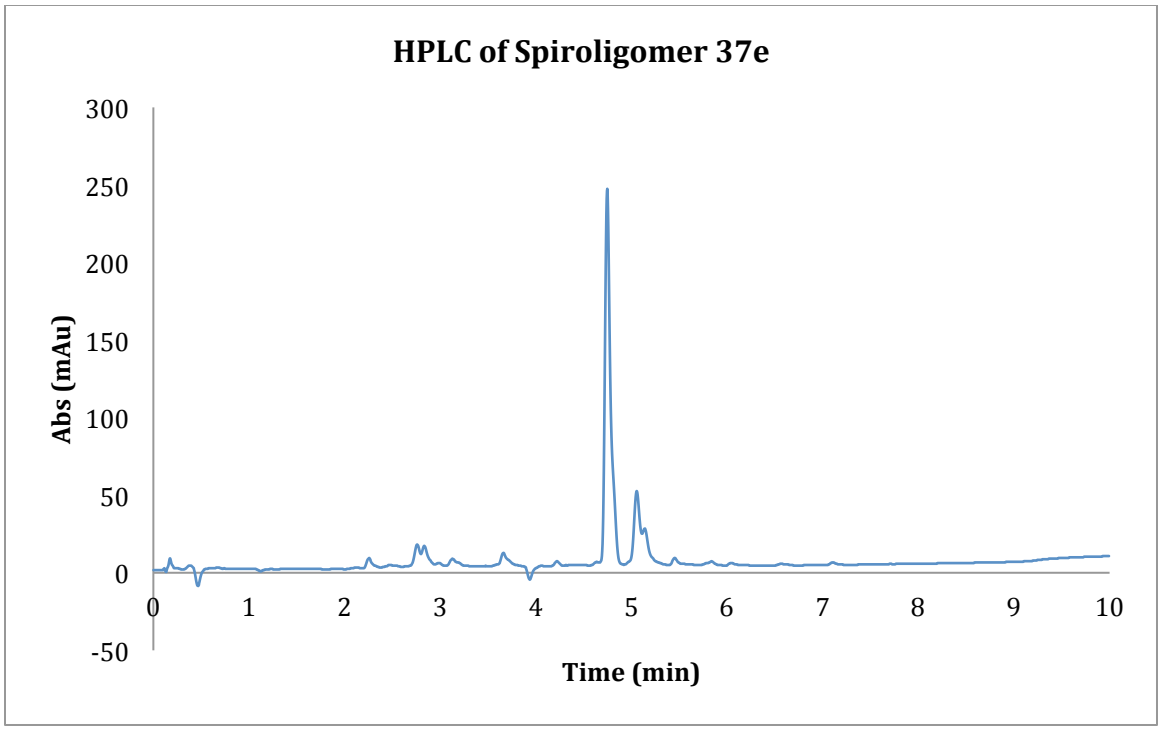

Figure 4-16. HPLC of Spiroligomer **37e**

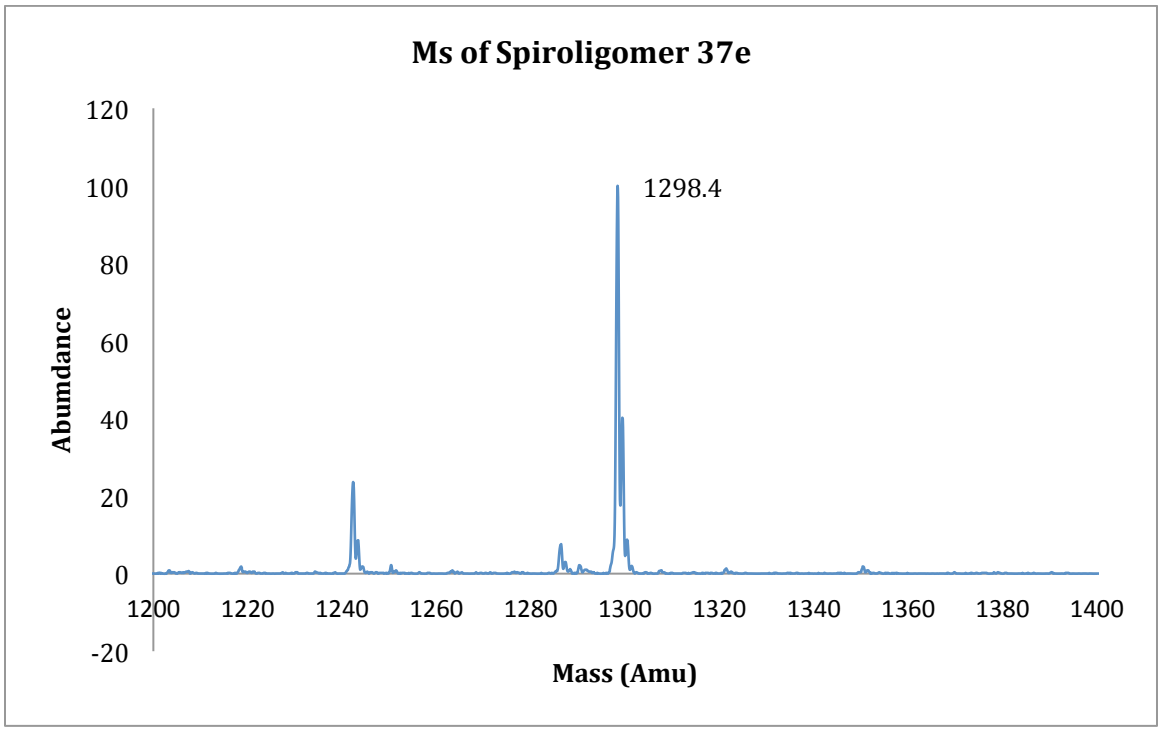

Figure 4-17. MS of Spiroligomer **37e**

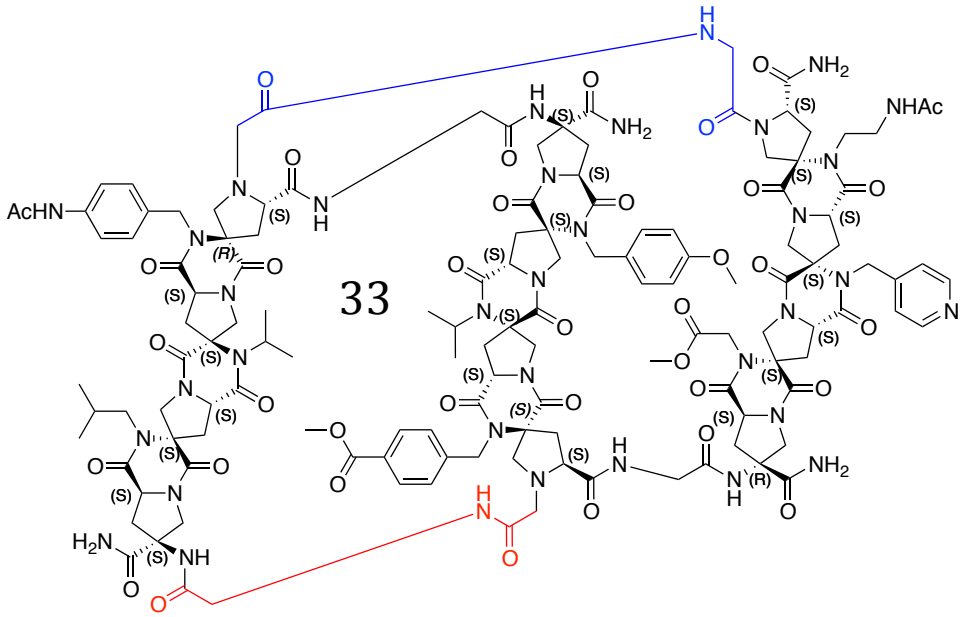

Chemical Formula: $C_{133}H_{157}N_{35}O_{37}$
Exact Mass: 2836.15

Fauxtein 33:

NovaPEG Rink Amide Resin (81.1mg, 30umoles loading) was placed in an 8mL solid phase reactor. Oligomer **37e** (116.8mg, 90umoles) was coupled according to general procedure (G) using PyAOP (46.9mg, 90umoles), NMP (450uL), and DIPEA (31.4uL, 180umoles). The terminal pNZ group was removed according to general procedure (T) using the 4M tin (II) chloride solution (1mL). Boc-Gly-OH (49.2mg, 90umoles) was coupled according to general procedure (F) using HATU (34.2mg, 90umoles), NMP (450uL) and DIPEA (31.4uL, 180umoles).

The oligomer's Fmoc group was removed according to general procedure (J) using 20% piperidine in DMF (900uL). Fmoc-Gly-OH (49.2mg, 90umoles) was coupled according to general procedure (F) using HATU (34.2mg, 90umoles), NMP (450uL) and DIPEA (31.4uL, 180umoles). The terminal Fmoc group was removed according to general procedure (J) using 20% piperidine in DMF (900uL).

Oligomer **37d** (122.4mg, 90umoles) was coupled according to general procedure (G) using PyAOP (46.9mg, 90umoles), NMP (450uL), and DIPEA (31.4uL, 180umoles). The oligomer's Fmoc group was removed according to general procedure (J) using 20% piperidine in DMF (900uL). Fmoc-Gly-OH (49.2mg, 90umoles) was coupled according to general procedure (F) using HATU (34.2mg, 90umoles), NMP (450uL) and DIPEA (31.4uL, 180umoles). The terminal Fmoc group was removed according to general procedure (J) using 20% piperidine in DMF (900uL).

Oligomer **37c** (116.5mg, 90umoles) was coupled according to general procedure (G) using PyAOP (46.9mg, 90umoles), NMP (450uL), and DIPEA (31.4uL, 180umoles). The terminal Fmoc group was removed according to general procedure (J) using 20% piperidine in DMF (900uL). Boc-Gly-OH (49.2mg, 90umoles) was coupled according to general procedure (F) using HATU (34.2mg, 90umoles), NMP (450uL) and DIPEA (31.4uL, 180umoles).

The terminal pNZ group was removed according to general procedure (T) using the 4M tin (II) chloride solution (1mL). Bromoacetates were introduced according to general procedure (M) using bromoacetic anhydride (46.8mg, 180umoles), NMP (900uL), and DIPEA (62.8uL, 360umoles). The linear assembly of spiroligomer was liberated from the resin according to general procedure (P) using 95% TFA/2.5% Tips/2.5% Water (1.8mL) to **32**.

32 (4.1mg, 2umoles) was cross-linked according to general procedure [R] or [S] using DMF (44mL) and 1.5% TEA in DMF (88mL/umole) or 50% MeCN in water (44mL) and 0.05M pH7 Phosphate Buffer (88mL). The residue was reconstituted in 50% MeCN in water (0.1% formic acid) and purified by reverse-phase chromatography (gradient elution over

30 minutes from water (0.1% formic acid) to 50% MeCN in water (0.1% formic acid). Desired fractions were combined and freeze-dried to yield **33** as a white powder.

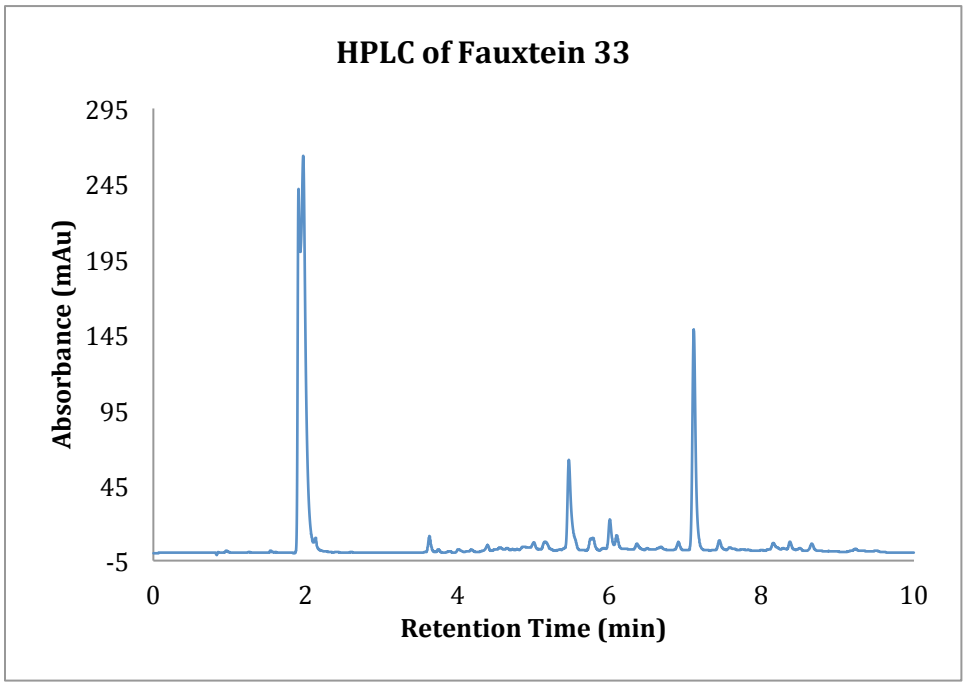

Figure 4-18. HPLC of Fauxtein **33**

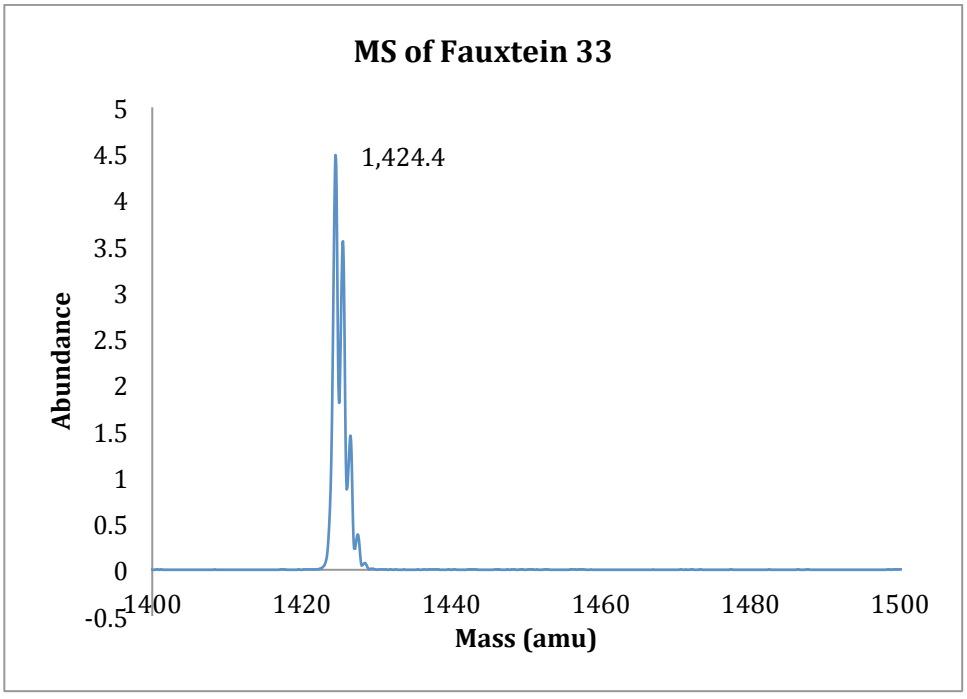

Figure 4-19. MS of Fauxtein **33**

4.5 References

[1] Gellman, S. H. Foldamers: A Manifesto. *Acc. Chem. Res.* **1998,** *31,* 173-180.

[2] Merkle, R. C. Molecular building blocks and development strategies for molecular nanotechnology. *Nanotechnology* **2000,** *11,* (2), 89-99.

[3] Breslow, R. Biomimetic Chemistry and Artificial Enzymes: Catalysis by Design. *Acc. Chem. Res.* **1995,** *28,* (3), 146-153.

[4] Schwab, P. F. H.; Levin, M. D.; Michl, J. Molecular rods. 1. Simple axial rods. *Chem. Rev.* **1999,** *99,* (7), 1863-1933.

[5] Kohnke, F. H.; Mathias, J. P.; Stoddart, J. F. Structure-Directed Synthesis of New Organic Materials. *Angew. Chem. Int. Ed.* **1989,** *28,* 1103-1110.

[6] Petkova, A. T.; Baldus, M.; Belenky, M.; Hong, M.; Griffin, R. G.; Herzfeld, J; *J. Mag. Res.* **2003**, 160, 1-12.

[7] Brown, Z. Z.; Schafmeister, C. E.; *Org. Lett.* **2010,** 12, (7), 1436-1439.

[8] Brown, Z. Z.; Alleva, J.; Schafmeister, C. E.; *Pep. Sci.* **2010**, 96, (5), 578-586.

[9] Carpenter, F. H.; Gish, D. T. *J. Am. Chem. Soc.* **1952**, 74, 3818–3821; (b) Gish, D. T.; Carpenter, F. H. *J. Am. Chem. Soc.* **1953**, 75, 950–952; (c) Shields, J. E.; Carpenter,F. H. *J. Am. Chem. Soc.* **1961**, 83, 3066–3070.

[10] Hocker, M. D.; Caldwell, C. G.; Macsata, R. W.; Lyttle, M. H. *Pept. Res.* **1995**, 8, 310–315; (b) Peluso, S.; Dumy, P.; Nkubana, C.; Yokokawa, Y.; Mutter, M. *J. Org. Chem.* **1999**, 64, 7114–7120.

[11] Isidro-Llobet, A.; Guasch-Camell, J.; A ´ lvarez, M.; Albericio, F. *Eur. J. Org. Chem.* **2005**, 14, 3031–3039. (b) Isidro-Llobet, A.: Alvarez, M.; Albericio, F.; *Tet Lett.* **2005**, 46, 7733-7736

[12] Suzuki, K.; Sasaki, Y.; Endo, N.; Mihara, Y.; *Chem. Pharm. Bull.* **1981**, 29, (1), 233-237.

[13] Isidro-Llobet, A.; Murillo, T.; Bello, P. Cilibrizzi, A.; Hodgkinson, J. T.; Galloway, W. R. J. D.; Bender, A.; Welch, M.; Spring, D. R.; *PNAS.* **2011**, 108, (17), 6793-6798.

[14] Borthwick, A. D.; *Chem. Rev.* **2012**, 112, 3641-3716.

5.0 Exploration of Cycloaddition Routes to Bis-Amino Acids

Chapter 5 details cycloaddition chemistry, specifically [3+2] cycloaddition to explore alternative routes to our principle building block, Pro4. Highlights of this work are success synthesis of Pro4 with either “sr” or “rs” stereochemistry. This synthetic route is complimentary to the current synthesis from trans-hydroxyproline, where the “sr” and “rs” stereochemistry are the minor diastereomer components.

5.1 Introduction

As shown in Chapter 1, the Pro4 monomer for solid phase assembly into spiroligomers is synthesized in 9 steps. Chapter 2 and 3 illustrated how Pro4 can be bifunctionalized for application development. However, the desire to access higher degrees of functionalization and more exotic oligomer assemblies never ceases. Gaining access to new synthetic routes toward bis-amino acids would expand the capabilities to form more advanced structures and configurations of functional groups. This can be achieved either through synthesis of new bis-amino acid building blocks or the synthesis of bis-amino acids bearing functionality built in as shown in Figure 5-1. The difficulty with the latter is installation of additional functional groups at the C-2, C-3, and C-5 positions could elongate the 9 step linear synthesis and introduce new challenges for control of stereochemistry and separation of stereoisomers. Despite this, success has been attained in the development of bis-amino acids that display additional functionality at R_2 or the C-3 position. [1]

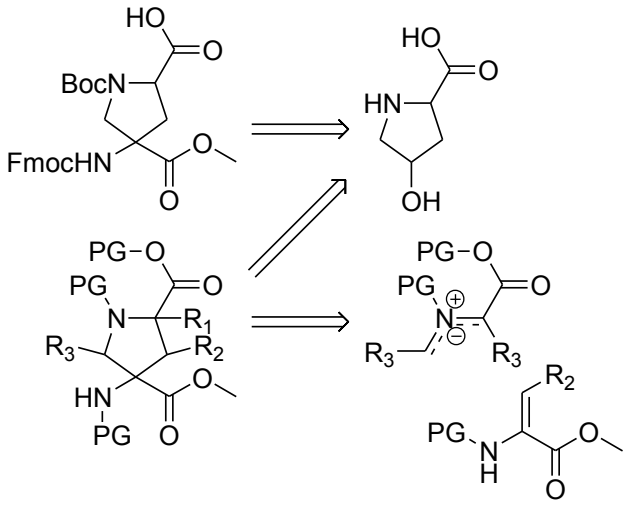

Figure 5-1. Retrosynthetic analysis of Pro4 monomer class possessing additional functional groups.

An alternative approach to the synthesis of bis-amino acids is utilizing a convergent strategy. A convergent strategy would allow complex molecules to be made in shorter syntheses and from smaller, simpler fragment that can be synthesized in parallel, while introducing several stereocenters at once. A convergent strategy to highly functionalized pyrrolidine rings, the ring type in the Pro4 monomer class, is to use [3+2] cycloaddition chemistry. In general, [3+2] cycloaddition chemistry reacts a 1,3 dipole with a dipolarophile. [2] Several different dipoles and dipolarophiles exist, but for the synthesis of pyrrolidine ring systems, the azomethine ylide is used as the 1,3 dipole fragment.

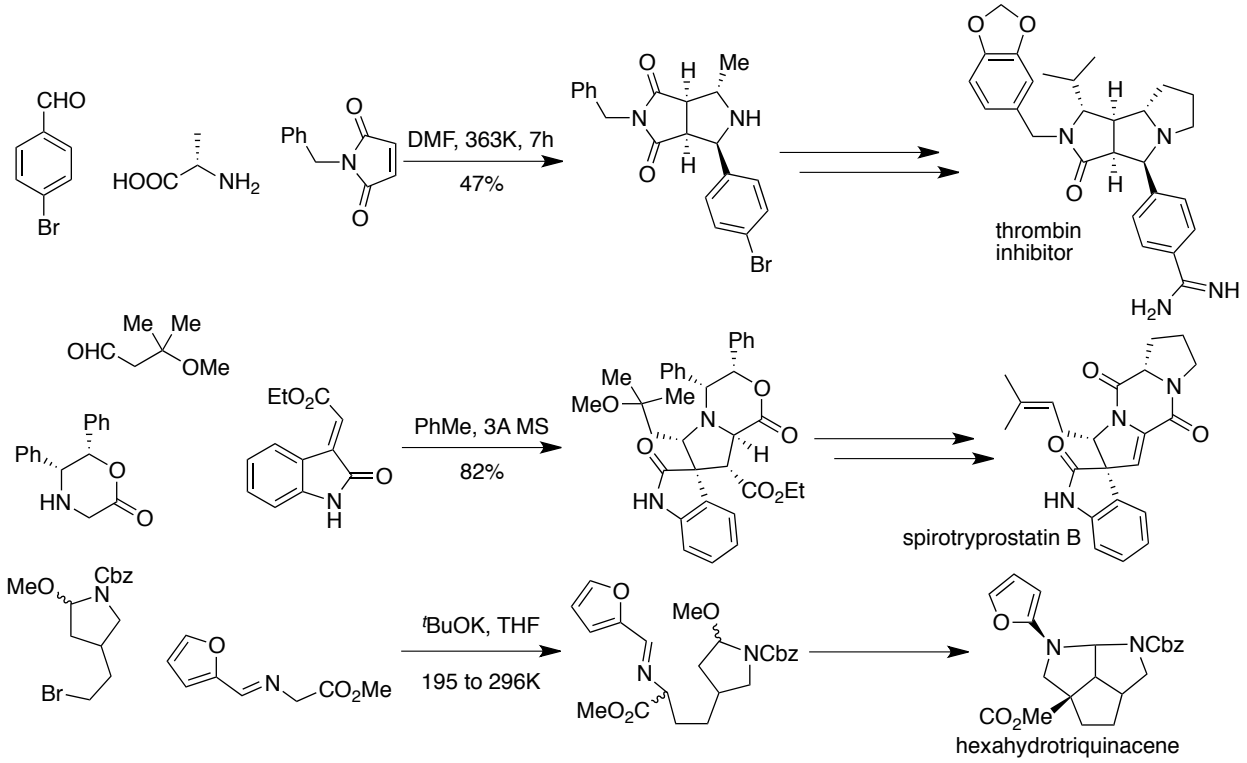

Figure 5-2. [3+2] Cycloaddition reactions and azomethine ylides used in total synthesis.

Natural product synthesis has utilized the azomethine ylide to make very complex and highly substituted pyrrolidine ring systems. [39-41] Figure 5-2 highlights some

examples of azomethine ylides used in total synthesis and the [3+2] reaction that led to the pyrrolidine ring formation. A tetra-substituted fused bicyclic ring system was synthesized as an intermediate to a thrombin inhibitor. [3] A hexa-substituted pyrrolidine spiro bicyclic ring system was synthesized as an intermediate to spirotryprostatin B. [4] The synthesis of hexahydro-triquinacene utilized two [3+2] cycloaddition reactions in tandem to make fused pyrrolidine-pyrrolidine ring system. [5]

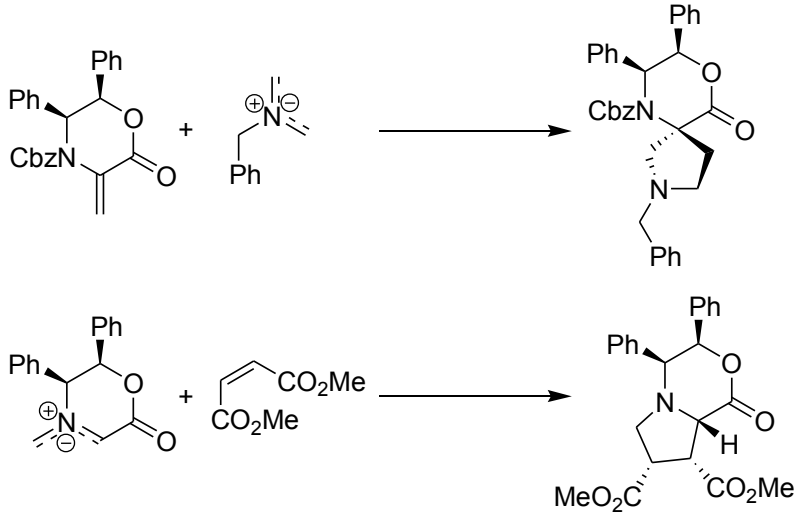

Figure 5-3. [3+2] Cycloaddition reactions and azomethine ylides used in synthesis of substituted proline and quaternary amino acids.

In addition to natural products, precedent exists for [3+2] reactions that have independently installed the two amino acids found in Pro4. Dehydroalanine derivatives have been reacted with azomethine ylides to synthesized α,α-disubstituted amino acids. [6] Azomethine ylides derived from protected glycine amino acids have been demonstrated to form highly functionalized proline amino acids. [7] Inspiration was drawn from both these exampled and used to develop new synthetic routes to Pro4. This work investigates the design and synthesis of Pro4 amino acid using [3+2] cycloaddition chemistry.

5.2 Results and Discussion

As shown in Chapter 1 and 2, the prototypical bis-amino acid design, compound **14** shown in Scheme 5-1. For making spiroligomers, a common protection scheme of compound **14** is a free acid at the C-2 position, an Fmoc protected amine and methyl esterified carboxylate at the C-4 position, and the pyrrolidine amine protected as a carbamate. Cbz and Boc are most frequently utilized but the Alloc group has been implemented as well (see Chapter 2). A [3+2] cycloaddition route to Pro4, shown in Scheme 5-1, required synthesizing two fragments: a glycinate (**41**) and a dehydroalanine (**40**) component. The previously shown literature examples demonstrate use of a chiral auxiliary in either fragment. Retrosynthetically, the use of a chiral auxiliary on the glycinate fragment (**41**) was of greater advantage. The (*S*) and (*R*) enantiomers of α-methylbenzylamine were implemented as the source of chirality. Both enantiomers are cheap and commercially available and they can easily be used to make N-substituted glycinates. A tert-butyl ester was chosen for the glycinate ester for its ease of removal, similar to the existing Pro4 synthesis (see Chapter 1). The azomethine ylide was generated *in situ* by the condensation of the glycinate and paraformaldehyde. In consideration of the dipolarophile fragment (**40**), the Fmoc group would not tolerate the reaction conditions of the cycloaddition and would need to be installed later in the synthesis. Instead, the Boc group was used to protect the amine of the dehydroalanine and the methyl ester was installed on the dehydroalanine prior to the cycloaddition step.

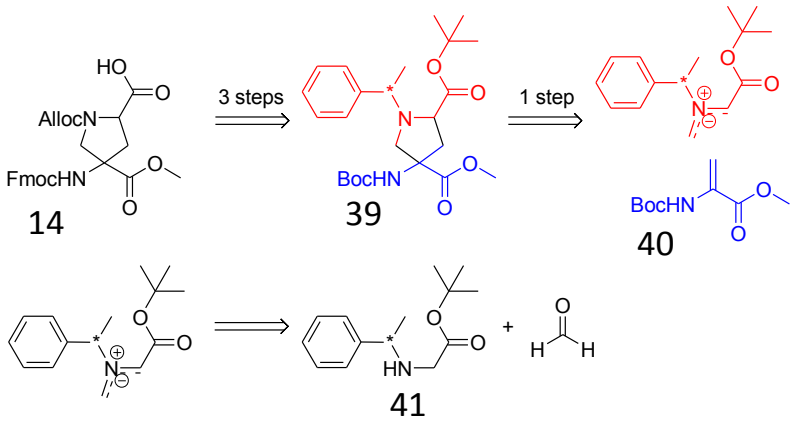

Scheme 5-1. Retrosynthetic analysis of the [3+2] route to Pro4 monomer class.

The fragment synthesis is shown in Scheme 5-2. The glycinate fragment, compound (**41**), was synthesized by combining tert-butyl bromoacetate and α-(R)-methylbenzylamine with TEA in THF. Its enantiomer (**ent-41**) is synthesized by combining tert-butyl bromoacetate and α-(S)-methylbenzylamine with TEA in THF. The dehydroalanine fragment (**40**) was synthesized in two steps starting from serine methyl ester, Boc_2O, and TEA in DCM followed by reacting with MsCl and TEA in DCM. The elimination was performed directly prior to the cycloaddition reaction, where the dehydroalanine derivative (**40**) was combined with the glycinate derivate (**41**) and paraformaldehyde in PhMe. The reaction vessel was fitted with a Dean-Stark trap and refluxed overnight accompanied by the azeotropic removal of water. The cycloaddition reaction yielded a single isomer (**39X**), which was purified by gradient flash chromatograph.

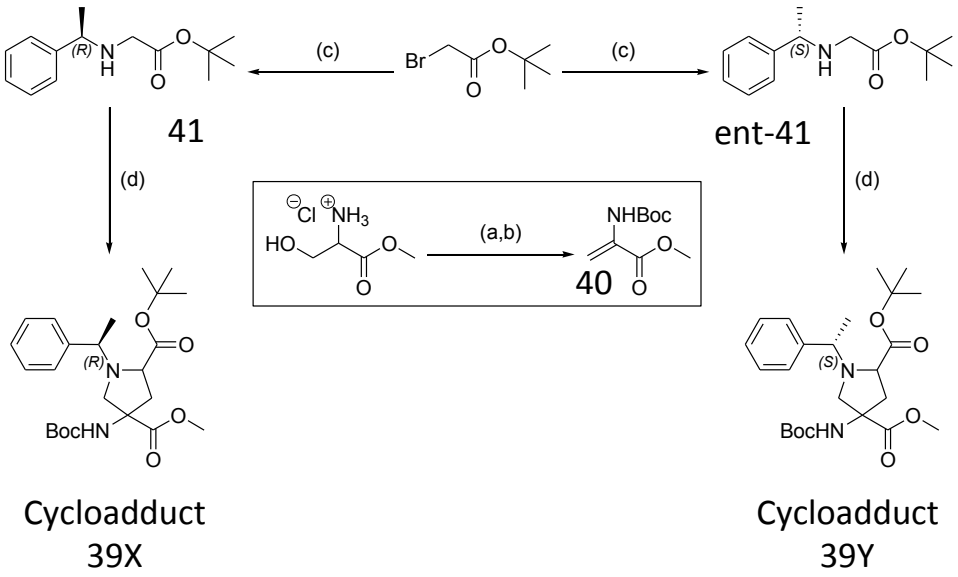

Scheme 5-2. Synthesis of cycloaddition components and cyclization reaction. a) Boc_2O, TEA, DCM; b) MsCl, TEA, DCM; c) tert-butylbromoacetate, TEA, THF; d) $(CH_2O)n$, PhMe, Δ.

Figure 5-4 shows the possible outcomes of the [3+2] cycloaddition reaction. The presentation of the dipolarophile with respect to the 1,3 dipolar yields eight different possible products. Four of the possible products represent stereoisomers of the Pro4 monomer class. The other four possibilities make up four stereoisomers of a Pro3 monomer class, derived from the same nomenclature.

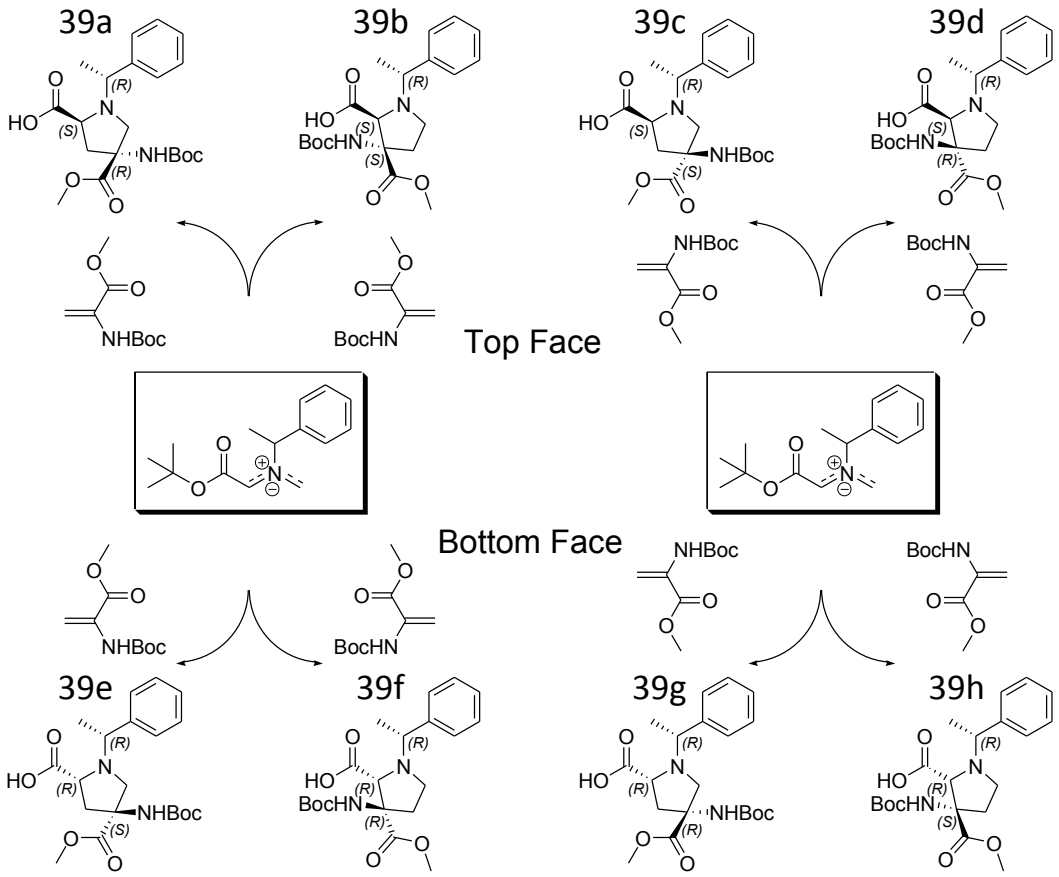

Figure 5-4. [3+2] cycloaddition facial and orientation presentations of alkenes and azomethine ylides and formed products.

NMR analysis of the cycloadduct (**39X**) provided evidence that the quaternary center was positioned at the C-4, shown in Figure 5-5, which is consistent with compounds (**39a, c, e, g**). The Cosy spectrum showed the α-proton coupling into the β-protons. Also the δ-protons were present as an isolated spin system, appearing as a pair of doublets. Conversely, the Pro3 ring system (**39b, d, f, h**) would show the α-proton as a singlet since it is an isolated spin system. Also, the β-protons and δ-protons would couple one another. From the NMR characterization, it was apparent that a Pro4 isomer was formed (**39a, c, e,**

g) and the remainder of the synthesis was carried out. However, we could not assign stereochemistry at this intermediate.

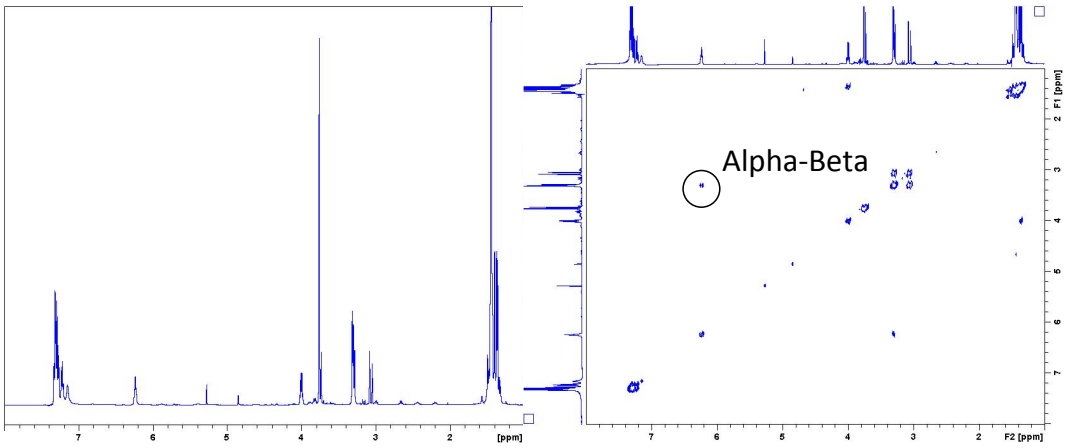

Figure 5-5. 1H and Cosy NMR of cycloadduct, compound **39X**.

With both chiral centers of the cycloadduct (**39X**) set, the chiral auxiliary was removed and replaced with an allyl carbamate in two steps, using $Pd(OH)_2/C$ in THF under $H_2(g)$ followed by Alloc-Cl and DIPEA in THF, shown in Scheme 5-3. The Boc and tert-butyl esters were cleaved with TFA in DCM. Finally, the C-4 amine was protected with a fluorenylmethyl carbamate using Fmoc-OSu and DIPEA in DCM to yield compound **42X**.

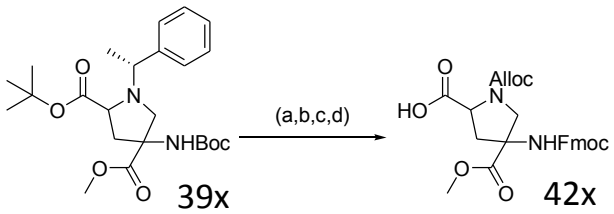

Scheme 5-3. Synthesis of Pro4 monomer (**42X**) from cycloadduct (**39X**). a) Pd(OH)2, H2, THF; b) Alloc-Cl, DIPEA, THF; c) 1:2 TFA/DCM; d) Fmoc-OSu, DIPEA, DCM.

The absolute stereochemistry was determined by derivatizing compound **42X** by attachment and DKP closure of an amino at the C-4 quaternary amino acid, illustrated in Scheme 5-4. Compound **42X** was attached to Trityl resin using DIPEA in DCM. The C-4 Fmoc group was cleaved using 1:4 piperidine in DMF followed by attachment of Fmoc-Tyr(tBu)-OH using HATU and DIPEA in NMP. The Tyr Fmoc group was cleaved and accompanied by spontaneous DKP formation. The Alloc group was cleaved using $(PPh_3)_4Pd$ and BH_3:DMA in DCM and compound **43X** was liberated from the solid support using TFA. To assist in determining the absolute stereochemistry of compound **43X**, the four known stereoisomers of Pro4 were derivatized in the same manner to provide compounds **43ss**, **43sr**, **43rr**, and **43rs**.

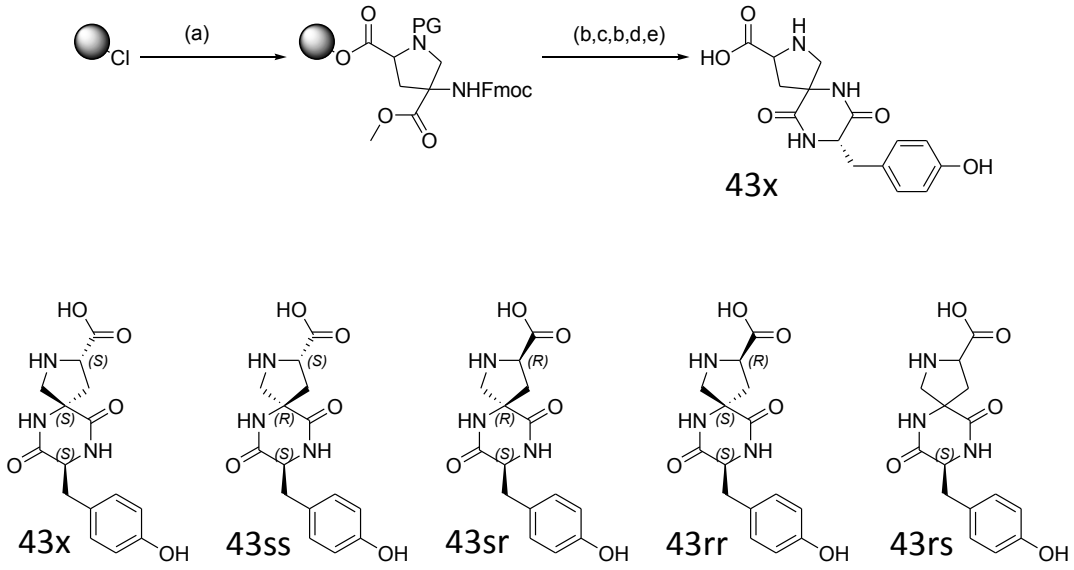

Scheme 5-4. Synthesis of Pro4 derivative for stereochemistry analysis. a) Pro4 monomer, DIPEA, DCM; b) 1:4 piperidine/DMF; c) Fmoc-Tyr(tBu)-OH, HATU, DIPEA, NMP; d) $(PPh_3)_4Pd$, BH_3:DMA, DCM; e) 48:1:1 TFA/TIPS/H_2O.

NMR analysis of the 5-member library provided the stereochemistry of compounds **43X** through comparisons with the known stereoisomers. The comparisons were most

profound when viewing the Cosy spectra of compound **43X** on top of the Cosy spectra of the known stereoisomers, Figure 5-6. Much like fingerprints, subtle differences were observed except of one perfect match for the unknown. According to the NMR data, compound **43X** is the same as **43rs**.

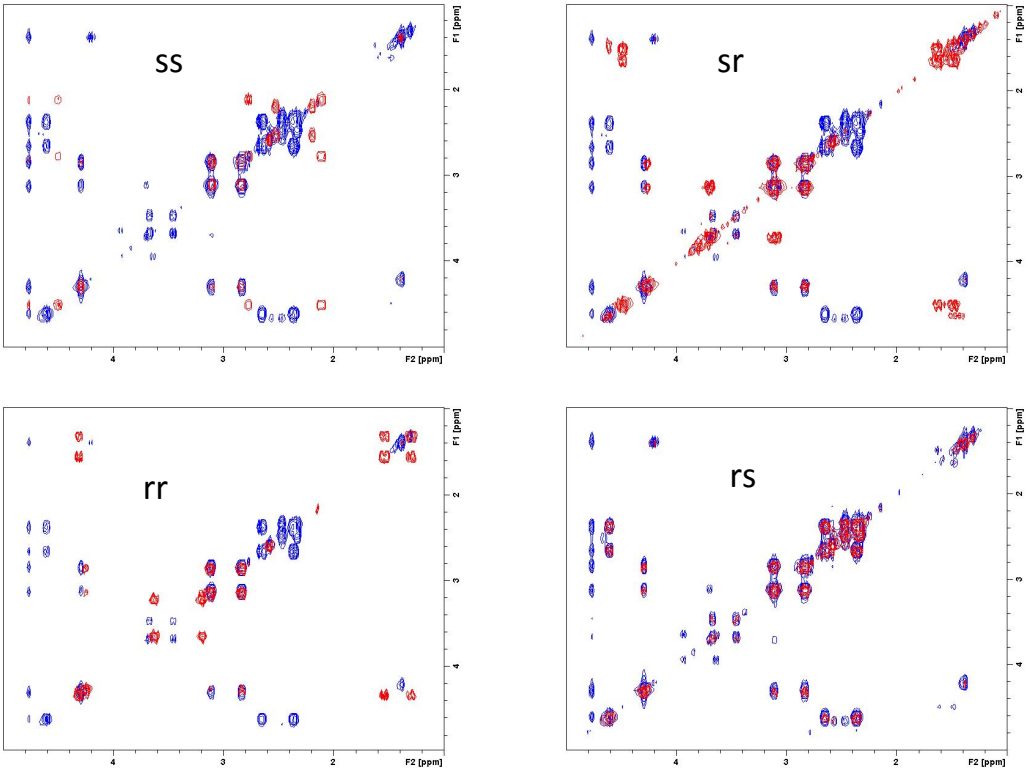

Figure 5-6. Cosy NMR of compound **43X** overlaid with compounds **43ss**, **43sr**, **43rr**, and **43rs**.

The enantiomer of (**43X**) was synthesized from glycinate (**ent-41**) and derivatized in a similar manner to provide (**43Y**). Figure 5-7 shows the Cosy spectra overlaid over the compounds **43ss**, **43sr**, **43rr**, and **43rs**. An identical match was also observed. According to the NMR data, compound **43Y** is the same as **43sr**.

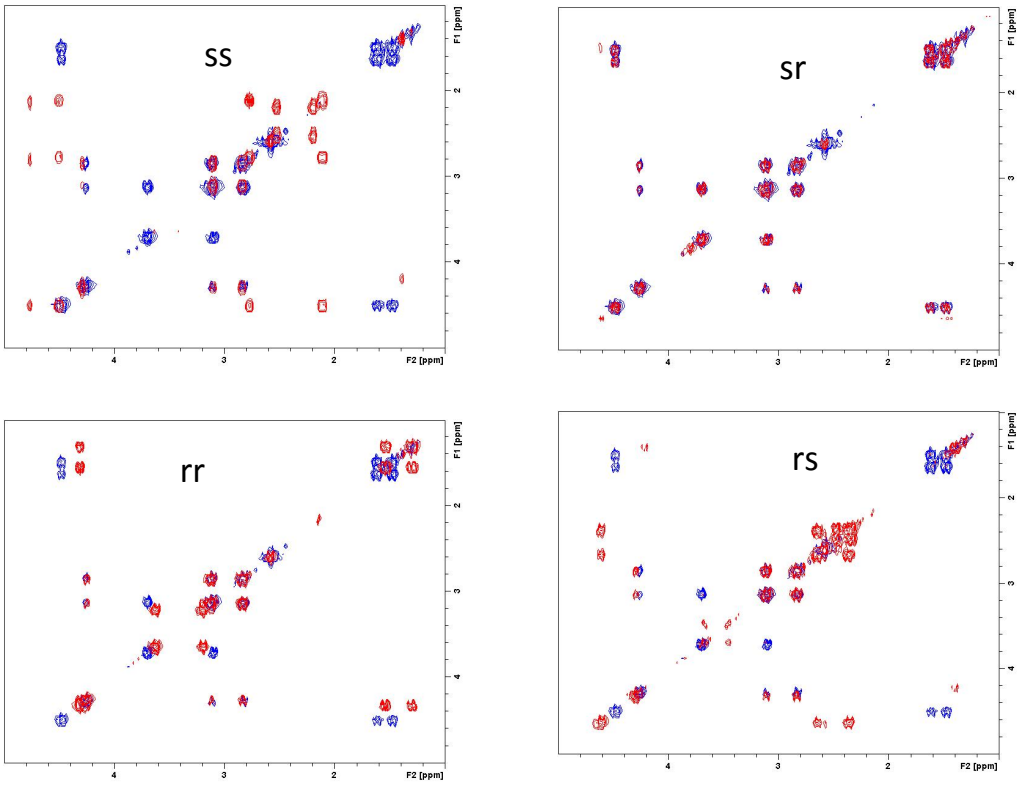

Figure 5-7. Cosy NMR of compound **43Y** overlaid with compounds **43ss**, **43sr**, **43rr**, and **43rs**.

5.3 Conclusion

An alternative route to the "minor" diastereomers of Pro4 was established. The use of α-(R)-methylbenzylamine provided the 2R4S stereoisomer of Pro4 and the use of α-(S)-methylbenzylamine provided the 2S4R stereoisomer of Pro4. This strategy is complimentary to the existing Pro4 synthesis from 4-trans-hydroxyproline. Furthermore, the cycloaddition strategy provides the 2R4S and the 2S4R stereoisomers in a shorter synthesis and in much higher yields (~40% overall yield in comparison to ~25% overall yield for the hydroxyproline synthesis).

5.4 Experimental Details

Solution Synthesis:

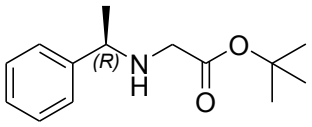

41

(R)-tert-butyl 2-(1-phenylethylamino)acetate (41):

To a stirring solution of (R)-1-phenylethanamine (1.3mL, 10.1mmoles) in THF (20mL) was added tBuOAcBr (1.5mL, 10.1mmoles, 1equiv) followed by a dropwise addition of TEA (2.8mL, 20.2mmoles, 2equiv) in THF (20mL). The reaction mixture was stirred overnight then diluted with EtOAc. The solution was washed with sat. NaCl (aq) x 3, dried over Na_2SO_4, filtered, and concentrated under reduced pressure yield as colorless oil (2.3g, 9.77mmoles, 97%). ^{1}H NMR (500 MHz, rt, $CDCl_3$): δ 7.31 (m, 5H), 3.80 (q, J=7.1 Hz, 1H), 3.21 (q, J=17.7 Hz, 15.9 Hz, 2H), 2.03 (br s, 1H), 1.44 (s, 9H), 1.38 (d, J=7.1, 3H); ^{13}C NMR (125MHz, rt, $CDCl_3$): δ 172.0, 144.9, 128.5, 127.2, 126.8, 125.9, 81.1, 57.8, 49.8, 28.1, 24.4.

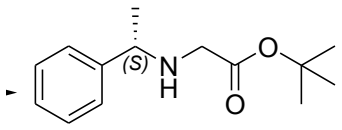

ent-41

(*S*)-tert-butyl 2-(1-phenylethylamino)acetate (ent-41):

To a stirring solution of (S)-1-phenylethanamine (1.3mL, 10.1mmoles) in THF (20mL) was added tBuOAcBr (1.5mL, 10.1mmoles, 1equiv) followed by a dropwise addition of TEA (2.8mL, 20.2mmoles, 2equiv) in THF (20mL). The reaction mixture was stirred overnight then diluted with EtOAc. The solution was washed with sat. NaCl (aq) x 3, dried over Na_2SO_4, filtered, and concentrated under reduced pressure yield as colorless oil (2.3g, 9.77mmoles, 97%). ^{1}H NMR (500 MHz, rt, $CDCl_3$): δ 7.31 (m, 5H), 3.80 (q, J=7.1 Hz, 1H), 3.21 (q, J=17.7 Hz, 15.9 Hz, 2H), 2.03 (br s, 1H), 1.44 (s, 9H), 1.38 (d, J=7.1, 3H); ^{13}C NMR (125MHz, rt, $CDCl_3$): δ 172.0, 144.9, 128.5, 127.2, 126.8, 125.9, 81.1, 57.8, 49.8, 28.1, 24.4.

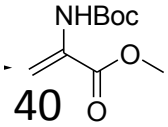

40

Methyl 2-(tert-butoxycarbonylamino)acrylate (40):

To a stirring solution of Serine-methyl ester hydrochloride (3.11g, 20mmoles) in DCM (40mL) was added Boc_2O (4.37g, 20mmoles, 1equiv) followed by TEA(8.4mL, 60mmoles, 3equiv). The reaction mixture was stirred overnight then diluted with EtOAc. The solution

was washed with sat. NH_4Cl (aq) x 3, sat. NaCl (aq) x 2, dried over Na_2SO_4, filtered, and concentrated under reduced pressure. The residue was dissolved in DCM (40mL) and cooled to 0°C in an ice/water bath. MsCl (3.4mL, 22mmoles, 1.1equiv) was added followed by a dropwise addition of TEA (8.4mL, 60mmoles, 3equiv) in DCM (20mL). The reaction mixture was stirred overnight then diluted in EtOAc. The solution was washed with sat. NH_4Cl (aq) x 3, sat. NaCl (aq) x 2, dried over Na_2SO_4, filtered, and concentrated under reduced pressure yield as orange oil (4.1g, 19.9mmoles, 99%). ^1H NMR (500 MHz, rt, $CDCl_3$): δ 5.48 (br s, 1H), 4.38 (br s, 1H), 3.97 (dd, J=3.7 Hz, 7.3 Hz, 1H), 3.91 (dd, J=3.7 Hz, 7.3 Hz, 1H), 3.78 (s, 3H), 1.48 (s, 9H), 4.08 (s, 3H); ^{13}C NMR (125MHz, rt, $CDCl_3$): δ 171.3, 155.8, 80.4, 63.6, 55.8, 52.7, 28.3.

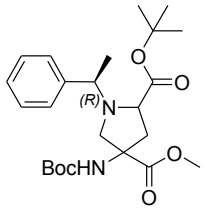

Cycloadduct
39X

2-tert-butyl 4-methyl 4-(tert-butoxycarbonylamino)-1-((R)-1-phenylethyl)pyrrolidine-2,4-dicarboxylate (39X):

To a stirring solution of **41** (2.3g, 9.77mmoles) and **40** (2.0 g, 10mmoles) in PhMe (100mL) was added $CH_2O_{(n)}$ (600mg, 20mmoles, 2equiv). The reaction mixture was fitted with a Dean-Stark trap and heated to reflux. The reaction mixture was stirred overnight then chromatographed on silica (gradient elution over 16 column volumes from 0-50% EtOAc in Hexanes). The desired fractions were combined and concentrated to yield as yellow oil

(2.6g, 5.8mmoles, 58%). ^{1}H NMR (500 MHz, rt, $CDCl_3$): δ 7.33 (m, 5H), 6.25 (t, J=5.81 Hz, 1H), 4.02 (q, J=6.8 Hz, 1H), 3.76 (s, 3H), 3.32 (m, 3H), 3.08 (d, J=17.4, 1H), 1.44 (s, 9H), 1.37 (d, J=6.2, 3H); ^{13}C NMR (125MHz, rt, $CDCl_3$): δ 172.3, 170.9, 165.1, 143.3, 129.4, 127.6, 127.0, 81.1, 81.0, 60.4, 52.7, 52.3, 48.7, 28.3, 19.2; LRESIQMS calcd for $C_{24}H_{36}N_2O_6$ ($M + H^+$) 449.2573, measured 449.4.

2-tert-butyl 4-methyl 4-(tert-butoxycarbonylamino)-1-((*S*)-1-phenylethyl)pyrrolidine-2,4-dicarboxylate (39Y):

To a stirring solution of **ent-41** (2.3g, 9.77mmoles) and **40** (2.0 g, 10mmoles) in PhMe (100mL) was added $CH_2O_{(n)}$ (600mg, 20mmoles, 2equiv). The reaction mixture was fitted with a Dean-Stark trap and heated to reflux. The reaction mixture was stirred overnight then chromatographed on silica (gradient elution over 16 column volumes from 0-50% EtOAc in Hexanes). The desired fractions were combined and concentrated to yield as yellow oil (2.5g, 5.6mmoles, 56%). ^{1}H NMR (500 MHz, rt, $CDCl_3$): δ 7.33 (m, 5H), 6.25 (t, J=5.8 Hz, 1H), 4.02 (q, J=6.8 Hz, 1H), 3.76 (s, 3H), 3.32 (m, 3H), 3.08 (d, J=17.4, 1H), 1.44 (s, 9H), 1.37 (d, J=6.23, 3H); ^{13}C NMR (125MHz, rt, $CDCl_3$): δ 172.3, 170.9, 165.1, 143.3, 129.4, 127.6, 127.0, 81.1, 81.0, 60.4, 52.7, 52.3, 48.7, 28.3, 19.2; LRESIQMS calcd for $C_{24}H_{36}N_2O_6$ ($M + H^+$) 449.2573, measured 449.4.

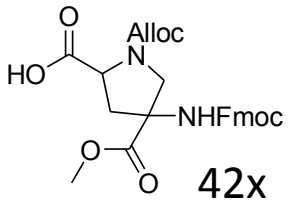

42x

4-(((9H-fluoren-9-yl)methoxy)carbonylamino)-1-(allyloxycarbonyl)-4-(methoxycarbonyl) pyrrolidine-2-carboxylic acid (42X):

To a stirring solution of **39X** (2.3g, 5mmoles) in THF (50mL) was added $Pd(OH)_2$ (75mg). The reaction mixture was then degassed and charged with H_2 (g) and stirred overnight then sparged with Ar (g). To this solution was added Alloc-Cl (530uL, 5mmoles, 1equiv) followed by DIPEA (1.75mL, 10mmoles, 2equiv). The reaction mixture was stirred for 4 hours then diluted with EtOAc. The solution was filtered then washed with sat. NH4Cl (aq) x 3, sat. NaCl (aq) x 2, dried over Na_2SO_4, filtered, and concentrated under reduced pressure. The residue was dissolved in DCM (20mL). To this reaction mixture was added TFA (10mL) and the reaction mixture was stirred for 4 hours then concentrated under reduced pressure. The residue was diluted with PhMe and concentrated under reduced pressure and further dried overnight under high vacuum. The residue was dissolved in DCM (50mL) and DIPEA (1.75, 10mmoles, 2equiv) was added followed by Fmoc-OSu (1.69g, 5mmoles, 1equiv). The reaction mixture was stirred overnight then diluted with EtOAc. The solution was washed with sat. NH4Cl (aq) x 3, sat. NaCl (aq) x 2, dried over Na_2SO_4, filtered, and concentrated under reduced pressure. The residue was chromatographed on silica (gradient elution over 16 column volumes from 0-5% MeOH in DCM). The desired fractions were combined and concentrated to yield a yellow solid (1.7g,

3.5mmoles, 70%). ^{1}H NMR (500 MHz, 365K, DMSO-d6): δ 8.49 (bs, 1H), 8.11 (d, J = 7.45 Hz, 2H), 7.92 (d, J = 7.1 Hz, 2H), 7.64 (t, J = 7.3 Hz, 7.4 Hz, 2H), 7.56 (t, J = 7.3 Hz, 7.2 Hz, 2H), 6.17 (m, 1H), 5.52 (t, J = 16.7 Hz, 16.7 Hz, 1H), 5.43 (dd, J = 10.5 Hz, 17.9 Hz, 10.5 Hz, 1H), 4.77 (m, 2H), 4.54 (m, 4H), 4.29 (dd, J = 11.2 Hz, 24.2 Hz, 11.2 Hz, 1H), 3.82 (s, 3H), 3.80 (m, 1H), 3.11 (m, 1H);); ^{13}C NMR (125MHz, 365K, DMSO-d6): δ 174.8, 171.8, 157.6, 155.6, 155.6, 143.6, 141.0, 133.5, 128.7, 128.4, 128.2, 126.8, 116.4, 67.3, 65.1, 55.0, 54.8, 52.2, 50.9, 37.2; LRESIQMS calcd for $C_{132}H_{138}N_{10}O_{40}$ ($M + H^+$) 494.1689, measured 494.2.

4-(((9H-fluoren-9-yl)methoxy)carbonylamino)-1-(allyloxycarbonyl)-4-(methoxycarbonyl) pyrrolidine-2-carboxylic acid (42Y):

To a stirring solution of **39Y** (2.3g, 5mmoles) in THF (50mL) was added $Pd(OH)_2$ (75mg). The reaction mixture was then degassed and charged with H_2 (g) and stirred overnight then sparged with Ar (g). To this solution was added Alloc-Cl (530uL, 5mmoles, 1equiv) followed by DIPEA (1.75mL, 10mmoles, 2equiv). The reaction mixture was stirred for 4 hours then diluted with EtOAc. The solution was filtered then washed with sat. NH_4Cl (aq) x 3, sat. NaCl (aq) x 2, dried over Na_2SO_4, filtered, and concentrated under reduced pressure. The residue was dissolved in DCM (20mL). To this reaction mixture was added TFA (10mL) and the reaction mixture was stirred for 4 hours then concentrated under reduced pressure. The residue was diluted with PhMe and concentrated under reduced pressure and further dried overnight under high vacuum. The residue was dissolved in DCM (50mL) and DIPEA (1.75, 10mmoles, 2equiv) was added followed by Fmoc-OSu (1.69g, 5mmoles, 1equiv). The reaction mixture was stirred overnight then diluted with EtOAc. The solution was washed with sat. NH4Cl (aq) x 3, sat. NaCl (aq) x 2, dried over Na_2SO_4, filtered, and concentrated under reduced pressure. The residue was

chromatographed on silica (gradient elution over 16 column volumes from 0-5% MeOH in DCM). The desired fractions were combined and concentrated to yield a yellow solid (1.7g, 3.5mmoles, 70%). ^{1}H NMR (500 MHz, 365K, DMSO-d6): δ 8.49 (bs, 1H), 8.11 (d, J = 7.5 Hz, 2H), 7.92 (d, J = 7.1 Hz, 2H), 7.64 (t, J = 7.3 Hz, 7.4 Hz, 2H), 7.56 (t, J = 7.30 Hz, 7.20 Hz, 2H), 6.17 (m, 1H), 5.52 (t, J = 16.7 Hz, 16.7 Hz, 1H), 5.43 (dd, J = 10.5 Hz, 17.9 Hz, 10.5 Hz, 1H), 4.77 (m, 2H), 4.54 (m, 4H), 4.29 (dd, J = 11.2 Hz, 24.2 Hz, 11.2 Hz, 1H), 3.82 (s, 3H), 3.80 (m, 1H), 3.11 (m, 1H);); ^{13}C NMR (125MHz, 365K, DMSO-d6): δ 174.8, 171.8, 157.6, 155.6, 155.6, 143.6, 141.0, 133.5, 128.7, 128.4, 128.2, 126.8, 116.4, 67.3, 65.1, 55.0, 54.8, 52.2, 50.9, 37.2; LRESIQMS calcd for $C_{132}H_{138}N_{10}O_{40}$ ($M + H^{+}$) 494.1689, measured 494.2.

Solid Phase Synthesis

General procedure (A): Attachment to Trityl resin

To a solution of the amino acid (10 equivalents based on resin loading) in DCM (3mL/mmole of amino acid) was added DIPEA (5 equivalents based on resin loading). The reaction mixture was added to a portion of resin in a solid phase reactor. The reaction mixture was stirred for 4 hours. The resin was filtered and washed with DMF, DCM, IPA, DCM and DMF.

General procedure (B): HATU coupling

To a solution of amino acid (3 equivalents based on resin loading) and HATU (3 equivalents based on resin loading in NMP (5mL/mmole of amino acid) was added DIPEA (6 equivalents based on resin loading). The reaction mixture was agitated for 5 minutes then

added to a pre-swelled (with DMF) portion of resin in a solid phase reactor and stirred for 45 minutes. The resin was filtered and washed with DMF, DCM, IPA, DCM and DMF.

General procedure (C): Fmoc deprotection

A solution of 20% of piperidine in DMF (15mL/mmole based on resin loading) was added to a pre-swelled (with DMF) portion of resin in a solid phase reactor and stirred for 15 minutes. The resin was filtered and washed with DMF, DCM, IPA, DCM and DMF.

General procedure (D): Alloc deprotection

A solution of borane:dimethylamine complex (6 equivalents based on resin loading) in DCM (10mL/mmole based on resin loading) was added to a pre-swelled (with DMF) portion of resin in a solid phase reactor and stirred for 5 minutes. To this solution was added a solution of tetrakis(triphenylphosphine)palladium (0) (0.1 equivalents based on resin loading) in DCM (10mL/mmole based on resin loading). The reaction mixture was stirred for 1 hour. The resin was filtered and washed with DMF, DCM, IPA, DCM and DMF.

General procedure (E): Liberation from Trityl resin

A solution of 5% TIPS and 5% water in TFA (25 mL/mmole based on resin loading was added to a portion of resin (successively washed with DCM and MeOH, and thoroughly dried under vacuum) and stirred for 4 hours. The resin was filtered and rinsed with TFA. The filtrate was concentrated, reconstituted in 50% MeCN in water (0.1% formic acid) and freeze-dried.

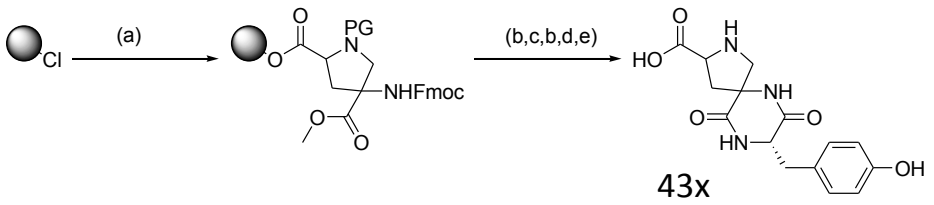

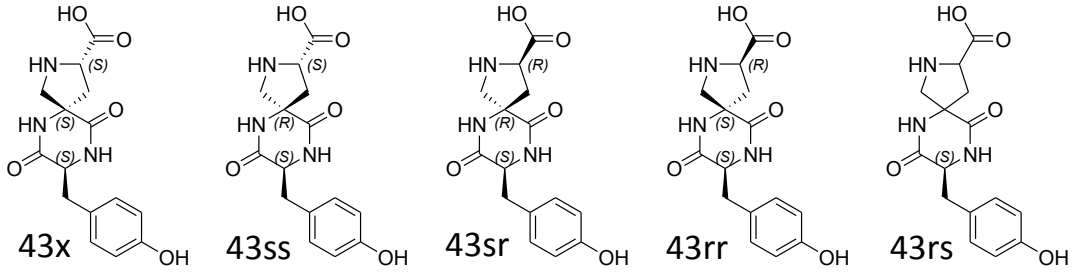

a) Pro4 monomer, DIPEA, DCM; b) 1:4 piperidine/DMF; c) Fmoc-Tyr(tBu)-OH, HATU, DIPEA, NMP; d) $(PPh_3)_4Pd$, BH_3:DMA, DCM, 48:1:1 TFA/TIPS/H_2O.

43X

Trityl resin (100mg, 100umoles loading) was placed in a 4mL solid phase reactor. **42X** was attached according to general procedure (A) using DCM (4.5mL) and DIPEA (116uL, 750umoles). The terminal Fmoc group was removed according to general procedure (C) using 20% piperidine in DMF (2.25mL).

Fmoc-Tyr(tBu)-OH (211mg, 450umoles) was coupled according to general procedure (B) using HATU (171mg, 450umoles), NMP (2.25mL), and DIPEA (156uL, 900umoles). The terminal Fmoc group was removed according to general procedure (C) using 20% piperidine in DMF (2.25mL) and the reaction time was extended to 2 hour.

The Alloc group was removed according to general procedure (D) using borane:dimethylamine complex (53mg, 900umoles) in DCM (2.5mL) and tetrakis(triphenylphosiphine)palladium(0) (17mg, 15umoles) in DCM (2mL).

43X was liberated from the resin according to general procedure (E) using 3.75 mL of the cleavage cocktail. The residue was reconstituted in 50% MeCN in water (0.1% formic acid) and purified by reverse-phase chromatography (gradient elution over 30 minutes from water (0.1% formic acid) to 50% MeCN in water (0.1% formic acid). Desired fractions were combined and freeze-dried to yield a white powder.

43Y

Trityl resin (100mg, 100umoles loading) was placed in a 4mL solid phase reactor. **42Y** was attached according to general procedure (A) using DCM (4.5mL) and DIPEA (116uL, 750umoles). The terminal Fmoc group was removed according to general procedure (C) using 20% piperidine in DMF (2.25mL).

Fmoc-Tyr(tBu)-OH (211mg, 450umoles) was coupled according to general procedure (B) using HATU (171mg, 450umoles), NMP (2.25mL), and DIPEA (156uL, 900umoles). The terminal Fmoc group was removed according to general procedure (C) using 20% piperidine in DMF (2.25mL) and the reaction time was extended to 2 hour.

The Alloc group was removed according to general procedure (D) using borane:dimethylamine complex (53mg, 900umoles) in DCM (2.5mL) and tetrakis(triphenylphosiphine)palladium(0) (17mg, 15umoles) in DCM (2mL).

43Y was liberated from the resin according to general procedure (E) using 3.75 mL of the cleavage cocktail. The residue was reconstituted in 50% MeCN in water (0.1% formic acid) and purified by reverse-phase chromatography (gradient elution over 30 minutes from water (0.1% formic acid) to 50% MeCN in water (0.1% formic acid). Desired fractions were combined and freeze-dried to yield a white powder.

43ss

Trityl resin (100mg, 100umoles loading) was placed in a 4mL solid phase reactor. **Pro4SS** (**1**) was attached according to general procedure (A) using DCM (4.5mL) and DIPEA (116uL, 750umoles). The terminal Fmoc group was removed according to general procedure (C) using 20% piperidine in DMF (2.25mL).

Fmoc-Tyr(tBu)-OH (211mg, 450umoles) was coupled according to general procedure (B) using HATU (171mg, 450umoles), NMP (2.25mL), and DIPEA (156uL, 900umoles). The terminal Fmoc group was removed according to general procedure (C) using 20% piperidine in DMF (2.25mL) and the reaction time was extended to 2 hour.

43ss was liberated from the resin according to general procedure (E) using 3.75 mL of the cleavage cocktail. The residue was reconstituted in 50% MeCN in water (0.1% formic acid)

and purified by reverse-phase chromatography (gradient elution over 30 minutes from water (0.1% formic acid) to 50% MeCN in water (0.1% formic acid). Desired fractions were combined and freeze-dried to yield a white powder.

43sr

Trityl resin (100mg, 100umoles loading) was placed in a 4mL solid phase reactor. **Pro4SR** (**2**) was attached according to general procedure (A) using DCM (4.5mL) and DIPEA (116uL, 750umoles). The terminal Fmoc group was removed according to general procedure (C) using 20% piperidine in DMF (2.25mL).

Fmoc-Tyr(tBu)-OH (211mg, 450umoles) was coupled according to general procedure (B) using HATU (171mg, 450umoles), NMP (2.25mL), and DIPEA (156uL, 900umoles). The terminal Fmoc group was removed according to general procedure (C) using 20% piperidine in DMF (2.25mL) and the reaction time was extended to 2 hour.

43sr was liberated from the resin according to general procedure (E) using 3.75 mL of the cleavage cocktail. The residue was reconstituted in 50% MeCN in water (0.1% formic acid) and purified by reverse-phase chromatography (gradient elution over 30 minutes from water (0.1% formic acid) to 50% MeCN in water (0.1% formic acid). Desired fractions were combined and freeze-dried to yield a white powder.

43rr

Trityl resin (100mg, 100umoles loading) was placed in a 4mL solid phase reactor. **Pro4RR** (**3**) was attached according to general procedure (A) using DCM (4.5mL) and DIPEA (116uL, 750umoles). The terminal Fmoc group was removed according to general procedure (C) using 20% piperidine in DMF (2.25mL).

Fmoc-Tyr(tBu)-OH (211mg, 450umoles) was coupled according to general procedure (B) using HATU (171mg, 450umoles), NMP (2.25mL), and DIPEA (156uL, 900umoles). The terminal Fmoc group was removed according to general procedure (C) using 20% piperidine in DMF (2.25mL) and the reaction time was extended to 2 hour.

43rr was liberated from the resin according to general procedure (E) using 3.75 mL of the cleavage cocktail. The residue was reconstituted in 50% MeCN in water (0.1% formic acid) and purified by reverse-phase chromatography (gradient elution over 30 minutes from water (0.1% formic acid) to 50% MeCN in water (0.1% formic acid). Desired fractions were combined and freeze-dried to yield a white powder.

43rs

Trityl resin (100mg, 100umoles loading) was placed in a 4mL solid phase reactor. **Pro4RS** (**4**) was attached according to general procedure (A) using DCM (4.5mL) and DIPEA (116uL, 750umoles). The terminal Fmoc group was removed according to general procedure (C) using 20% piperidine in DMF (2.25mL).

Fmoc-Tyr(tBu)-OH (211mg, 450umoles) was coupled according to general procedure (B) using HATU (171mg, 450umoles), NMP (2.25mL), and DIPEA (156uL, 900umoles). The terminal Fmoc group was removed according to general procedure (C) using 20% piperidine in DMF (2.25mL) and the reaction time was extended to 2 hour.

43rs was liberated from the resin according to general procedure (E) using 3.75 mL of the cleavage cocktail. The residue was reconstituted in 50% MeCN in water (0.1% formic acid) and purified by reverse-phase chromatography (gradient elution over 30 minutes from water (0.1% formic acid) to 50% MeCN in water (0.1% formic acid). Desired fractions were combined and freeze-dried to yield a white powder.

5.5 References

[1] Gupta, S.; Schafmeister, C. E.; *J. Org. Chem.* **2009**, *74*, 3652–3658.

[2] Yoshida, K.; Kawamura, S.; Morita, T.; Kimura, S. JACS, **2006**, 128, 8034-8041

[3] Obst, U.; Betschmann, P.; Lerner, C.; Seiler, P.; Diederich, F. *Helv. Chim. Act.* **2000**, *83*, 855.

[4] Sebahar, P. R. and Williams, R. M. *J. Am. Chem. Soc.* **2000**, *122*, 5666.

[5] Overman, L. E. and Tellew, J. E. *J. Org. Chem.* **1996**, *61*, 8338.

[6] Chinchilla, R., Falvello, L.R., Galindo, N., Najera, C., (2001) *Eur. J. Org Chem*, 3133-3140.

[7] Williams, R.M., Fegley, G.J., (1992) *Tetrahedron Letters*, **33(45)**, 6755- 6758.

6.0 Concluding Remarks

This dissertation details the efforts to the progress towards a class of synthetic molecules with the eventual goal to serve as an alternative to natural proteins. Proteins possess a structural hierarchy of sequence (primary structure), local environments (secondary structure), global environments (tertiary structure) that are all require for protein function. Following this dogma we have created a series of chiral building blocks that carry chemically relevant functional groups. We can assemble these building blocks into rod-like oligomers that position small collections of functional groups in 3-dimensional space for diverse applications. To increase our effectiveness to discovering useful functional molecules, we have gained access to our principle building block (Pro4 class, based on the 5-membered ring heterocycle) through means of reaction optimization and scale up to 600 millimoles. We are continuing to modify and optimize a general solid phase synthesis strategy for making the oligomers. Our current strategy has allowed for the concurrent synthesis of 6 oligomers and has been demonstrated effective on scales up to 2 millimoles for each oligomer. With these oligomers, we have demonstrated competent modeling strategies for hypothesis driven application development toward electron transfer processes, catalysis, and molecular recognition, all three important functions of natural proteins. We have expanded on these principles to create larger, 3-dimensional assemblies by utilizing the oligomers as intermediate building materials. We have developed strategies to selectively cross-link 2 and 3 oligomers together to create something more protein-like. We are just now actualizing the first macromolecules of this kind, which we call “Fauxteins”. We are currently concerned with understanding their structures and have developed tools to characterize them, principally, the implementation

of the NMR active ^{15}N isotope of nitrogen. Once we gain information of the structure of these large macromolecules, we will develop them for the recreation of protein binding surfaces and enzyme active sites. Successful development and execution of "Fauxteins" would mark a gigantic leap into the chemical space, which up until now, has only been accessible via proteins.